ALKALI ACTIVATED MATERIALS: INTERACTIONS BETWEEN INGREDIENTS TO ACHIEVE SUSTAINABILITY

Mohammad Almakhadmeh

A Thesis

in

The Department of

Building, Civil and Environmental Engineering

Presented in Partial Fulfillment of the Requirements

for the Degree of Master of Applied Science (Civil Engineering) at

Concordia University

Montréal, Quebec, Canada

August 2020

CONCORDIA UNIVERSITY

School of Graduate Studies

This is to certify that this thesis prepared
by: Mohammad Almakhadmeh

Entitled: Alkali activated materials: Interactions between ingredients to achieve sustainability

and submitted in partial fulfillment the requirements for the degree of

Master of Applied Science (Civil Engineering)

Complies with the regulations of the University and meets the acceptable standards with respect to originality and quality.

Signed by the final examining Committee:

_____ Chair

_____ Examiner
Dr. Biao Li

_____ Examiner
Dr. M. Nokken

_____ Examiner
External (to program)
Dr. Mojtaba Kheiri

_____ Supervisor
Dr. A. Soliman

Approved by _____
Dr. M. Nokken, GPD
Department of Building, Civil and Environmental Engineering

_____
Dr. M. Debbabi, Dean
Gina Cody School of Engineering and Computer Science

Date _____

ABSTRACT

ALKALI ACTIVATED MATERIALS: INTERACTIONS BETWEEN INGREDIENTS TO ACHIEVE SUSTAINABILITY

Mohammad Almakhadmeh

Extensive researches were conducted on alkali-activated materials (AAM) as a green sustainable alternative for ordinary Portland cement (OPC). Recently, there was a shift to one-part alkali-activated materials to avoid the use of corrosive activator and also to reduce the carbon footprint. Most of the researches had focused on these powder activators types and impacts on the final product properties. However, limited research had investigated the interaction of these activators and other ingredients. Hence, the novelty of this work stems from studying these interactions and illustrating their effect on the developed One-Part AAM properties. Mixing water is a critical parameter in controlling the fresh and hardened properties of construction materials. Hence, the interaction between mixing water and the anhydrous activator was examined. Also, water effluents from various industrial recourses were tested. The study highlighted, for the first time, the role of water temperature in controlling the dissolution rate of solid activators. It emphasizes how this interaction can significantly change the fresh and hardened properties. On the other hand, superplasticizer and other chemical admixtures are commonly added to enhance cementitious materials flowability. However, the high alkalinity of AAM had drastically affected their effectiveness. Hence, a premixing technique was tested to produce AAM with high flowability. Various wastes, namely, red Mud, paper mill sludge, and paper mill fly ash, were examined as a potential precursor for AAM. The study showed the potential for developing a new smart, sustainable construction material/product incorporating such industrial wastes while maintaining adequate mechanical and durability performance. It is anticipated that the findings of this study

will i) lead to saving energy/reducing fossil fuel consumption to heat water during cold weather concreting will increase the sustainability level of the construction sector, ii) replace or reduce the demand for admixtures leading to both economic and environmental benefits, and iii) reduce the amount of industrial wastes sent to reservoirs through recycling/reusing in various construction applications leading to social and environmental benefits. Also, the outcomes of this research will allow the industrial sector to economically and sustainably transforming wastes into a high-value product.

CO-AUTHORSHIP STATEMENT

Substantial parts of this thesis were either published in or submitted for publication to peer-reviewed technical journals and an international conference. The candidate himself carried out all experimental work, data analysis, and writing of initial versions of all publications listed below. The contribution of the research advisor and any other co-author, if applicable, consisted either providing advice and/or helping in the development of the final versions of publications:

1. **M. Almakhadmeh** and A. Soliman "Effects of Mixing Water Temperatures on Properties of One-part Alkali-Activated Slag Paste," Construction and Building Materials, (Manuscript # ID CONBUILDMAT-D-20-07335), **Submitted**

2. **M. Almakhadmeh** and A. Soliman "Effects of Mixing Time on Properties of One-part Alkali-Activated Slag Paste," Construction and Building Materials, (Manuscript # ID CONBUILDMAT-D-20-08432), **Submitted**

ACKNOWLEDGMENT

I would first like to thank God, the Almighty, for the blessings he has given me throughout my time as a research student and for all the help I received when I needed it the most. I would now like to gratefully acknowledge various people who have been incredibly helpful and without whom it would have been impossible to write this thesis.

I would like to express my most profound appreciation to my supervisor, Dr. Ahmed Soliman, for his invaluable advice, persistent help, and financial support. Throughout my time as his research student, Dr. Soliman was very supportive and gave me access to fantastic research opportunities. I could not have imagined having a better supervisor for my MASc.

I am also particularly grateful for my mother, father, sisters, and brother for their prayers and continuous support. I would also like to thank my colleagues and friends for their support and all the precious moments spent outside the University.

1.1 List of Abbreviations

AAM	Alkali-Activated Materials
AAS	Alkali-Activated Slag
OPC	Ordinary Portland Cement
PPFA	Pulp and Paper Mill Fly-Ash
GGBFS	Ground Granulated Blast Furnace Slag
C-A-S-H	Calcium Aluminum Silicate Hydrate
C-S-H	Calcium Silicate Hydrate
CH	calcium hydroxide
NRC	Noise Reduction Coefficient
DSC-TGA	Thermogravimetric Tests

TABLE OF CONTENT

List of Abbreviations

AAM	Alkali-Activated Materials
AAS	Alkali-Activated Slag
OPC	Ordinary Portland Cement
PPFA	Pulp and Paper Mill Fly-Ash
GGBFS	Ground Granulated Blast Furnace Slag
C-A-S-H	Calcium Aluminum Silicate Hydrate
C-S-H	Calcium Silicate Hydrate
CH	calcium hydroxide
NRC	Noise Reduction Coefficient
DSC-TGA	Thermogravimetric Tests

List of Figures

List of Tables

CHAPTER ONE

INTRODUCTION

1.2 Background

Manufacturing waste management is the key to any successful and sustainable industry. Three leading practices are involved in mitigating the environmental impacts of manufacturing by-products, namely reduce, reuse, and recycle. Hence, the landfill is supposed to be the final destination in the waste management cycle [1].

Several industrial sectors are facing significant environmental challenges threatening the sustainability of their business. Therefore, they are searching for other alternatives having fewer environmental impacts [2,3]. The cement industry is one of these industries. It is considered a substantial sector that contributes to 8% of carbon dioxide (CO_2) emissions, with more than 2.8 Billion tonnes produced in 2015 [4]. Two main reasons are behind the cement industry's vast amounts of CO_2 emissions. The first reason is the high energy consumption during the manufacturing processes. The high burning temperature of 1400 °C is required for the decomposition of limestone during the Clinkerzation process, consuming massive amounts of fossil fuel. The second reason is the high demand for concrete as primary building materials, especially with the rapid civilization growth [5].

Different techniques have been used to mitigate the environmental impacts of the cement industry. One of the most common methods is the usage of chemical admixtures, such as superplasticizers.

These admixtures can disperse water and cement particles helping in reducing cement content in the mixture while maintaining adequate workability and strength [6]. Another environmentally friendly technique is to replace the OPC partially by rich aluminosilicate by-products such as Slag, Fly-Ash, and Silica Fume. This method offers environmental and economic benefits while enhancing concrete properties [7].

In the last decade, serious steps have taken toward entirely replace the OPC by the rich aluminosilicate by-products under the term Alkali Activated Materials (AAM). AAMs are known as the new building materials generation. Its final products have the same binding properties of cement or even better. Three main components to produce AAM are aluminosilicate precursor, alkali activator, and water. [8].

The thesis initially focused on the Alkali Activated Slag (AAS) as a concrete binding system, which has some features that distinguish it from the other precursors. AAS system has high early strength and does not need heat curing. This is attributed to the high calcium content in the precursor. Despite these features, AAS has several challenges related mainly to its fresh properties. These include high slump loss and fast setting time, which vanish its presents in many construction applications, such as Ready-Mixed concrete as delivery time is essential [8].

Two techniques have been investigated to enhance AAS fresh properties while maintaining mechanical performance, 1) the effect of mixing water temperature and 2) the effect of remixing. Moreover. AAS used as a binding system for a novel building material application incorporating with other by-products, two different industries by-products were examined, alumina manufacturing industry and wood pulping industry.

1.3 Objectives and Scope

This thesis aims to investigate different techniques that could enhance Alkali Activated Slag properties along with examining local rich aluminosilicate as potential precursors. It is anticipated that incorporating these domestic manufacturing waste in AAS technology will produce novel construction building materials. Hence, the goals of this study are to explore:

1) Providing general Knowledge about Alkali Activated Slag (AAS) and the challenges encounter behind the utilization of AAS.
2) Examining two different green and sustainable techniques could improve AAS's fresh and mechanical properties, 1) the effect of mixing water temperature on AAS paste and, 2) the effect of remixing on AAS paste.
3) Investigating the possibility of using the local rich aluminosilicate by-products as AAM precursors.
4) Examining the possibility of reusing Pulp and Paper Mill sludge and water effluent incorporating with AAS system in new building materials.

1.4 Structure of the Thesis

This thesis has been prepared according to the guidelines of the Faculty of Graduate Studies at Concordia University. It consists of seven chapters focusing on Alkali Activated Materials properties as the primary binding system and evaluating its properties as follow:

contains a critical review of the recent Knowledge about Alkali Activated Materials. The chapter highlights vital factors controlling the properties of AAM. These factors represent the basis for the following chapters. Chapter 3 highlights the effects of different mixing water temperatures on AAS activated by 6%,8%, and 10% anhydrous sodium meta-silicate activator. Four different mixing

water temperatures were used to simulate cold and hot weather conditions. Chapter 4 was allocated to investigate the effect of the remixing of AAS paste; three mixing regimes were studied to evaluate the effect of mixing time on both fresh and mechanical properties. Chapter 5 is assigned to examine local rich aluminosilicate by-products. Two by-products were included in this investigation. Red Mud as the by-product of the alumina manufacturing and pulp and paper mill Fly-Ash. Chapter 6 discussed the reuse of wood pulping industry solid waste, water effluent, and pulp and paper sludge in AAM to produce greener construction building materials. This chapter contains a novel building material made by zero virgin row materials. Finally, Chapter 7 provides a conclusion and summary of the achievements done out of this thesis.

1.5 Original Contributions

The originality of this research stems from the novel, simple ideas used to introduce AAS for a broader range of applications. Furthermore, utilizing and examine local waste in construction building materials which will reflect on the Canadian environment and economy. In sum, two significant contributions are involved in this thesis:

1) Providing a critical review of challenges encountering One-Part AAS and the recent work done related to this subject.

3) Improving One-Part AAS fresh properties through new sustainable techniques. These techniques would extend the use of the AAS binding system in various construction applications.

4) Investigating the effect of mixing ingredients temperatures on the One-Part AAS dissolution rate.

5) Solving serious One-Part AAS challenges related to its fresh properties by eco-friendly techniques while maintaining the mechanical properties, which will help the market in AAS concrete delivery.

6) Finding real solutions for two massive Canadian industries wastes, which will positively impact the environment and the economy.

7) Introducing new sound and thermal insulation board products using zero virgin materials made out of local manufacturing waste.

CHAPTER TWO

LITERATURE REVIEW

2.1 Industrial Issues

Recently, voices were raised for demanding serious steps toward climate change and global warming, especially with the rapid civilization progression [9]. Greenhouse gases (GHGs), including carbon dioxide (CO_2), Sulphur hexafluoride, hydrofluorocarbons, perfluorocarbons, and methane, are taking part in climate change and global warming [10]. Among those GHGs, CO_2 is considered as the primary contributor to climate change. About 70% of CO_2 emissions are the result of burning fossil fuel for several civilization sectors such as transportations, manufacturing, and construction industries [11]. These climate changes and global warming issues had urged governments to establish new legislation and policies toward maintaining global temperature rise below 2 ºC as discussed in Copenhagen and Paris summits for climate change [12,13].

The concrete industry is a significant CO_2 emissions producer. Cement industry, the primary binding material in concrete, contributed with about 8% of total CO_2 emissions in 2016. Cement industry required burning large amounts of fossil fuel to heat the first manufacturing reaction “calcination (decarbonation) of limestone” at 1400 –1450 °C [14]. Several eco-friendly practices have been developed to limit cement consumption while maintaining quality and economic benefits such as using chemical admixtures "superplasticizers," well-graded particles distribution, paste volume optimization, supplementary cementitious materials replacement “slag, fly ash and

silica fume," and more other techniques leading to a lower environmental impact [15]. Despite employing all these practices, Ordinary Portland Cement (OPC) is still highly demanded material. This motivates researchers to utilize rich aluminosilicates manufacturing by-products such as fly ash, slag, metakaolin, and silica fume as an alternative to OPC. Activating these aluminosilicates to produce environmentally friendly materials with a remarkable lower carbon footprint with similar or even higher mechanical properties to OPC binding system [14].

Alkali-activated materials (AAM) are inorganic materials made by dissolution, precipitation, and condensation of aluminosilicate precursors under high Alkaline medium [16]. Activating aluminosilicate using alkaline activators forms (Si-O-Al) and (Si-O-Ca) amorphous or crystalline networks depends on the activated binder chemistry. The rich calcium binders have a higher tendency to form (Si-O-Ca) bonds [17]. They will have similar properties to OPC materials or even better [18].

Several terminologies are used to express the reaction process the hydration products of this system, such as Alkali Activated Materials and Geoplymers. Both terms have been addressed under two different reaction mechanisms that do not express the same hydration process. For example, Slag is a glassy precursor called "melilite", it consists of gehlinite (Ca-silico aluminate) and akermanite (Mg-silicate), under the high alkaline medium of alkaline activator, gehlinite dissolve to form (K, Ca)-ortho-sialate-hydrate and precipitated aluminum hydroxide. On the other side, the dissolution of akermanite forms C-S-H and precipitated magnesium hydroxide, the interaction between (K, Ca)-ortho-sialate-hydrate, and C-S-H form a new structure with free K+, the free Ions leach rapidly at contact with water. In the case of geopolymers, the reaction process continues using additional precursors able to create a new network, the new network consumes the free Ions leads to form a sound and durable microstructure [16].

“Geopolymers is NOT a subset of AAM because they are not a calcium hydrate alternative (no NASH, no KASH). They belong to two very different and separate chemistry systems” [16].

2.2 General Overview of Alkali Activated Materials

Slag is the by-product of the steel industry. Around 1607 (Mt) of steel was produced in 2013, resulting in a massive amount of slag. This enormous quantity had many environmental issues that need to be managed. One of the main actions taken by big steelmakers to mitigate slag environmental impacts is grinding slag and reuse it in construction as partially replacing OPC. Moreover, it was found that slag and OPC combination has tangible enhancement on strength and durability compared to OPC concrete only [19].

For more than 125 years, utilizing slag in construction applications is under research and development. In 1895 combining slag, lime, and caustic soda was the first alkali-activated slag (AAS) attempt, which opened the horizon for new building materials generation. Later in 1957, Victor Clukhovsky reported the potential of producing new binding materials from calcium-free or low calcium precursors “aluminosilicate” under the term (Soil Cement) [20]. Despite environmental, durability, and mechanical advantages, AAS faced several challenges that limit its presence in many construction applications such as ready-mixed concrete. The main challenge to utilize AAS in ready-mixed concrete is its low followability and short setting time. These properties make delivery and consolidation very hard, along with high safety measures that need to be considered during handling the alkali activators [21].

2.3 Alkali Activated Materials Precursors

Alkali Activated Materials hydration products are the yield products of the dissolution, polymerization, and precipitation of aluminosilicate precursors under high alkali mediums. Rich aluminosilicate by-products have been examined to be AAM precursors, such as Slag, Fly-Ash, Metakaolin, Red Mud, and more other by-products, several studies attempt to explore the potential of these precursors to be OPC alternatives. From the literature, each processor has its properties depends on the chemical composition and the physical properties such as the fineness and particle shape [22,23].

2.4 Various Precursors:

2.4.1 Slag

Steel manufacturing required melting large amounts of iron ore, limestone, and coke under 1500^{o}C blast furnace. The melting process generates mainly two materials: iron and rich Ca-aluminosilicate light by-product float on the surface called Blast Furnace Slag. Slag formed during the rapid cooling process with granular particles with 5 mm in diameter. This slag is ground to reduce its particle size producing ground granulated blast furnace slag (GGBFS) [24].

Even though it is steel manufacturing by-product, steel slag chemical composition and properties differ based on the production method and manufacturing raw materials. In general, steel slag consists of four main chemical components dominate AAS hydration properties, which are Al_2O_3 (8-24%), SiO_2 (28–38%), MgO (1–18%), and CaO (30–50%). For example, CaO affects slag basicity index [(CaO + MgO)/(SiO_2 + Al_2O_3)]. Increasing CaO content increases GGBFS basicity leading to higher strength and more compacted microstructure [24]. Moreover, the milling

process affects slag hydration properties. It was reported that particle size finer than 20 μm is relatively higher reactivity comparing to the slag particles coarser than 20 μm in diameter [25].

2.4.2 Red Mud

Bauxite is a mixture of minerals. It contains aluminum, iron oxides, sand, clay, and small amounts of a form of titanium oxide. This raw material is bathed in a solution of sodium hydroxide (i.e. a strong base) at a high temperature and pressure to dissolve aluminum components. All the remaining undissolved components form the red mud. This red mud is kept in reservoirs. In order to avoid leakage and flood, aluminum producers use powerful presses to squeeze the water out of the mud and evaporators to dry most of the rest [22,26].

2.4.3 Pulp and Paper Mill Fly-Ash

PFA is the biomass by-product generated from the combustion process of wood, the chemical and physical properties of PPFA are vary depending on the combusted wood and the manufacturing operation, mainly the combustion temperatures which controls PPFA properties. Generally, PPFA specific gravity ranges between 2.4 - 2.8 with bulk density 150-1300 Kg/m3, where the particle size distribution ranges between 150 to 250 μm and surface area 4200 - 100,600 m2/kg. PPFA pH rangs between (8-12) [27]. PPFA consists of major six chemical oxides (SiO 6.5-50.7), (Al2O3 9-28), (Fe2O3 2.34-5.4), (MgO 3-6.5) and (Na2O 1.7-2.8) [28, 29]. This chemical composition makes PPFA a high promising precursor in the building materials field.

2.5 Effect of Combining Different Precursors

The Slag-fly ash combination is rich calcium precursors. Slag is known to be highly reactive, unlike low calcium fly ash type (F), which known as low reactive precursors. The low CaO content in the fly ash precursors required heat curing, which is not available for all applications. Therefore, tuning between fly ash and slag is required to achieve acceptable fresh and harden properties at reasonable curing conditions. Several studies reported the effect of increasing the slag portion from the total binder. Increasing slag portion reduces slump and shortens setting time. Contrary, it increases strength, especially in the early stage. This is attributed to the high CaO content in the mixture provided by Slag. Moreover, one-part AAM reported very high slump loss, where less than 20 minute was enough to lose almost 150 mm flow even with 0% slag substitution [30].

2.6 Alkali Activators

Generally, the OPC hydration process promotes mixture alkalinity, which activates aluminosilicate materials when added as a partially replaced OPC. However, with the absence of OPC, AAS required another material to activate aluminosilicate precursors, which called alkali activators [31]. Numerous studies have investigated the potential of utilizing different high alkaline materials. The most common activators examined are sodium hydroxide (NaOH), sodium silicate (Na_2SiO_3), Sodium meta-silicate (Na_2SiO_3) potassium hydroxide (KOH) and potassium silicate (K_2SiO_3), these activators used in two forms, two-Part which is the most common and One-Part. [18,32-34]. Alkali activator working mechanism can be understood through monitoring AAM hydration processes. AAM reaction process starts with the dissolution of the activator in water. Hence, the alkaline medium of activator solution starts desolating aluminosilicate precursors under the high

alkaline (pH > 12). The higher concentration of OH^- increases aluminosilicates dissolution to Al-O and Si-O monomers. Moreover, high activator alkalinity accelerates reaction kinetics resulting in a higher degree of reaction, which in turn maximizes final hydration products. From a durability point of view, it was reported that the higher activator alkalinity helps in producing more stable and compacted hydration products [35].

2.6.1 Alkali Activators Forms

Two forms of alkali activators are used to activate aluminosilicate binders: the solution form "two-part," which is the conventional one, and the solid form "one part." Two parts alkali activators are prepared by adding water to the solid form of the activator, forming a corrosive solution. Contrary, the one-part is used in its solid form directly added to the mixture. However, every alkali activator form has its advantages and disadvantages. For the most common activator form, two-part alkali activators are distinguished by their high workability, strength, and their tendency to form more zeolite as final hydration product rather than one-part activators. Despite its positive features, two-part activators have higher efflorescence. Also, the issue of safety as two-part activators are very corrosive materials that need strict safety procedures during preparation, handling, and mixing. [20]

Several studies have investigated the combination of different types of alkali activators, such as the combination of sodium hydroxide and sodium silicate [12,16,36,37]. Moreover, many other combinations have investigated targeting better AAM fresh and hardened properties while maintaining low environmental impacts [38]. For example, combining both sodium carbonate and sodium hydroxide offers better strength than using each activator separately [39].

2.6.2 Effect of Combining Different Activators

The use of different activators or combining them is another technique that was implemented to achieve sufficient workability while maintaining strength. Many types of activators were studied, such as sodium silicate, sodium hydroxide, sodium carbonate, and sodium meta-silicate, etc. It was reported that the same alkali activator dosage, same binder, and water to binder ratio (W/B), sodium hydroxide exhibited very high slump loss followed by potassium hydroxide (KOH) and sodium silicate. This is attributed to the high heat generated at the contact point of the activator with water. Moreover, the rapid set does not mean higher strength, where activator chemistry has its role in the quality of the final hydration products [40].

2.6.3 Influence of Activator Concentration "Alkalinity MOH."

Increasing activator alkalinity offers a richer Na^+ or K^+ solution, which has a tremendous effect on the hydration process. The influence of activator alkalinity on setting time and strength is tightly related to reaction kinetics. In general, two peaks accrue in AAM reactions, the first happens in the first few minutes, and the second happens later on based on several variables. Setting time and workability are linked to the first peak; subsequently, higher heat released results shorter setting time and lower workability. Isothermal calorimeter analysis showed that increasing alkalinity increase dissolution, and precipitation rates yielding a higher exothermic reaction, which affects AAM properties significantly [41].

It was reported that increasing activator molarity accelerates the reaction leading to shorter setting time and low workability. This effect refers to a high rate of dissolution and precipitation process of the precursor under the high alkaline mediums [42]. On the other hand, the effect of activator

molarity on strength development had been investigated in several studies. The major effect was reported on the early strength. The higher the molarity, the higher the early strength. This observation confirmed by high reaction kinetics during dissolution and polymerization mentioned earlier.

2.7 Slag Activation Process

Generally, the activation process of rich aluminosilicate precursors passes through a series of chemical reactions. Three chemical reactions are involved in the formation of the hydration products: i) dissolution of aluminosilicate precursor into silica and aluminum monomers under the alkaline medium, ii) oligomer formation from precursors ions “precipitation” and iii) condensation “Polycondensation” of monomers to form the geopolymer. Geopolymrization is an exothermic reaction that releases heat during the reaction process. The heat generated is affected by curing temperature, which affects both setting and mechanical properties [17,43,44]. As a rich calcium and aluminosilicates binder, GGBFS presence in the mixture results in forming (Si-O-Ca) gel similar to calcium silicate hydrate (C-S-H) in OPC binding system and precipitates in the form of Portlandite $Ca(OH)_2$. Based on calcium availability in the system and medium alkalinity, the higher alkaline medium tends to form more (C-S-H) bonds. Therefore, integrating calcium content binders such as GGBFS and type C Fly-Ash and high alkaline activators offer higher mechanical strength, especially at an early age [45].

2.8 Chemical Admixtures

Admixtures are chemical additives that are added to concrete or grout to promote its properties in both fresh and harden stages. Various types of admixtures used for different purposes. Commonly, chemical admixtures added in the wet stage of mixing by dosage ranges between 0.3% up to 5% of cement content, including supplementary cementitious materials. Generally, the admixture dosage depends on the amount of the active materials in the designed formula. Several mechanisms interacting with mixture ingredients mainly to retard or accelerate hydration process depending on admixture type such as 1) affecting hydration process speed, 2) dissipation binder particles (plasticizer effect), 3) affecting water surfers tension (air entrain agent), 4) changing mixture rheology by changing its viscosity, or 5) affecting harden properties using additional chemicals to enhance durability against corrosion in the case of using corrosion inhibitors as an example. The most common admixtures which help in getting targeted workability, strength, and durability are dissipating admixtures. The main three species, with different chemical structures, that fall under this category are:

a) **Lignosulphonate:** heavy spherical micro-gel polymer. The dissolution of its sulphonate group resulting in Na+, SO-3, and negative charge micro-gel, which has the role of the dispersing action [46].

b) **Sulphonated naphthalene formaldehyde (SNF):** is the product of Sulphonated and polymerized naphthalene under high temperatures and high sulphuric acid concentration. The mixture is then neutralized by calcium Ca and sodium Na salts. The dispersion mechanism of SNF depends on the dissolution of the polymer chain into Na+ and SO-3. The negative charge of SO-3 adsorbed on cement particle and did the

electrostatic dissipation. SNF dissipation time depends on molecular weight. The higher the molecular weight, the longer the dissipation time, resulting in longer setting time and lower slump loss [46].

c) **Polycarboxylate (PCs):** is considered as the most recent dissipation admixture technologies, especially polyether type. PCs consist of a backbone and a micro monomer. The backbone produced by the polymerization of acrylic acid. Different types of micro monomers can be attached to the backbone providing liaison point on cement particles and does the dissipations by the steric effect. This effect keeps cement particles away from each other. Moreover, polyether is distinguished by its high molecular weight. This high molecular weight promotes PCs admixture properties to give longer slump retention and higher water reduction which has positive impact on workability and strength [46].

2.8.1 The Effect of Chemical Admixtures on AAS

Several researchers examined the possibility of using the same chemical admixtures to improve Alkali activated slag (AAS) properties. These included lignosulphonate based water-reducing and retarder (WRRe), modified naphthalene formaldehyde polymers based superplasticizer (SNF), modified polycarboxylate polymers based superplasticizer (PC), shrinkage-reducing (SRA) admixtures [39]. Air-entraining agent (AEA) tested as another technique to increase mixture workability [48]. The potential of combined chemical admixtures to reach reasonable properties with optimizing admixtures was also examined [47].

a) **Lignosulphonate based water-reducing and retarder (WRRe)** effect on AAS concrete activated by sodium silicate and a combination of sodium silicate and sodium hydroxide was examined. Higher initial slump and low sump loss for mixtures activated by sodium silicate and sodium hydroxide were reported. These results indicate that activator type is an essential factor affecting fresh properties [48].

b) **Liquid modified based polymer admixture (SSRe)** have been examined to achieve better workability of AAS while maintaining strength. Generally, SSRe effect on setting time and workability was powerful with Portland cement paste mixtures; however, no significant effect of admixture on AAS. This is attributed to the collapsing of the admixture polymer structure under the high alkali mediums. It was reported that SSRe admixture was more effective on fresh properties for mixtures with low activator concentration, but a significant impact on the early and ultimate strength was also reported [47].

c) **Shrinkage reducer admixture (SHR) admixture** had shown significant effects on the workability and setting time at low Ms (SiO_2/Na_2O). Moreover, inadequate early and ultimate strength reported due to insufficient amount of sodium in the mixture to produce the hydration products N-A-S-H gel was also reported [47].

d) **Alkyl Aryl sulphonate based air-entraining agent admixture (AEA)** potential to enhance AAS fresh properties was examined. AEA showed significant AAS workability improvement and adequate strength compared with the AAS mixture without AEA [48].

e) **Modified polycarboxylate admixtures (PC)** considered as a new generation of concrete admixtures, moreover its became widely used in Portland cement concrete manufacturing, the effect of (PC) admixtures on different activators types and concentrations were

investigated, regardless its effect on setting time, no significant effect on workability was reported [48].

2.8.2 Effects of Chemical Admixtures on One-Part Meta-Silicate AAS

Although it is safer in production and handling than two-part AAM, maintaining sufficient workability and setting time without effecting strength using one-part alkali activators is a challenge[33,40]. This is linked to the heat generated instantly after adding water due to activator dissolution leading to a rapid setting [40]. As discussed earlier, admixtures' effects on AAS is subjected to several variables related to activator type, activator concentration, Ms, admixture type, and GGBFS chemical composition. Many studies had examined the effect of different admixtures on two-parts AAM. However, very limited researches studied the effect of admixtures on one-part AAM.

The effect of different admixtures on AAS mixtures prepared by anhydrous "powder" sodium silicate and sodium met-silicate activators have been investigated [41]. For sodium metasilicate, a significant slump increased initially under the effect of both PC and SNF admixtures. However, setting time was very short compared to sodium silicate mixtures. This is attributed to the high pH of sodium meta-silicate solution, which accelerates the dissolution of aluminosilicate particles and the rapid formation of hydration products [41].

Another study investigated lignosulphonate, polycarboxylate, sodium gluconate based admixtures and sodium tetraborate decahydrate-Borax (B)-($Na_2B_4O_7 \cdot 10H_2O$) admixtures on slag/fly ash (85%:15%) mixtures. mixtures were activated by 8% solid sodium metasilicate with Ms (Na_2O/SiO_3) = 1. The study showed that sodium gluconate and Borax had a positive effect on

workability. Moreover, calcium Lignosulphonate increased slump loss even more than the mixture without chemical additives. Borax significantly increases slump and reduce slump loss. The impact on compressive strength was tangible, especially when Borax content goes beyond 4% by binder mass [40].

It was confirmed that the effect of using some of the chemical admixtures with one-part AAM could enhance fresh properties for very limited periods. Considering the side effects on compressive strength in both early and later stages, it is an acoustical issue that needs to be solved with other techniques [14].

2.9 Effect of Curing

Curing temperature is a crucial factor that affects AAM properties. Different curing regimes have been tested to investigate their effects on geopolymrization and final product properties. By isothermal calorimeter, geopolymrization reaction kinetics was characterized under different curing temperatures providing a clear understanding of its properties [49].

2.9.1 Effect of Curing Temperature

A Previous work on AAM studied three different curing temperatures kinetics (20 ºC, 35ºC, and 50ºC) [44]. Two peaks were recorded at two different reaction stages. The first one happens in the early stage within the first few minutes and the second one during the first 5 hours. It can be observed that the higher curing temperature offered higher peaks in both stages, while shorter elapsed time till the second peak. The overall heat generated was higher for the moderate curing temperatures (20 and 35 ºC), which is confirmed by higher strength results obtained. This is attributed to the rapid dissolution and polymerization process of high curing temperature at the

moment of contact between the precursor and the alkali activator solution. This consumes a high amount of Si and Al during the first stage forming gel products quickly, which cover the particles and preventing the reaction progress later [49].

As shown in **Fig.2.1,** the effects of different curing temperatures (7–30 °C) on ***setting time, strength development, shrinkage, and the microstructure*** for both AAS and OPC mortars were investigated. Generally, ***setting time*** reduced with increasing curing temperatures for both types of cement. Shorter setting time was recorded for AAS mixtures in the normal curing temperature

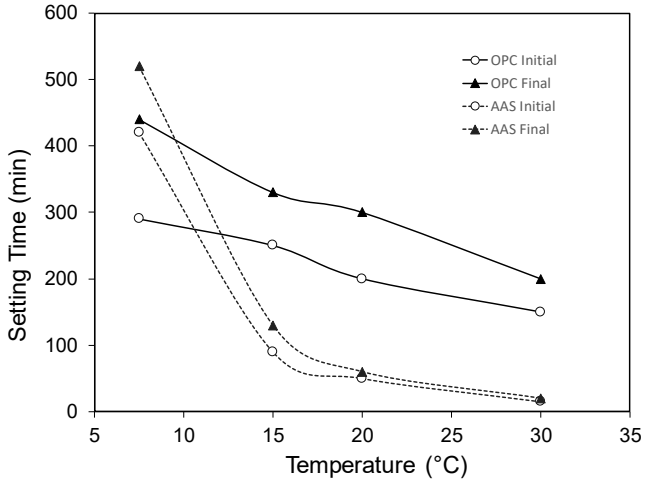

Figure 2-1 Effect of curing temperature on Setting time [50]

In terms of ***strength development*****, Fig.2.2** shows a tangible impact of curing temperature on the AAS strength gaining rate rather than OPC samples, especially during an early age. The three days' strength results show high strength difference, about three times strength gaining for the high curing temperature compared to that of low curing. In comparison, 28 days' strength results showed high strength for the higher curing temperatures in both binding systems. Moreover, the study

shows that higher strength value for AAS than the OPC can be an advantage in favor of AAS in ***cold weather concreting*** [50].

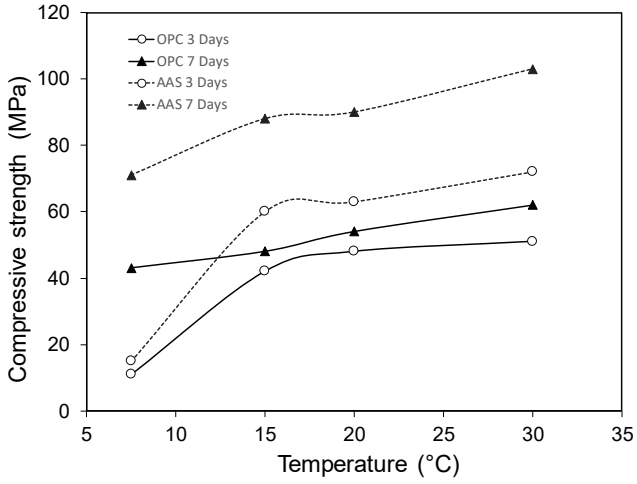

Figure 2-2 Effect of curing temperature on Compressive strength [50]

2.10 Effect of Calcium Content with Different Curing Temperatures

Calcium content has a tremendous effect on both binding systems AAM and OPC properties. Generally, calcium-rich precursors had faster setting time, higher early, and later strength; this is attributed to its ability to develop more C-S-H gel in the OPC system and C-A-S-H gel in AAM systems, this is attributed to the high presence of Ca ions in the precursor. These features can potentially expand AAM applications, especially in low curing temperatures conditions.

A comparison study between Alkali activated fly ash and OPC paste with additional calcium hydroxide (CH) in different percentages to both binding systems showed that increasing CH percentage by binder decreases setting time and increases strength development in both stages. [51].

2.11 The Effect of Mixing Time

Mixing time is a crucial factor that controls the quality of the final product, especially in Ready-Mix concrete applications, several studies have covered this topic in the OPC concrete base system [52-54]. In contrast, limited research has done studding the effect of mixing regimes on the AAM. AAS fresh and harden properties were investigated under three different continuous mixing times, it was evident that increasing mixing time leads to longer setting time and higher slump retention time this was attributed to the continuous breaking of the early formation gel structure. The effect on strength was noticeable as well; the longer the mixing time, the higher strength reported; these results were attributed to denser microstructure formed, which was confirmed by SEM and porosity tests [55,56].

2.12 Conclusion

Alkali Activated Materials (AAM) are promising materials that can be an alternative to the OPC binding system in the future. Moreover, AAM can be a massive landfill for many waste by-products such as Slag, Red Mud, and Pulp and Paper Mill Fly-Ash. However, several challenges encounter the presence of AAM in many construction applications; this limited presence is due to the fast setting, curing temperature, and safety precautions, these challenges make AAM delivery and consolidation a hard job, many techniques have been investigated toward enhancing AAM fresh properties while maintaining consistent mechanical performance. At the same time, most of these practices harmed the other features.

CHAPTER THREE

EFFECTS OF MIXING WATER TEMPERATURES ON PROPERTIES OF ONE-PART ALKALI-ACTIVATED SLAG PASTE

During hot and cold weather, mixing water temperature is a critical parameter in controlling the fresh and hardened properties of cement-based materials. With the advent of Alkali Activated Materials (AAMs), the effectiveness of such a technique becomes questionable as the hydration mechanism differs from that of the ordinary Portland cement (OPC). Therefore, this study focuses on evaluating the effects of mixing water temperature on the performance of the One-Part Alkali Activated Slag (AAS) paste. Various AAS paste mixtures prepared by different mixing water temperatures (i.e., 0°C, 10°C, 20°C, and 30°C) were tested. Fresh and hardened properties, including mini-slump, slump loss rate, setting time, the heat of hydration, compressive strength, and shrinkage, were investigated. Results reveal that the mixing water temperature plays a dominant role in controlling solubility and dissolution rates for different ingredients (i.e., solid activator and Slag). This, in turn, had affected the hydration process and, consequently, the development of various properties. Slump life and setting time were found to extend as mixing water temperature reduced while the strength was not harmed. Saving energy consumed for warming water during cold weather concreting will also increase concrete sustainability. It is

anticipated that these findings will pave the way for a broader implementation of such green sustainable materials in the construction sector.

3.1 Introduction

Cement manufacturing is one of the primary sources of CO_2 emissions [57]. This severe environmental impact had urged researchers to find alternative eco-friendly materials to cement [58]. Alkali activated materials (AAMs) are a promising alternative that is known under the term polymer as "the third generation of cement" [59]. AAMs are formed by dissolving alumino-silicates under high alkalinity conditions to free $[SiO_4]^-$ and $[AlO_4]^-$ tetrahedral units. These tetrahedral units are alternatively linked, forming polymeric [–Si–O–Al–O–] bonds [60]. Fly ash, metakaolin, blast furnace slag, and other industrial by-products are being used as sources for alumino-silicate precursors [61-63]. A high alkalinity solution of sodium hydroxide, sodium silicate, or sodium meta-silicate, is used as a chemical activator for these precursors [51,64]. Among various types of AAMs, alkali-activated Slag (AAS) is the most promising as it has a fast setting, high early strength development, low permeability, and does not need heat curing [57,66]. These features make AAS a promising material that can fit many constructional applications [67]. On the other hand, in the concrete industry, fresh concrete properties are critical from different aspects, including how easy to cast, compact, and finish [68]. Hence, having mixtures with long slump-life while maintaining adequate strength is a desire. In hot regions, cold water or ice is used to lower concrete mixture temperatures. Consequently, the hydration rate is reduced, and the slump-life is extended [69]. On the contrary, heating concrete ingredients is recommended in cold weather concreting [70]. Conversely, in cold weather, mixing with hot water was found to enhance

the hydration process resulting in a reasonable setting time [71]. Hence, the mixing water temperature has a dominant role in achieving targeted properties for concrete.

The hydration mechanism of AAS and formed products differ from that of the OPC. The activation for slag results in the formation of hydrated calcium aluminates and alumino-silicates (C-A-H and C-A-S-H phases) [72]. The formation and growth rates for these products vary from that of calcium silicate hydrated (CSH) and calcium hydroxide (CH) and other products formed during OPC hydration [73]. Consequently, the response of AAS will be governed by a set of factors that differ from that controlling OPC. For instance, the AAS hydration rate is affected by the activator type and dosage, which does not apply to OPC. Even for the same factor, the response of AAS is anticipated to differ from OPC response (i.e., admixture dosages) [74]. Most of the researches conducted on fresh and hardened properties of AAS had focused on exploring the effects of varying slag composition, combining Slag with other precursors, using different activators, varying activator dosages, adding various admixtures, and applying different curing regimes [75-77]. Moreover, enormous researches were conducted on AAS activated by very corrosive solutions (known as two-part AAS) [78-80]. Limited attention was given to AAS activated with powder activators (known as one-part AAS) due to its lower performance compared to two-part AAS [81-83]. However, recent development in powder activator had made it a promising safe, easy to handle activator for AAS.

Therefore, this paper will explore the effects of mixing water temperatures on the fresh and hardened properties of one-part AAS. Selected mixing water temperatures included 0°C and 10°C to simulate sub-freeze and cold conditions, 20 °C represents normal condition (tap water), and 30 °C was used to simulate hot weather conditions. This temperature range will emphasize the economic and energy save side of avoiding cooling or heating mixing water for AAS concrete at

various conditions. The reported results of this study will contribute to understanding the interrelationships between AAS ingredients' temperatures and achieved properties.

3.2 Research Significance

The effects of types and contents of precursor materials, activators, and additives on AAM properties were extensively studied in the literature. To the best of the authors' Knowledge, very limited research had investigated the effects of mixing water temperature on AAM properties. A parameter that had proven to have significant effects on OPC-based materials properties. The study provides first-time data on how water temperature controls the dissolution rate of different ingredients and, consequently, various properties developments. Hence, this study bridges the knowledge gap on the interactions between water temperature and other one-part AAS ingredients.

3.3 Experimental Program

3.3.1 Materials

For all mixtures, granulated blast furnace slag (hereafter referred to as Slag) with specific gravity 2920 kg/m^3, and Blaine fineness 515 m^2/kg and d_{50} value around 14.5 μm and basicity coefficient 1.06 was used as the precursor material. The chemical compositions of used Slag are summarized in **Table 3.1**. Anhydrous sodium meta-silicate was used as a powder activator. The chemical and physical properties of used activators are shown in **Table 3.2**. Three different activator dosages of 6%, 8%, and 10% by weight of Slag were used, all mixtures ingredient had the room temperature of (i.e., temperature (T) =23 ± 2°C). Four groups of mixtures with different mixing water temperatures, namely, 0°C, 10°C, 20°C, and 30 °C were cast mixed and tested. For all mixtures, a constant liquid-to-solid ratio (l/s) = 0.40 was used.

3.3.2 Mixtures Preparation and Testing Procedure

All paste mixtures were prepared and tested under the laboratory ambient condition (i.e., temperature (T) =23 ± 2°C and relative humidity (RH) = 45 ± 5%). Initially, slag and powder anhydrous sodium meta-silicate activator were dry mixed for 2 minutes. Then, mixing water was gradually added while mixing continued for about 2 min. For the setting time, samples were prepared and tested using a Vicat needle according to ASTM C191-19 "Standard test method for time of setting of hydraulic cement by Vicat needle." Flowability was evaluated using the mini-slump cone test. After removing the filled mini-cone, the final spread diameter (D_f) of the fresh paste sample was taken as an average of two measurements made in two perpendicular directions.

Table 3-1Chemical compositions of used Slag

Items	SiO_2	Al_2O_3	CaO	Fe_2O_3	SO_3	MgO	K_2O	Na_2O	TiO_2	M_nO_2
(%)	36.5	10.2	37.6	0.5	3.1	11.8	0.4	0.3	1.0	0.4

Table 3-2 Chemical and physical properties of Anhydrous sodium meta-silicate [84]

Property	W_t % Na_2O	W_t % SiO_2	W_t % H_2O	Density (g/cm^3)	Particle Size	Melting Point (°C)	The heat of solution (kJ/mol)
Typical Data	50.5	46.2	<3	1.09	93% in 20 to 65 mesh	1088	-31.7

Moreover, following ASTM C143 (Standard Test Method for Slump of Hydraulic-Cement Concrete), the slump was measured every 2.5 minutes for the first 10 minutes, then at 5 minutes intervals until 100 mm slump value (i.e., equivalent to the mini-slump cone diameter) was

achieved. Cubic specimens 50 mm were used to evaluate the compressive strengths at ages 1, 3, 7, and 28 days following the ASTM C 109-20 "Standard Test Method for Compressive Strength of Hydraulic Cement Mortars (Using 2-in. Or [50-mm] Cube Specimens". After 24 hrs, specimens were demolded and stored inside a plastic bag at laboratory ambient temperature until the time of testing. For drying shrinkage measurements, prismatic specimens, 25 × 25 × 285 mm, were made according to ASTM C 157/C127-17 "Standard Test Method for Length Change of Hardened Hydraulic-Cement Mortar and Concrete." After demolding, specimens of each mixture were exposed to dry at the ambient laboratory conditions to evaluate the total shrinkage. The unrestrained one-dimensional deformations were measured using a comparator provided with a dial gauge with an accuracy of 10 μm/m.

The heat flow at the wetting point (i.e., once the water comes in contact with solid materials) and dissolution of solid particles was captured by mixing solid ingredients (i.e., anhydrous sodium meta-silicate and Slag) with water inside an isothermal calorimeter. Initially, only anhydrous sodium meta-silicate was mixed with water to avoid interference due to slag particle dissolution. The heat flow for Slag, activator, and water was evaluated in the second phase. For each test, the powder sample was inserted inside a single-use glass ampoule and sealed. After that, the ampoule was installed inside the insulated chamber, and water was injected using an especial syringe while mixing using a manual stirring.

Moreover, semi-adiabatic calorimetry studies were conducted on specimens during the first 48 hrs of hydration using a custom-built experimental setup. Specimens were prepared and cast into a cylinder mold with a diameter of 75 and a height of 150 mm. The mold was immediately placed in a micro-porous insulation box. Three Type-T thermocouples were inserted into the center of the concrete volume along its height to monitor its temperature. Temperature readings were recorded

continuously using a data acquisition system. Replicate specimens indicated a standard deviation of 1.8°C for the maximum specimen temperature. Moreover, another set of the same cylinder specimens was stored under ambient conditions and monitored to capture the heat profile.

The formation of different hydration products was evaluated through conducting Differential Scanning Calorimetry (DSC) using a TA instrument. The hydration product formation was evaluated at ages 1and 28 days. At the selected testing age, hydration of paste samples was stopped using the freeze-drying technique. Then, chunks taken from the center of the specimens were ground to powder and sieved on No. 200 sieve. Samples weighing approximately 40 mg were heated from 23°C to 670°C at a heating rate of 10 °C/min. Collected data and curves were analyzed using a TA Instruments thermal analysis software.

3.4 Results and Discussion

3.4.1 Effect of Mixing Water Temperatures on Fresh Properties of AAS Paste

3.4.1.1 Mini-Slump Results

Figure 3.1 illustrates the measured slump-loss over time for mixtures mixed with various mixing water temperatures and activator dosages. Generally, the higher the mixing water temperature, the faster the slump loss rate. For instance, at an activator dosage of 6%, spread diameter for mixtures mixed with 30°C water decreased from 190 mm to 100 mm in only 10 min, while for mixtures mixed with 10°C water, it took around 55 min. This confirms that mixing water temperature will have a significant effect on the slump-life for AAS mixtures. Increasing the water temperature will increase the mixture temperature; hence, more thermal energy is available for water evaporation leading to a higher water loss [85]. Losing water will reduce the water content in the mixture,

which will increase its stiffness [86]. Moreover, potentially the pH will rise after the reduction of the water content as alkalis concentration will increase [87]. This is anticipated to accelerate the formation of hydration products and losing flowability due to the formation of new physical and chemical bonds between new products [86]. Moreover, water will be consumed in the hydrolysis of silicate and aluminate from the activator and the Slag into the solution. Hence, less water is available to disperse solid aggregates by forming water layers between particles [88]. This reduction in slump retention correlates with the short induction period, as will be discussed in heat flow measurements.

In agreement with the literature, increasing activator dosage had shortened the slump retention time [89]. For example, mixtures mixed with 0°C water, spread diameter decreased from 190 mm to 100 mm in 70 min and 25 min at activator dosages 6% and 10% (i.e., about 64% reduction in slump-life), respectively. A previous study showed that increasing sodium meta-silicate activator dosage promoted flocculation for suspended particles in AAS due to decreasing the zeta potential [86]. Zeta potential reflects the electrostatic repulsive forces between homogeneously charged particles due to the formation of a double layer of counter ions [90]. Hence, decreasing zeta potential will increase the net inter-particle forces leading to a lower flowability.

Moreover, it was noticed that the reduction in slump retention due to increasing activator dosage varied as mixing water temperature changed. For instance, mixtures mixed with 30°C water exhibited around 75% reduction in the slump-life as activator dosage increased from 6% to 10%, which is higher than that for mixtures with 0°C water (i.e., 64%). This reduction in the slump-life also can be attributed to the thermal effect of varying mixing water temperatures. However, the heat generated from activator dissolution is anticipated to have a role as will be explained later.

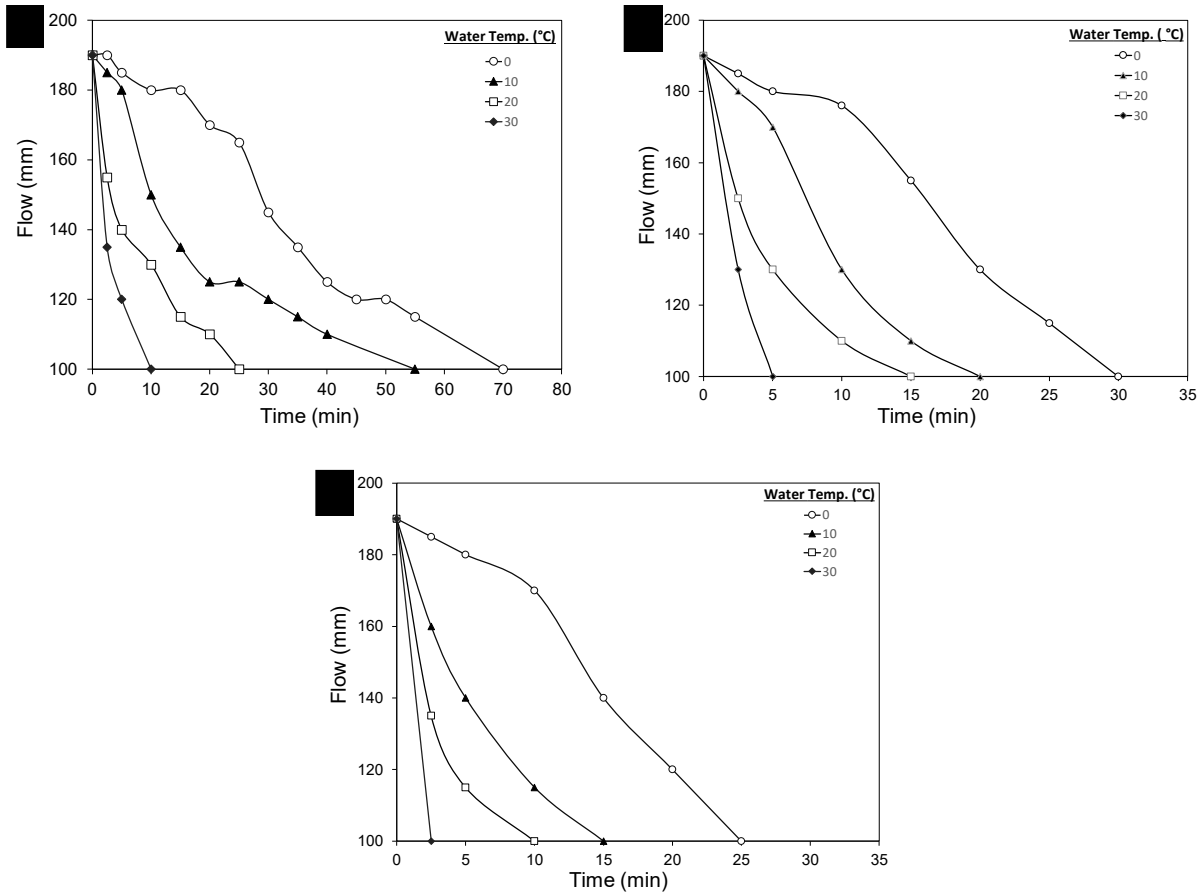

Figure 3-1 Flow results for AAS prepared by different mixing water temperatures and activator dosages of a) 6%, b) 8%, and c)10%.

3.4.1.2 Setting Time

Figure 3.2 illustrates the effect of mixing water temperatures on the initial and final setting times. Generally, regardless of activator dosages, increasing the mixing water temperature shortened the setting time and vice versa. For instance, for mixtures activated by 6%, the final setting time for mixtures mixed by 30°C water was around 42% shorter than that for mixtures mixed by 0°C water. This confirms the extended slump-life for mixtures prepared by cold mixing water (i.e., < 20 °C) (**Fig. 3.1**). The setting is defined as the process of the gradual development of rigidity due to hydration progress, which is a chemical reaction. Chemical reactions are directly affected by

exposed temperatures (i.e., high temperatures accelerate chemical reactions and vice versa) [91]. The dissolution of the solid activator and Slag are exothermic reaction processes, adding more heat to the system. Hence, the resultant for the thermal effects, induced by both varying water temperatures and heat of hydration, will control the duration of the setting. Low mixing water temperature partially compensates the dissolution heat effect, slowing the chemical reactions and extending the setting time. Conversely, warm mixing water adds up and accelerates the hydration leading to shorter setting time.

Interestingly, the elapsed time between the initial and final setting times did not change significantly as the mixing water temperature changed. For instance, for mixtures activated by 8%, the difference in the initial setting between mixtures prepared by 0°C to 10°C was around 28%, while both mixtures the same time to achieve final setting (i.e., less than 1%). This indicates that the thermal effects (i.e., induced by mixing water temperature and early liberated heat) will be limited to the early stages of hydration reactions (i.e., initiation). Later, this thermal effects diminished due to exchanging heat between mixtures and the surrounding environment resulting in the same temperatures profile for all mixtures. Hence, the setting process will be mainly controlled by the reactant materials characterizations. This is complying with the heat flow results during the dormant period, as discussed later.

On the other hand, the higher the activator dosage, the shorter the setting time. For instance, mixtures mixed with 10°C water, the setting time was shortened by 55% as the activator dosage increased from 8% to 10%. It should be mentioned that, for the same activator dosage, the elapsed time between the initial and final setting time was almost the same regardless of mixing water temperatures. This also confirms that the hydration progress after the initial setting will be mainly relying on the reaction of mixture ingredients rather than the initial mixing water temperature.

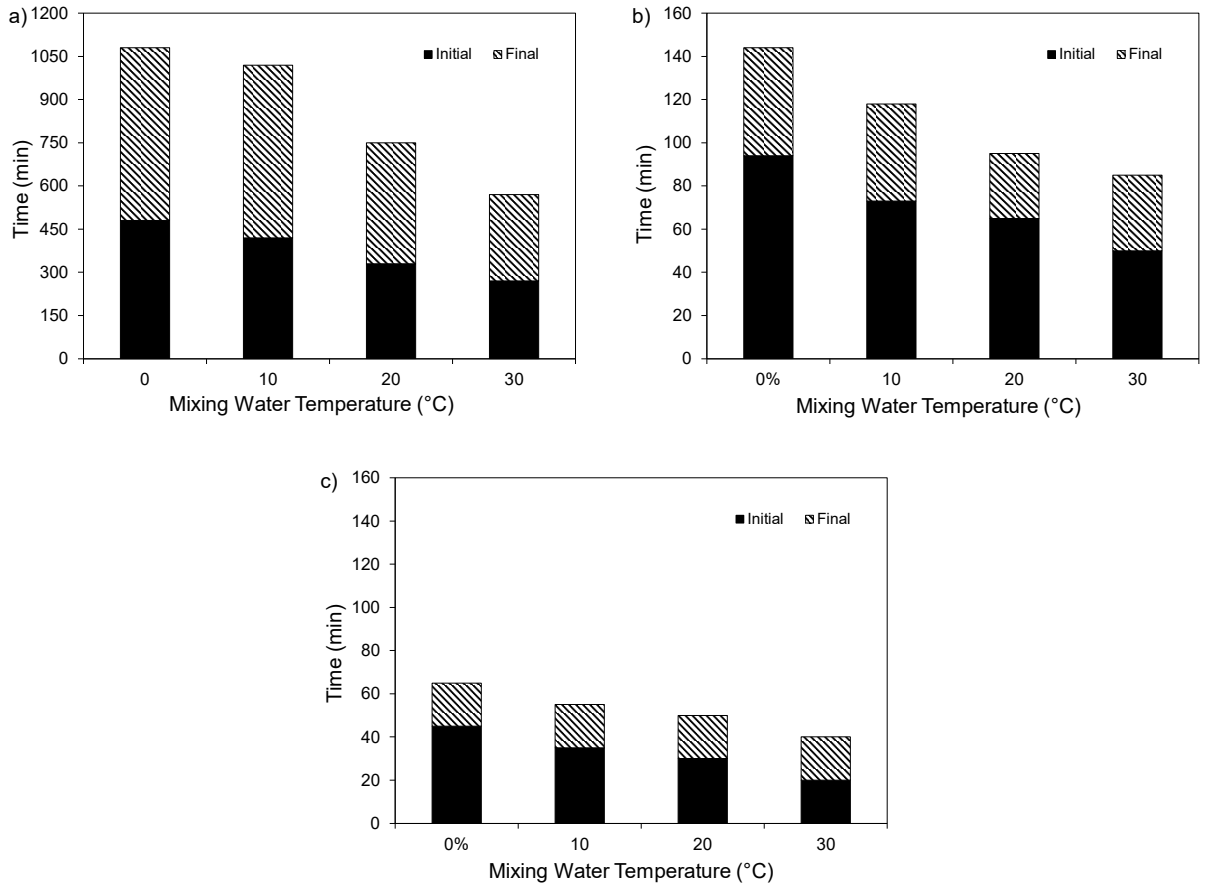

Figure 3-2 Setting time results for AAS prepared by different mixing water temperatures and activator dosages of a) 6%, b) 8%, and c)10%.

3.4.1.3 Heat Flow Profile

Monitoring the heat flow changes during alkali-activation reactions is a useful way to distinguish differences induced by varying mixing water temperature. Both the magnitude and duration of heat release will indicate the hydration progress and formation of reaction products that will directly be related to different properties development. In the following section, the heat profiles for three testing conditions were evaluated: a) Pre-wetting for solids ingredients, b) semi-adiabatic condition, and c) ambient condition.

a) Pre-wetting for solids ingredients and dissolution heat

In cement-based materials, a very high exothermic peak took place once the cement surface gets in contact with water, and anhydrous phases start to dissolute [92]. For conventional Two-Part alkali-activated materials, the precursor starts to dissolute once getting in contact with the activator solution (i.e., high pH) due to the availability of soluble silica and alkali ions [93]. This is expected to differ in the case of one-part alkali-activated materials as the precursor, and solid activators get simultaneously in contact with water. The solid activator starts to dissolute first, releasing alkali and silicon ions in the system. Once enough alkali ions are in the system, the precursor starts to dissolve [94]. The higher the alkalinity, the higher the dissolution rate of the precursor. The dissolution rate (D_r) can be expressed using the Noyes-Whitney equation (**Eq.3.1**):

$$D_r = A\frac{D}{d}\,(C_s - C_b) \qquad \textbf{Eq. 3.1}$$

Where; A is the surface area of the solute particles, D is the diffusion coefficient, d is the thickness of the concentration gradient, C_s saturation concentration of solute in solvent, C_b is the concentration in the bulk solvent. For the same solute, at the same concentration, the dissolution rate will be directly proportioned to the diffusion coefficient (D), which depends on the solvent temperature according to the Stokes-Einstein equation (**Eq. 3.2**):

$$D = \frac{kT}{6\pi\eta r} \qquad \textbf{Eq. 3.2}$$

Where k is Boltzmann constant, T is the absolute temperature, η is the viscosity of the solvent and r radius of the solute molecule. Hence, as the solvent temperature increases, the diffusion coefficient increases, and consequently, the dissolution rate will increase. Therefore, the initial attempt of this study had focused on understanding the effect of mixing water temperatures on the dissolution of the solid activator.

Figure 3.3 shows the heat generated once activator mixed with water with various temperatures (i.e., 0°C, 10°C, 20°C, and 30°C). Generally, the temperatures for mixtures prepared by cold water decreased then increased until reaching a plateau, for instance, as the activator (i.e., which had a temperature around 20°C) mixed with 0°C water, the temperature of the mixture (i.e., solution) dropped to 3°C, then it started to increase after that. This indicates that at the initial wetting point, the low temperature of the mixing water had dominated the temperature changes of the system. However, as the activator dissolution started, which is an exothermic reaction (i.e., generates heat), it dominated the temperature profile taking it up to around 20°C. The colder the mixing water, the lower the measured temperature.

Conversely, the temperature for mixtures mixed with warmer water immediately increased until reaching a plateau, as the exothermic heat is added up. The mixture temperature remained constant at various levels based on the initial mixing water temperatures after that. For instance, the initial temperatures were reached 22°C and 43°C for mixtures prepared with 0°C and 30°C water, then remained almost constant until the end of the investigated period. These changes in the temperature profile are attributed to the dissolution of the solid activator and the effects of mixing water temperatures.

For the used anhydrous meta-silicate, the dissolution enthalpy will be the sum of three energy components: i) energy needed to break the lattice structure of the solid activator (i.e., solute) which is an endothermic process, ii) energy required to break the water (i.e., solvent) lattice structure, which is also an endothermic process, and iii) energy due to the anhydrous meta-silicate attraction water molecules forming solvent-solute bonds [39]. Generally, the sum of the three components can be done following the Gibbs free energy equation (**Eq. 3.3**). Changes in Gibb's free energy

(ΔG) will depend on the changes in the enthalpy (ΔH) and entropy(ΔS) for each step of the dissolution process. Also, the temperature (T) will have a significant rule in controlling the ΔG value, as shown in **Eq. 3.3**.

$$\Delta G = \Delta H - T\Delta S \qquad \textbf{Eq. 3.3}$$

Generally, negative ΔG is required; hence, the dissolution process will be "thermodynamically favorable." This will be controlled by the nature of the process, which can be either exothermic or endothermic. For exothermic reactions, heat energy is released as a result of solute dissolving in the solvent, which increases the system temperature. According to Le Chatelier's Principle, the system will balance this increase in temperature by inhibiting the dissolution reaction to reduce heat energy contribution. Hence, the solubility of the solid activator will decrease. Conversely, in endothermic reactions, the system will promote more dissolution, to absorb the heat energy partially, leading to higher solubility [95].

Anhydrous meta-silicate has an enthalpy of solution around (-31.17 KJ/mol) [96]. Hence, the dissolution of anhydrous meta-silicate is an exothermal reaction (i.e., energy released from making bonds (iii) is higher than that used in breaking bonds ((i)+(ii)). Simultaneously, water needs around 4,186 Joule/kg to change its temperature by one degree [97]. Hence, once meta-silicate comes in contact with cold water, there will be a tendency towards thermal equilibrium. The heat liberated due to activator dissolution is consumed to raise the system temperature. Conversely, in the case of warm water, the liberated heat is added-up to the system resulting in a higher temperature. As shown in (**Fig. 3.3)**, the final system temperature was directly proportional to the initial mixing water temperature. Each 10°C difference in initial mixing water temperature-induced about 7°C difference in the final solution temperature.

On the other hand, at the same activator dosage, changing the mixing water temperature had the same effect when slag was added to mixtures, as shown in (**Fig. 3.3b)**. Generally, in the first stage, the heat is mainly released due to activator dissolution in water producing alkali ions. In the second stage, slag starts to dissolute, producing Si, Al, and Ca ions under the high alkaline medium, which is also considered as an exothermic reaction [98]. However, there were no significant differences between the curves for the system of water and meta-silicate with and without slag. This indicates that the reaction progress was still in the first stage, and the alkalinity for the pore solution did not increase enough to initiate slag dissolution [99]. This agreed with the recent study by [100], indicating a high energy barrier for hydration reaction for slag and water. During the first hrs, the dissolution of the sodium meta-silicate activator was dominating the chemical composition. Also, the temperatures for all mixtures remained constant at various temperature levels, similar to those for water and activator solutions. This indicates that the mixing water temperatures and dissolution of the solid activator were the dominating factors during that very early-stage. Generally, slag particles start to dissolute partially upon contact with an alkaline solution. The minimum pH for the solution to effectively activate slag is not yet defined. However, at least a pH of 11.7 (i.e., equivalent to the pH of slag-water suspension reacting very slowly) is required [86]. Hence, the pH values were measured for solutions of the activator and water with different temperatures. At the end of the early-stage, the pH values ranged between 12.13± 0.2 to 12.56 ± 0.2. This slight pH increase above 11.7 indicated the very low reactivity of slag, which confirms its low contribution to the heat flow at this stage.

Figure 3.4 illustrates the effect of the activator dosage on the system temperature. For the same activator dosage, the mixture temperature is linearly proportionated with the mixing water temperature for the first 60 seconds from the time of the ingredients contact with water. The higher

the activator dosage, the higher the mixture temperature. This is expected as at higher activator dosages; more sodium meta-silicate will be available to dissolute generating more heat.

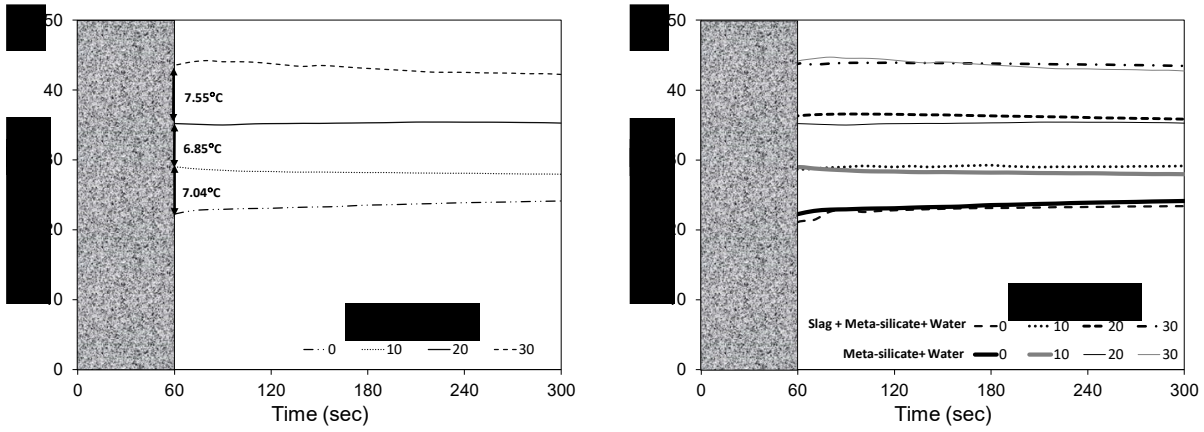

Figure 3-3 Wetting point heat generation, a) the contact between sodium meta-silicate and water, b) the contact between slag, sodium meta-silicate, and water.

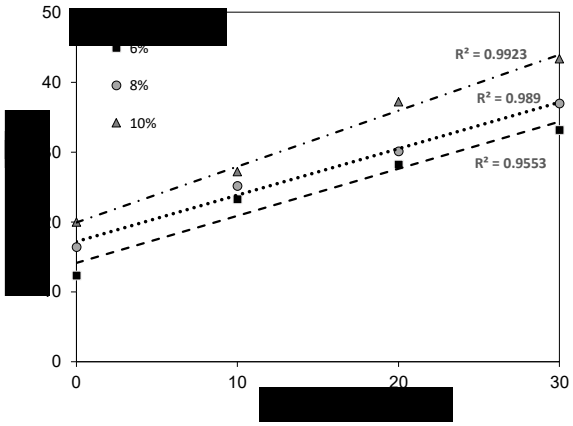

Figure 3-4 Effect of activator dosage one the system temperature.

b) The heat of hydration under the semi-adiabatic condition

Figure 3.5 illustrates the temperature profiles for various specimens under a semi-adiabatic condition. This test is dedicated to capturing the effect of mixing water temperatures on the heat evolution in the second stage, during which slag starts to dissolve. Generally, after the initial temperature peak, which was not captured in this test, the temperature goes through a dormant

period followed by a temperature peak [101]. As shown in the curves (**Fig. 3.5**), the initial temperature differed from one mixture to another based on the mixing water temperature and used activator dosage. The higher the mixing water temperature and activator dosage, the higher the initial mixture temperatures. For example, for mixtures prepared by 0°C and 30°C water, the initial temperatures were 12.4°C and 20.2°C for 6% activator, and 33.2°C and 43.3°C for 10% activator, respectively. This is mainly ascribed to the combined effect of the mixing water temperature and the increase in activator dosage (i.e., the heat liberated), as explained earlier.

Moreover, the lower the mixing water temperature, the longer the dormant period. For instance, for 6% activator, the dormant period for mixtures mixed with 0°C water was extended up to 23.6 hrs, while for mixtures mixed with 30°C water, it ended around 9.7 hrs. All tested mixtures with different activator dosages exhibited similar trends. This also complies with the flowability and setting time results.

For the same mixing water temperature, the higher the activator dosage, the shorter the dormant period, and the higher the temperature peak. For example, for mixture prepared by 0°C water, the dormant periods were 23.6 and 3.03 hrs for mixtures mixed with 6% and 10% activator, respectively. The influence of activator dosage on the temperature peak can be illustrated for mixtures mixed with 10°C water as temperature peak value increased from 50.18°C to 75.06°C as activator dosage increased from 6% to 10%. These observations can be attributed to the effects of water temperature and activator dosage on the rate of slag dissolution. Generally, the hydration of sodium silicate-activated slag is relatively slow. However, increasing temperature will advance and accelerate the hydration process of slag by improving solubility and diffusivity [99].

Moreover, increasing activator dosage resulted in the rapid dissolution of the slag precursor and the formation of various reaction products [102].

One more interesting finding is related to the increase in the mixture temperature after the induction period and up to the second peak. All mixture with the same activator dosage exhibited almost the same changes in the temperature profile regardless of the mixing water temperature. Moreover, the higher the activator dosage, the higher the difference in temperature. For instance, mixtures with a 6% activator exhibited around 25°C difference in temperature (**Fig. 3.6**), while mixtures with 8% and 10% activators exhibited around 33°C and 39°C, respectively. By referring all heat profiles to 0 ºC as a datum, the effect of mixing water temperature would mainly affect the heat profile by shifting the maximum peak location. In conclusion, the mixing water temperature role will be mainly as a regulator for the speed of hydration. Increasing the mixing water temperature will accelerate the hydration process while reducing water temperature will retard the hydration process [91]. This can be due to the effect of water temperature on the dissolution rates of activator and slag, as explained earlier. These findings were confirmed with compressive strength, as will be discussed in the next section.

c) Heat liberation under ambient condition.

Figure 3.7 shows the temperature profiles for the first 48 hrs for fresh specimens stored at the laboratory temperature after casting. All mixtures exhibited a similar heat profile, starting with an initial sudden change in the temperature followed by a dormant period and a strong peak. Mixing water temperatures controlled the initial temperatures for all mixtures. The colder the mixing water temperature, the lower the mixture's initial temperature, and vice versa. For instance, mixtures activated by 6%, using 0°C and 10°C mixing water temperatures reduced the initial mixture

temperatures to about 75% and 40% of that for mixture prepared with 20°C water, respectively. Conversely, in the case of mixing with warm water, the enthalpy of activator dissolution had

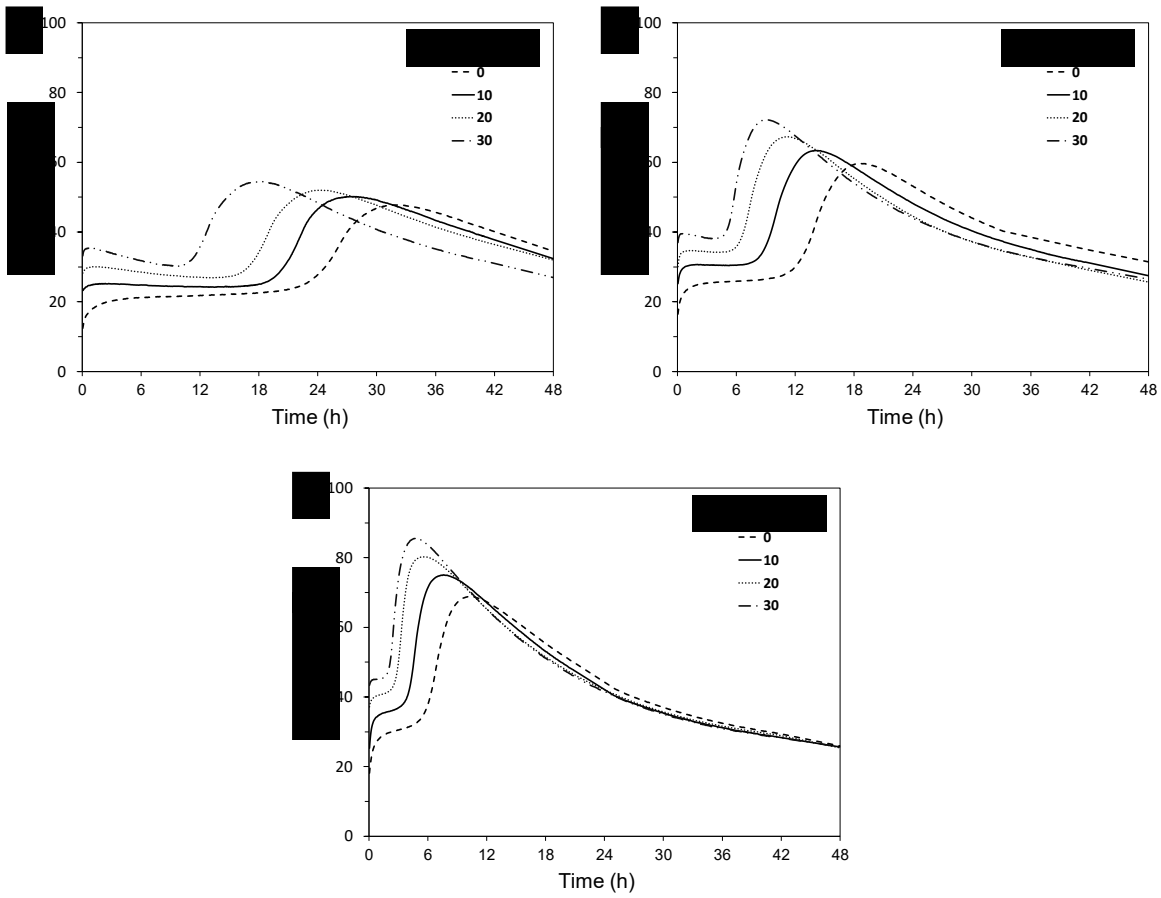

Figure 3-5 AAS heat of hydration for various mixing water temperatures and different activator dosages of a) 6 %, b) 8 %, and c) 10%.

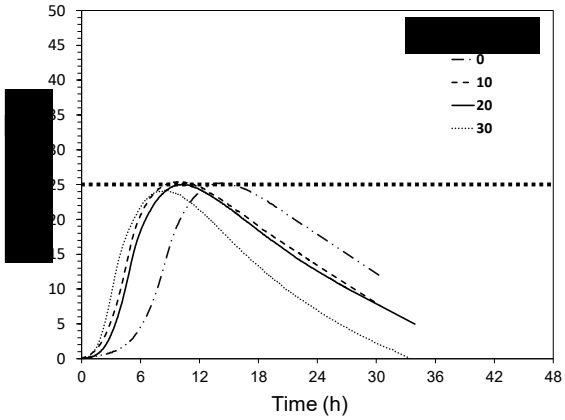

Figure 3-6 Differences in temperature for the hydration second peak for various mixtures

added on to the system temperature, leading to a higher initial peak. These initial peaks also increased as the activator dosages increased. For instance, mixing by 30°C water, the initial peak for 10% activator mixtures was about 28% higher than that of 6% activator mixtures. This can be attributed to the increase in alkalinity, resulting in a higher slag dissolution and hydration progress forming new products [103]. This can also explain the reduction in the dormant period as the activator dosages increased. Mixtures mixed with 10°C water temperature showed a shortening in the dormant period from 17 hrs to 6 hrs as the activator dosage increased from 6% to 10%.

Similar to the heat profile under semi-adiabatic condition, all mixtures with the same activator dosage showed the same increase in temperature regardless of the mixing water temperature. For instance, for mixtures with an 8% activator, the increase in the temperature at the second peak was around 6 ±0.5 °C regardless of the initial mixing water temperature. This is complying with the previous findings (**Fig. 3.6**). Also, the location for the second peak did not follow a trend. However, it seems that the peak for mixtures mixed by cold water took place slightly earlier than those mixtures by warmer water. For instance, at 10% activator, the second peaks for mixtures mixed

with 0°C and 10°C water took place after 13.1 hrs, while for mixtures mixed with 30 °C it took place after around 15.8 hrs. The hypotheses for this behavior can be related to the thermodynamic of the dissolution for the used activator.

At the very early, the temperature will be changing over a short period. There will be heat exchange between the specimens and the surrounding lab conditions, as illustrated by (**Fig 3.7)**, where mixtures temperature was evaluated from the time of ingredients contact with water. Mixtures with temperatures lower than ambient temperature will absorb heat to achieve thermal equilibrium, while mixtures with temperatures higher than the ambient temperature will lose heat. This will affect the dissolution rate (**Eq. 3.2**). For instance, at 6% activator, the temperature of mixtures prepared with 0°C water increased by 10°C (i.e. $\Delta T = +10°C$), while the temperature of mixtures prepared with 30°C decreased by 11°C (i.e. $\Delta T = -11°C$). The increase in temperature for mixtures prepared with cold water will increase the dissolution rate and consequently accelerate hydration (**Eq. 3.2**).

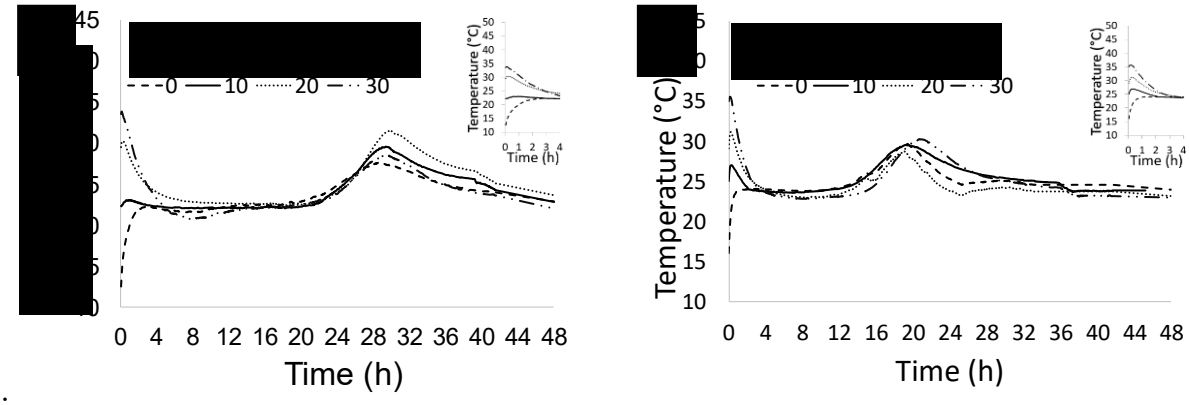

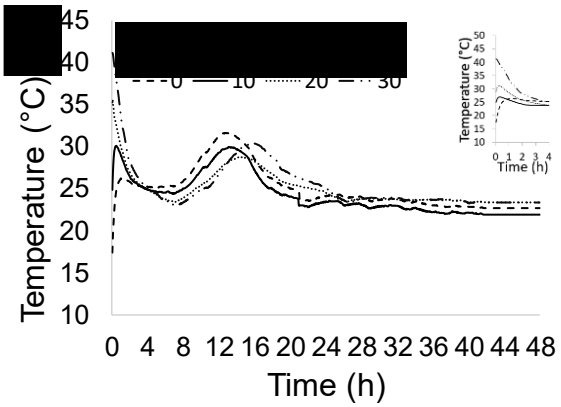

Figure 3-7 AAS activated by sodium meta-silicate heat evolution with different mixing water temperatures and activator dosages of a) 6 %, b) 8 %, and c) 10 %.

Conversely, the reduction in the temperature for mixtures prepared with warm water will decrease the dissolution rate and consequently slow the hydration. This can partially explain the early polymerization peak for mixtures with cold water. These results agreed with the DSC conducted on specimens from mixtures with a 10% activator at age one day, as shown in (**Fig. 3.8)**. Up to 200 °C, the weight loss is corresponding to the dehydration of calcium silicate hydrated phases C-(A)-S-H gel [104], along with the removal of physisorbed free evaporable water in the pore structure [105]. As shown, the peak at point (1) refers to the intensity of the C-S-H endothermic peak grows as the mixing water temperature decreased. This implies that more C-S-H is formed. The weak shoulder at around 220 °C and the broad endothermic peak between 300 and 400 °C is due to the decomposition of hydrotalcite-like phases [106]. The slight increase in the intensity of the hydrotalcite endothermic peak for mixtures with cold water indicates a higher formation of such a phase due to the advance of the hydration reactions [107]. Previous studies showed that early exposing slag to high-temperature results in rapid hydration and formation of a hard reaction shell completely surrounded particles surface [108]. This will delay further hydration. On the other hand, at the same pH, early exposing slag to cold temperature, a large number of intricately

connected network products accumulated on the surface of its particles. This will facilitate the penetration and diffusion of ions into the slag particles allowing further hydration [107]. This also was confirmed with the compressive strength results reported later.

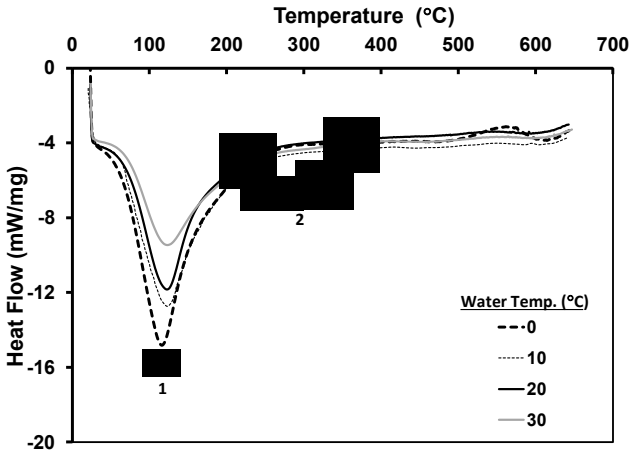

Figure 3-8 DSC for mixtures with 10% activators and different mixing water temperatures at age one day.

3.4.2 Effect of Mixing Water Temperatures on Hardened Properties of AAS Paste

3.4.2.1 Compressive Strength

Figure 3.9 shows strength development for AAS mixtures with various activator dosages and mixing water temperatures. Generally, the compressive strength increased with time for all mixtures. It seems that the mixing water temperature had a higher effect on early-age strength. For example, at activator 10%, the increase in one day strength for mixtures prepared by 0°C water was higher than that prepared by 30°C water. The same trend was found for all other activator dosages. This confirmed the results for the heat of hydration as the temperature peak values were the same as mixing water temperatures changed. Also, it agreed with the DSC results at one day

shown in (**Fig. 3.8)**. However, the strengths at later ages were almost the same regardless of mixing water temperature. For instance, for mixtures with 8% activator, the variation in the 28 days' compressive strength for mixtures mixed with various water temperatures was only ± 2.2 MPa. This indicates the marginal effect of mixing water temperature on the later strength. This also was confirmed by X-ray results, as shown in (**Fig. 3.10)**. At 8% activator, there was no significant difference in the X-ray for mixtures mixed with various water temperatures.

Moreover, the influence of activator dosages on early-age strength (i.e., one and three days) was higher than that at later ages (7 and 28 days), for instance, for mixtures mixed with 0°C water, increasing the activator dosage from 8% to 10% resulted in about 200% increase in the 1-day strength compared to only 2.6% increase in the 28 days strength. This agreed with the shorter induction period in the heat of hydration analysis. The high heat flow induced by increasing the activator dosage improved the slag reactivity, thereby, higher one-day compressive strength than lower activator dosages was achieved [64].

Moreover, for the 1-day strength, the increase in strength as activator dosage increased was higher for mixtures with cold water (i.e., ≤10°C) than those mixtures with warm water. For example, mixtures mixed with 30°C water, the change in strength as activator dosages increased from 8% to 10% was 112% compared with 200% for 0°C water. This can be ascribed to the exothermic nature of the activator and higher solubility, which accelerates the initial polymerization as discussed earlier and in agreement with previous findings and recommendations [64]. Moreover,

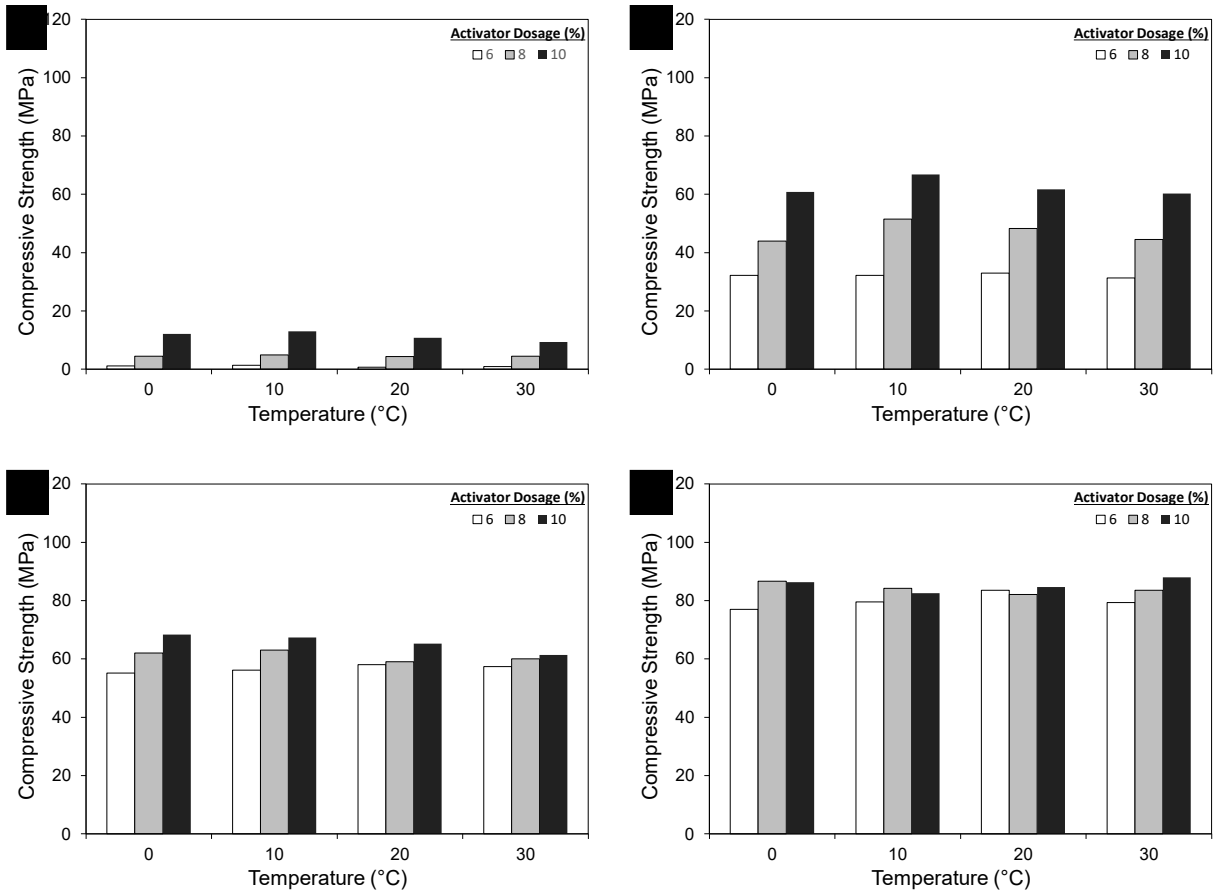

Figure 3-9 Compressive Strength results for AAS activated by 6,8 and 10% activator dosages and various mixing water temperatures at ages a) 1 day, b) 3 days, c) 7 days, and d) 28 days.

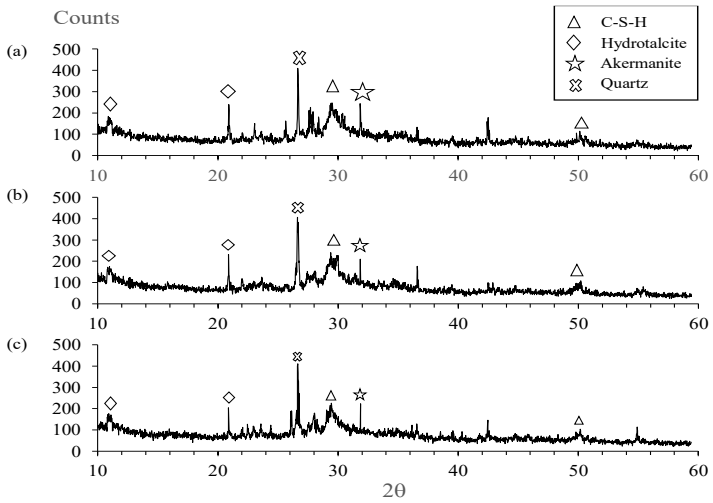

Figure 3-10X-ray results for mixtures with 8% activator mixed with a) 30□C, b) 20□C and c) 0ºC mixing water.

Slag activated by sodium silicate activator is known to hydrate slowly forming denser products with higher later strength. However, increasing the early temperature was reported to accelerated product formation leading to more pores, less density, and lower quality hydration products leading to a lower strength [108].

One interesting point, there were white spots on the broken surfaces for tested specimens, as shown in (**Fig. 3.11)**. These white spots were found to be anhydrous meta-silicate. This could partially explain the similarity in the compressive strength results at later ages (7 and 28 days). At high activator dosage, there are many particles of the activator ready to dissolve. The speed for hydration process for all mixtures will be controlled by two factors: the solubility, which reflects how much solute will ultimately dissolve in the solvent, and the dissolution rate, which is a kinetic process for how quick the solute will reach the solubility. The resultant of these two thermodynamically processes will be dominating the hydration kinetic. At the initial contact with cold water, many activator particles start to dissolute to balance the system, based on Le Chatelier's principle, as explained earlier. As the generated heat from the exothermal dissolution process increased the system temperature to the ambient temperature, the dissolution rate increase gradually. However, due to the availability of many particles to dissolve, it is expected that not all particles will not be fully dissolved. On the other hand, at the initial contact with warm water, fewer activator particles will start to dissolute as the system temperature starts dropping to the ambient temperature, the dissolution rate decrease gradually. Hence, it is also expected that some particles will not be fully dissolved. This confirms the heat of hydration results. Also, the higher the activator dosage, the higher the number of white spots. This is expected as more activator materials are available at high dosages than those at low dosages.

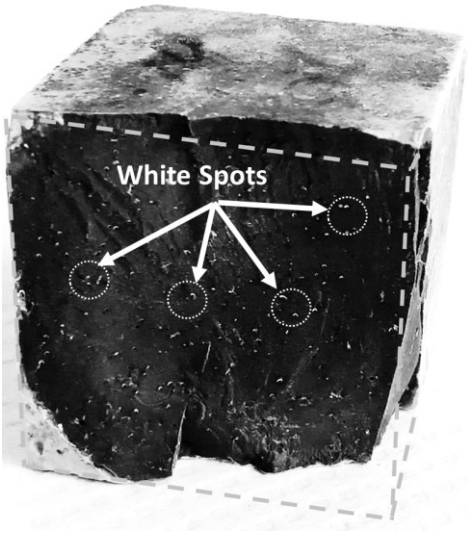

Figure 3-11White meta-silicate spots in 10% AAS samples

3.4.2.2 Early Shrinkage

Early shrinkage has been monitored immediately half an hour after the final setting time for all mixtures. Generally, shrinkage has increased for all mixtures over the investigated period (**Fig. 3.12a**). Mixtures prepared with cold mixing water showed a lower shrinkage compared to that mixed with warm water. The small cross-section of specimens allows fast heat dissipation and reaching equilibrium with the surrounding environment [70]. However, demolding at that early age, specimens' temperatures varied significantly. The temperature for the specimens of mixtures prepared with normal/warm water was obviously high. Hence, the temperature at the medial of a dummy specimen from each mixture was monitored. After about 30 min of demolding, all specimens' temperatures were around the ambient temperature. Considering this moment as a new initial point, the shrinkage deformations are shown in (**Fig. 3.12b)**. It seems that the changes in shrinkage were almost the same for all mixtures regardless of the mixing water temperatures. This highlights the significant role of mixing water temperatures on the early thermal deformation. Coldwater was capable of reducing the differences between specimens' temperatures and their

surroundings. This is anticipated to have a significant effect on the development of early shrinkage restraining stresses and carks formation, which will need further study. A similar trend was found for mixtures with different dosages of activator. However, the lower the activator dosage, the lower was the shrinkage and thermal effect. This reduction in deformation can be attributed to lower reactivity and heat liberation, as shown earlier.

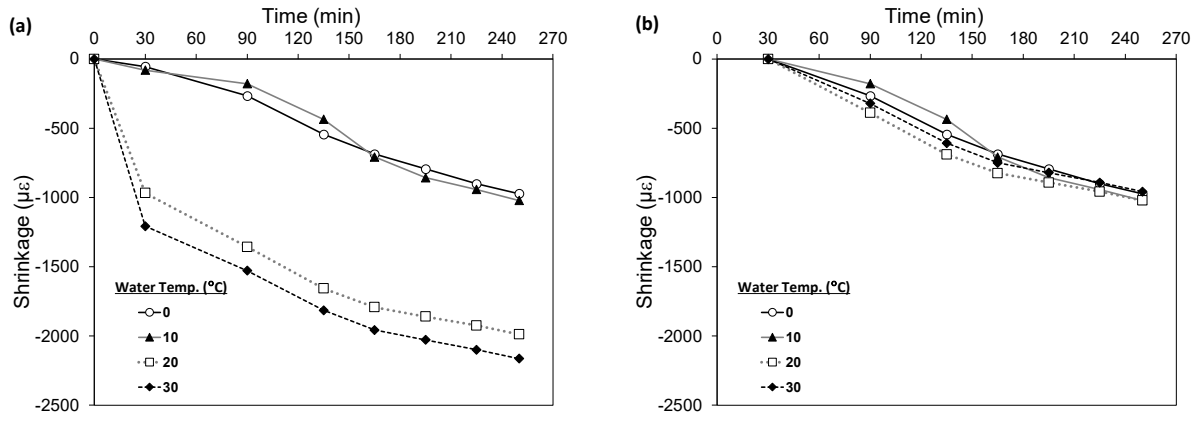

Figure 3-12 Early drying shrinkage for 10% sodium meta-silicate activator

3.5 Conclusion

This study investigated the effect of mixing water temperature on the fresh and hardened properties of one-part alkali-activated slag. Varying mixing water temperature induces thermal effects that affect the solubility and dissolution rate for the solid activator. Hence, the mixing of water temperature can be used to control the speed of the hydration process. The flowability and setting time of AAS were significantly affected by mixing water temperature. Similar to cement-based materials, using cold water can offset thermal deformation during early age. This paves the way for broader implementations of AAS in hot weather concreting. On the other hand, using cold water has been proved to be a useful technique to extend the slump-life while maintained strength

development, based on the high early strength results obtained and maintaining the fresh properties using this technique, AAS would be potentially a sustainable solution for Ready-Mixed concrete and precast concrete applications.

CHAPTER FOUR

EFFECT OF MIXING TIME ON AAS PASTE PROPERTIES

Agitating concrete mixtures is an essential practice for several concrete applications. Ready-Mixed concrete is the leading application required agitation, especially during concrete delivery. ASTM C94 “Standard Specification for Ready-Mixed Concrete” was allocated for equipment's testing to ensure the uniformity of concrete during the agitating process. This chapter investigates the effect of mixing time AAS mixtures. Three different mixing regimes have assigned: 1) initial mixing for a short period, 2) discontinues mixing, 3) continuous mixing. The study shows a positive impact of mixture agitating on fresh and mechanical properties.

4.1 Introduction

One-part alkali-activated Slag is produced by mixing granulated blast-furnace slag, powder activator, and water. However, the use of mortar and concrete made with this AAS is limited by two issues. Initially, the shrinkage which reaches six times that of the respective cement system. Also, the poor rheology for AAS and very fast setting result in on-site casting problems. Many studies showed that using stable fibers under the alkali environment and using shrinkage reducing admixtures can pointedly solve the shrinkage issue. The possibility of using chemical admixtures to extend setting times and maintain adequate flowability for AAS has also been investigated. However, other researchers had shown that varying the mixing time for two-parts AAS could

effectively extend the setting time. The longer the mixing time, the longer the setting time. This was ascribed to the breakage of calcium-silicate hydrated flocs. To date, however, nothing is known about the effect of this increase in mixing time on One-part alkali-activated slag. Consequently, the aim of this chapter was to explore the effect of increasing mixing time on the mechanical properties and drying shrinkage of one-part AAS as well as on the hydration kinetics [55,56].

4.2 Experimental Program

4.2.1 Materials

For all mixtures, granulated blast furnace slag (hereafter referred to as slag) with specific gravity 2920 kg/m^3, and Blaine fineness 515 m^2/kg and d_{50} value around 14.5 μm and basicity coefficient 1.06 was used as the precursor material. The chemical compositions of the used OPC and slag are summarized in **Table 4.1**. Anhydrous sodium meta-silicate was used as a powder activator. The chemical and physical properties of used activators are shown in **Table 4.2**. Three different activator dosages of 6%, 8%, and 10% by weight of slag were used. For all mixtures, a constant liquid-to-solid ratio (l/s) = 0.40 was used.

Table 4-1 Chemical and physical properties of cement

		OPC	GBFS
SiO_2	(%)	19.80	36.50
Al_2O_3	(%)	4.90	10.20
CaO	(%)	62.30	37.60
Fe_2O_3	(%)	2.30	0.50
SO_3	(%)	3.70	3.10
Na_2O	(%)	0.34	0.30
MgO	(%)	2.80	11.80

Table 4-2 Chemical and physical properties of Anhydrous sodium meta-silicate [84]

Property	**W_t % Na_2O**	**W_t % SiO_2**	**W_t % H_2O**	**Density (g/cm^3)**	**Particle Size**	**Melting Point (°C)**	**The heat of solution (kJ/mol)**
Typical Data	50.5	46.2	<3	1.09	93% in 20 to 65 mesh	1088	-31.7

4.2.2 Mixtures Preparation and Testing Procedure

All mixtures were prepared and tested under the laboratory ambient condition (i.e., temperature (T) =23 ± 2°C and relative humidity (RH) = 45 ± 5%) using an electrically driven mixer under-speed 139 RPM complying. Initially, slag and powder anhydrous sodium meta-silicate activator were dry mixed for 1 minute. Then, mixing water was gradually added while mixing continued for about 2 min. Three mixing regimes, as shown in (**Fig 4.1)**, were applied: 1) Mixing initially

for 3 minutes and rest for the whole testing period **R1**, 2) Dis-continues mixing for 8 minutes during the testing period **R2**, 3) Continues mixing for 8 minutes **R3**.

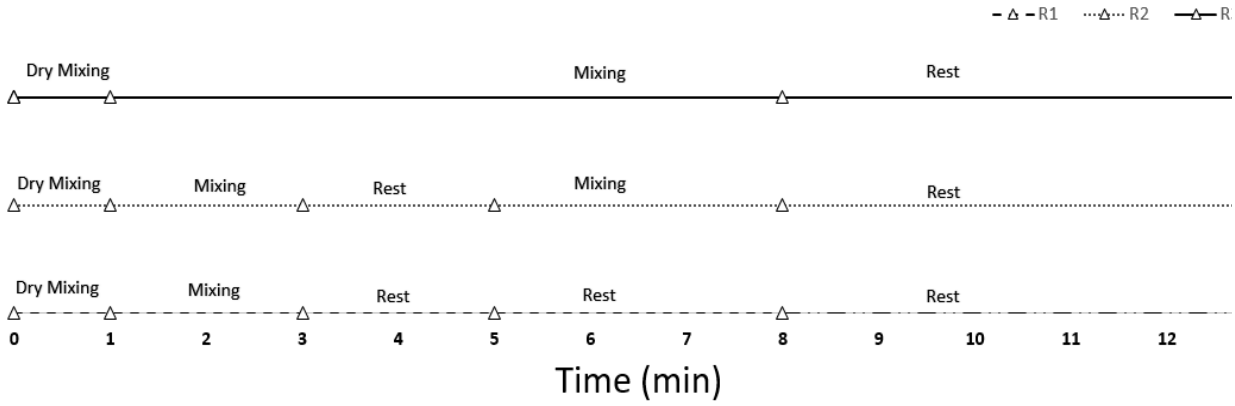

Figure 4-1 The three mixing regimes

For the setting time, samples were prepared and tested using a Vicat needle according to ASTM C191-19 "Standard test method for time of setting of hydraulic cement by Vicat needle" at the end of the final mixing of each regime. Flowability was evaluated in accordance with ASTM C143 (Standard Test Method for Slump of Hydraulic-Cement Concrete) at the assigned testing times (**Fig 4.1)**. After removing the filled mini-cone, the final spread diameter (D_f) of the fresh paste sample was taken as an average of two measurements made in two perpendicular directions. Cubic specimens 50 mm were prepared at the end of each remixing regime to evaluate the compressive strengths at ages 1, 3, and 7days following the ASTM C 109-20 "Standard Test Method for Compressive Strength of Hydraulic Cement Mortars (Using 2-in. Or [50-mm] Cube Specimens". After 24 hrs., specimens were demolded and stored inside a plastic bag at laboratory ambient temperature until the time of testing.

For the heat of hydration, semi-adiabatic calorimetry studies were conducted on specimens during the first 48 hrs of hydration using a custom-built experimental setup. Specimens were prepared and cast into cylinder molds with a diameter of 75 and a height of 150 mm directly at the last mixing time of each mixing regime. The mold was immediately placed in a micro-porous insulation box. Three Type-T thermocouples were inserted into the center of the concrete volume along its height to monitor its temperature. Temperature readings were recorded continuously using a data acquisition system. Replicate specimens indicated a standard deviation of 1.8°C for the maximum specimen temperature. Moreover, another set of the same cylinder specimens was stored under ambient conditions and monitored to capture the heat profile.

4.3 Results and Discussion

4.3.1 Effect of Mixing Time on Fresh Properties of AAS Paste

4.3.1.1 Mini-Slump Results

Figure 4.2 illustrates the measured slump-loss over time for mixtures mixed by different mixing regimes with OPC, and AAS activated by three different dosages, 6%, 8%, and 10%. Generally, the mixing regime has a significant effect on slump loss regardless of cement type or activator dosages, continuous mixing (R3) exhibits the least slump loss followed by the discontinuous regime (R2), this is the consequence of the continuous break of the early formed C-S-H in the OPC and C-A-S-H networks [55,56]. The effect of the mixing regime was more significant with AAS. For an instant, at activator dosage, 10%, slump decreased from 170 mm to 100 mm for the continuous mixing regime while slump was maintained 170 mm for the OPC. Moreover, the effect of activator dosage was tangible, the higher the activator dosage, the more slump loss regardless

to mixing regime, for example, 40% was the slump loss for the mixture activated by 10% dosage comparing to the mixture activated by 6% mixed continually (R3), this is attributed to the higher reaction kinetics, which speeds up the formation of hydration gel [110,111].

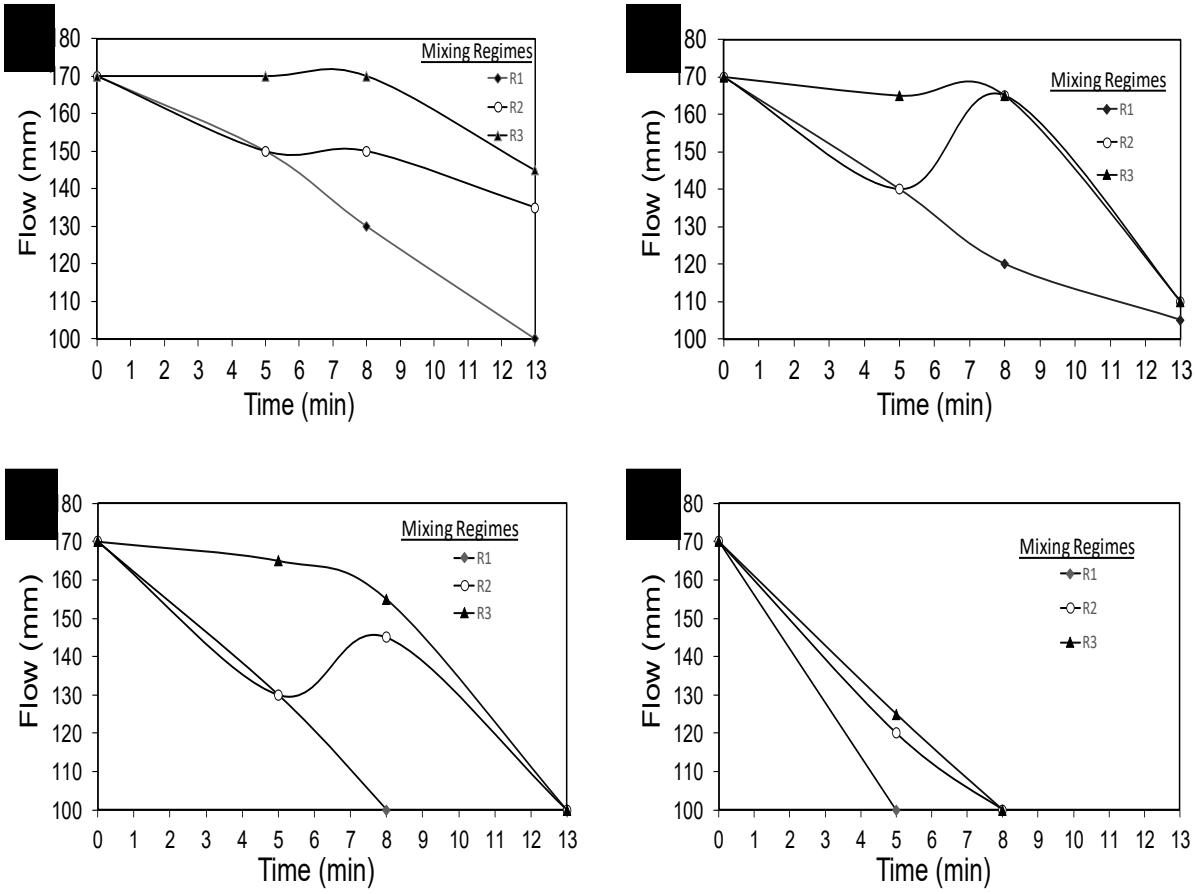

Figure 4-2 Flow results for OPC and AAS prepared by different mixing regimes and activator dosages of a) OPC, b) 6%, and c) 8%, d) 10%

4.3.1.2 Setting Time

Figure 4.3 illustrates the effect of different mixing regimes on the initial and final setting times. Regardless of activator dosage, discontinuous and continuous mixing regimes had significantly extended the setting time, respectively. For an instant, 380 minutes was the increase of setting time between mixing regime one and two for the AAS activated by 8%. Despite increasing activator

dosage reduces the setting time, discontinuous mixing and continuous mixing exhibited a tangible increase of setting time at each activator dosage, this is attributed to the same reason mentioned earlier, prolonged mixing breaks up the hydration products formation [55,56]. It was observed that the effect of the mixing procedure was more noticeable in the initial setting time for the higher activator dosage. For the OPC mixtures, the effect of the three mixing regimes was almost negligible.

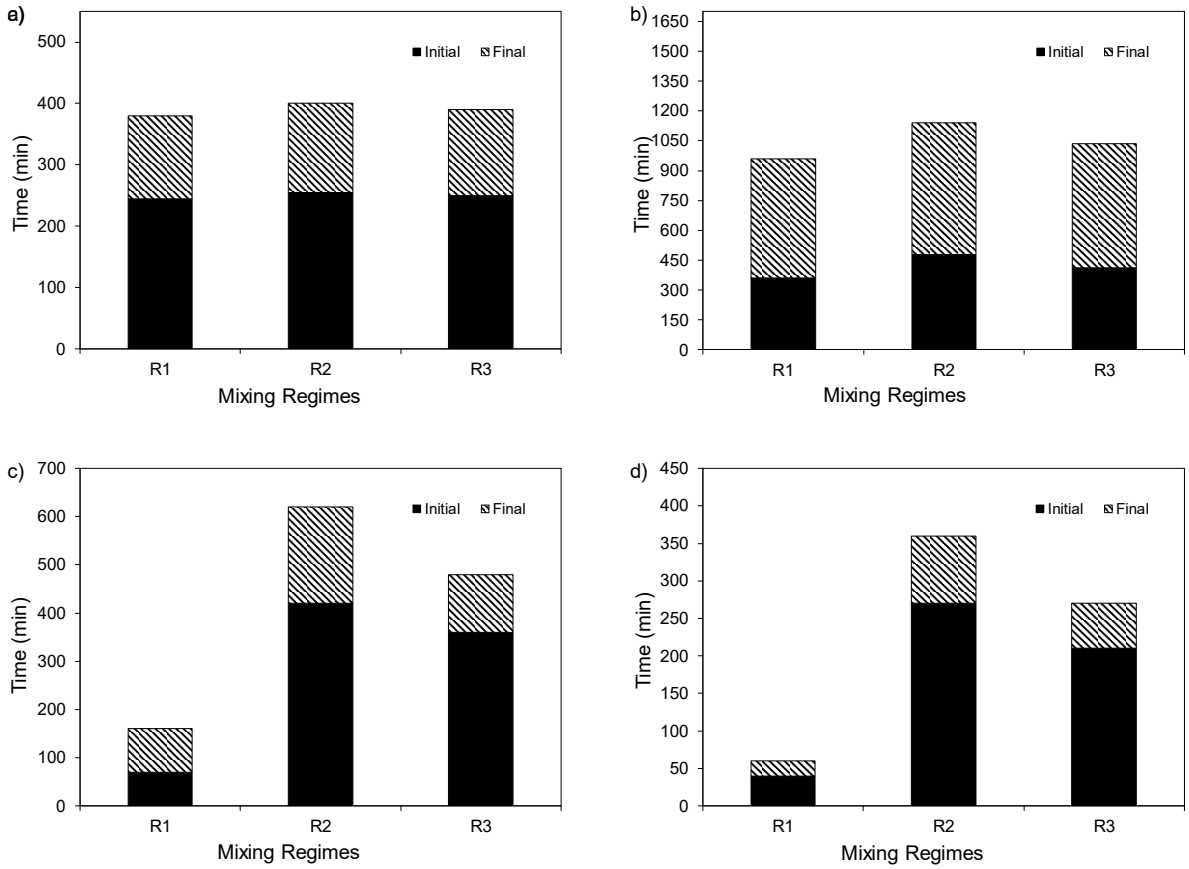

Figure 4-3 Setting time results for OPC and AAS prepared by different mixing regimes and activator dosages, a) OPC, b) 6%, and c) 8%, d) 10%

4.3.1.3 Heat Flow Profile

Monitoring the heat flow changes during alkali-activation reactions is a useful way to distinguish differences between the three mixing regimes. Both the magnitude and duration of heat release will indicate the hydration progress and formation of reaction products that will directly be related to different properties development. In the following section, the heat profiles for two testing conditions were evaluated: a) semi-adiabatic condition, and b) ambient condition.

d) The heat of hydration under the semi-adiabatic condition

Figure 4.4 illustrates the temperature profiles for various specimens under a semi-adiabatic condition; this test is dedicated to capturing the effect of mixing different mixing regimes on heat evolution. In general, OPC generated the highest heat of hydration, for the AAS, the higher the activator dosage, the shorter the dormant period, and the higher the temperature peak. Moreover, increasing activator dosage resulted in the rapid dissolution of the slag precursor and the formation of various reaction products [112]. Regardless of cement type or activator dosages, all mixing regimes exhibited the same hydration peak. For example, the OPC mixtures (**Fig 4.4a**) show that short time mixing, discontinuous mixing, and continuous mixing recorded almost 95 ^{o}C for the three mixing regimes at the same time, which indicates the same amount of hydration product formation, this could be attributed to the used speed which was fixed for all mixing regimes [113]. The same pattern was observed for AAS at each activator dosage.

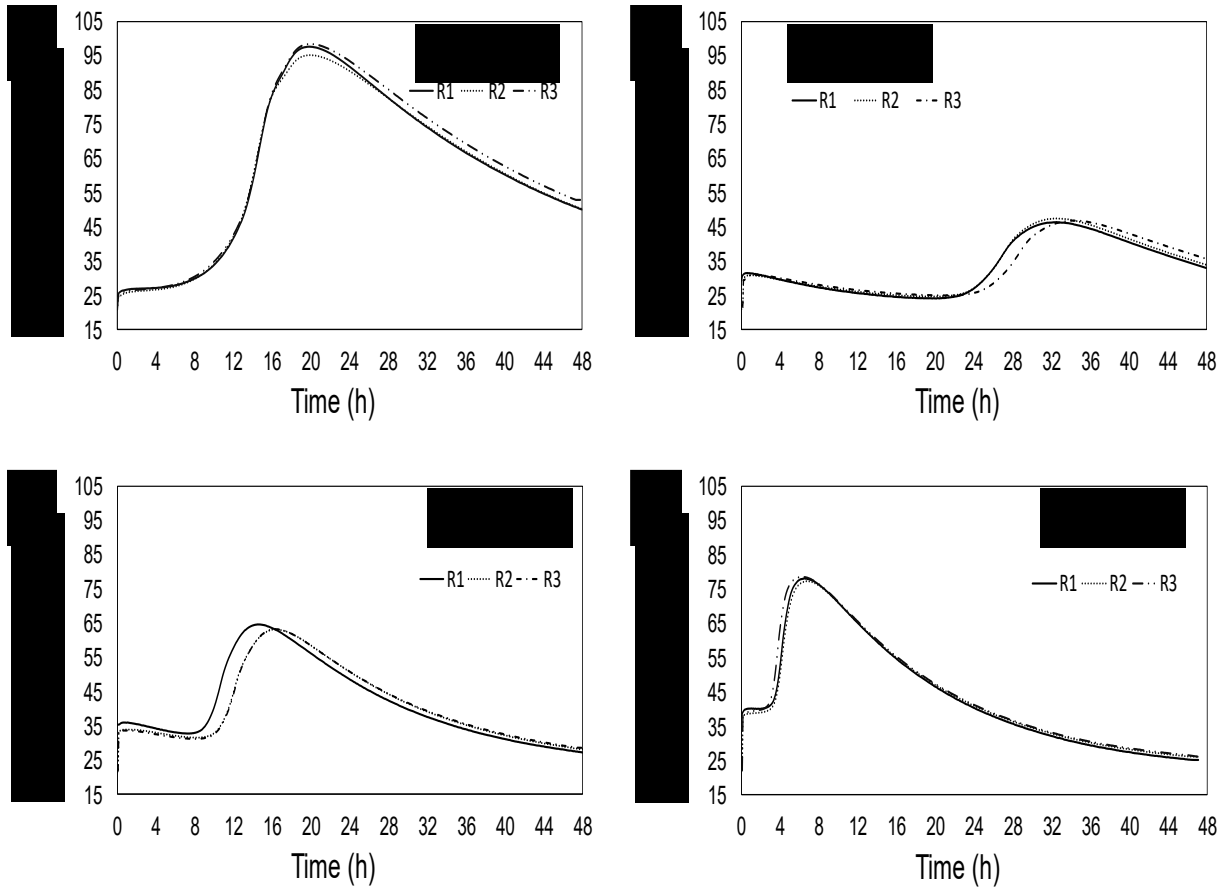

Figure 4-4 OPC and AAS heat of hydration for different mixing regimes and different activator dosages, a) OPC, b) 6%, and c) 8%, d) 10%

a) *Heat liberation under ambient condition*.

Figure 4.5 shows the temperature profiles for the first 48 hrs. for fresh specimens stored at the laboratory temperature after casting. Generally, the OPC mixtures recorded the highest heat generated, followed by the AAS mixtures activated by 10%, 8%, and 6%, respectively. Similar to the heat of hydration results, the higher the activator dosage, the shorter the dormant period, and the higher the temperature peak.

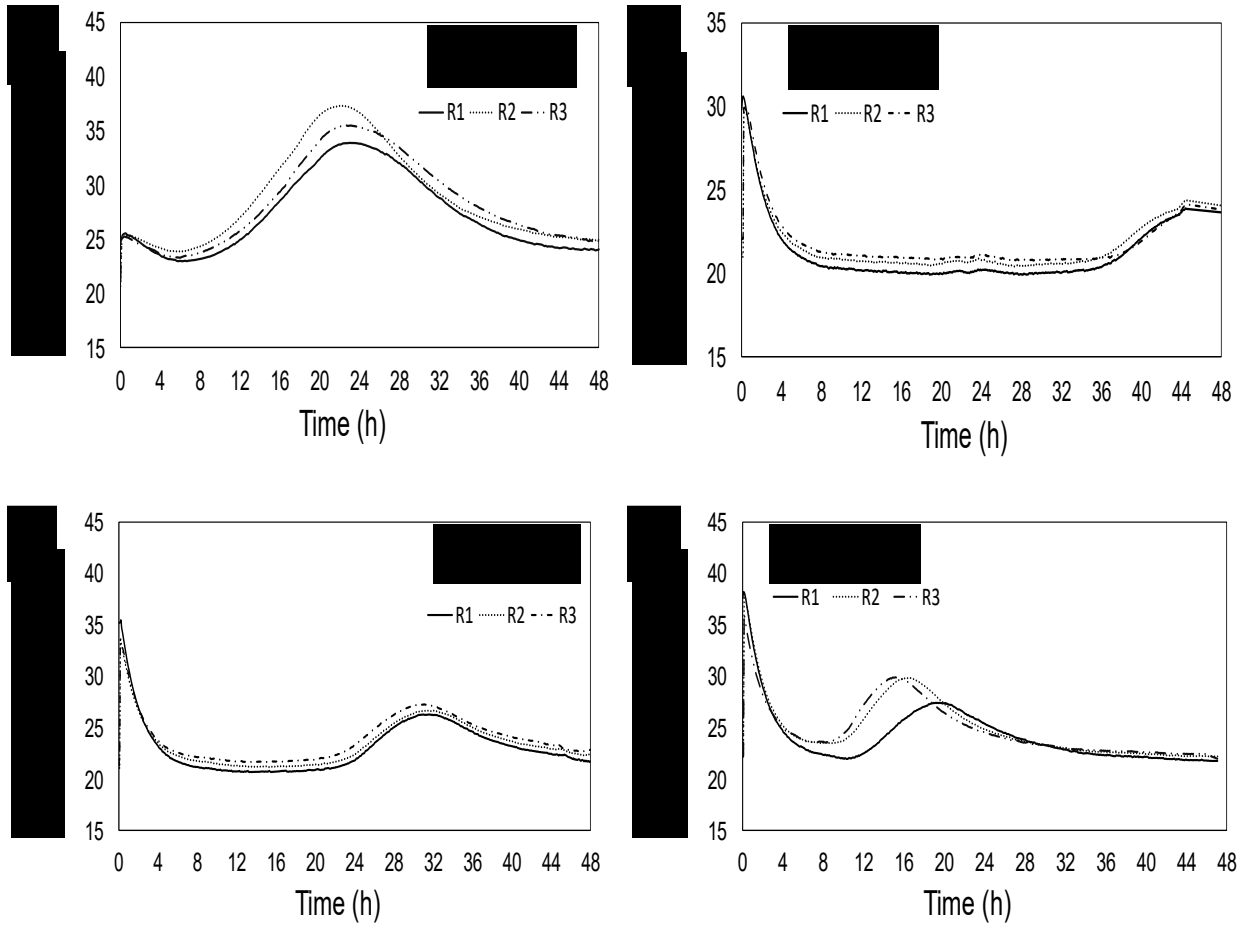

Figure 4-5 OPC and AAS heat evolution for different mixing regimes and different activator dosages, a) OPC, b) 6%, and c) 8%, d) 10%

4.3.2 Effect of Different Mixing Regimes on Hardened Properties

4.3.2.1 *Compressive strength*

Figure 4.6 shows strength development for OPC and AAS mixtures with the three different mixing regimes. Generally, the compressive strength increased with time for all mixtures. It seems that the effect of mixing on the early strength increases with the increase of activator dosages. For an instant, continuous mixing recorded 10 MPa strength increase on one day more than mixing regime one, while negligible increment was recorded for the 8% and 6% dosages. The same pattern was

reported at seven days' strength; the higher activator dosage, the more effect of continuous mixing on AAS mixtures. Referring to a study discussed the continuous mixing of AAS, the prolonged mixing time offers a denser microstructure; this observation was supported by microstructure analysis and porosity test, where the more extended the mixing time resulting in lower porosity value [55]. For the OPC, the results were almost negligible; this unexpected behavior could be attributed to the low speed used in all mixing regimes [113].

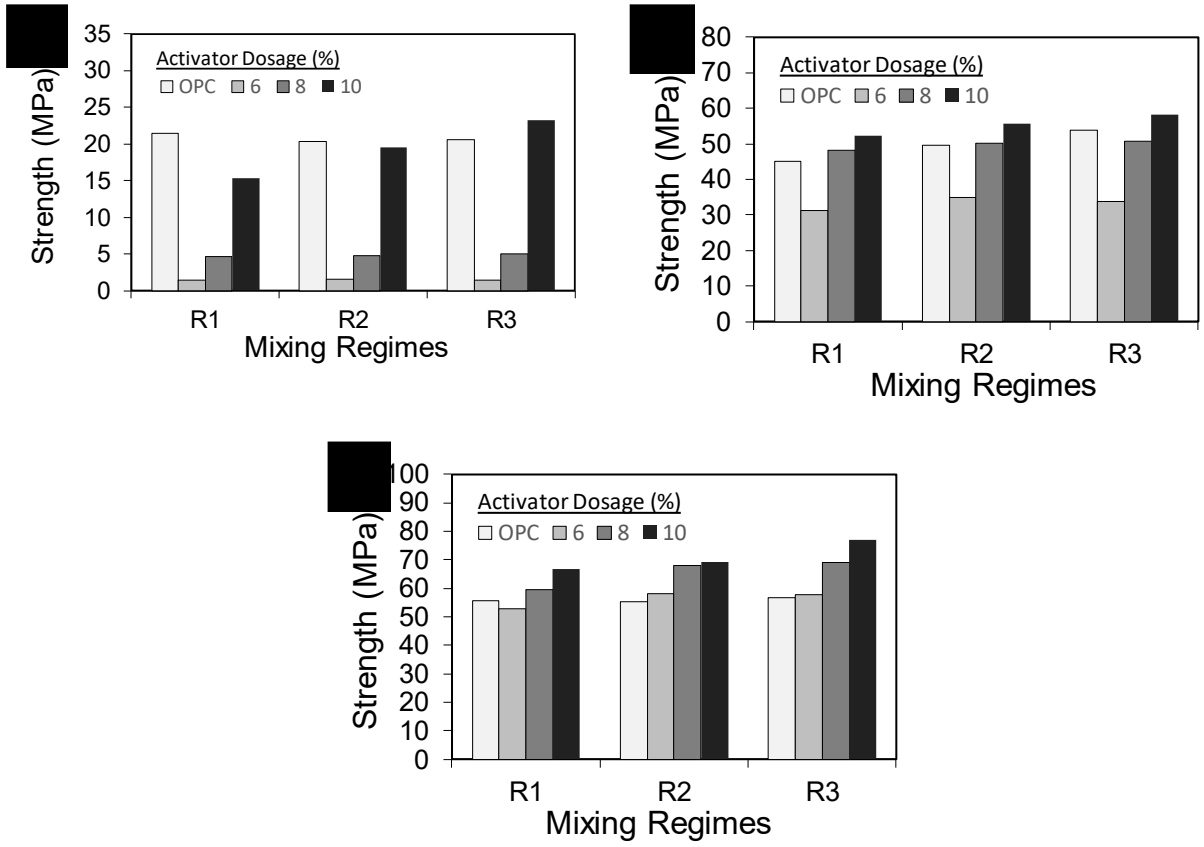

Figure 4-6 Compressive Strength results for OPC and AAS activated by 6,8 and 10% activator dosages different mixing regimes at ages a) 1 day, b) 3 days and c) 7 days

4.4 Conclusion

This chapter investigated the effect of different mixing regimes on AAS comparing to the OPC. Three mixing regimes were studied, mixing for a short period (3 minutes, discontinuous mixing for (8 minutes) and continuous mixing for (8 minutes), it is clear that mixing time effected both fresh and hardened properties. Longer mixing time enhances both fresh and hardened properties of one-part AAS; this could be considered as a technique toward introducing this system for more applications in the future.

CHAPTER FIVE

POTENTIAL UTILIZATION OF LOCAL AVAILABLE WASTE AS A PRECURSORS

This chapter highlights the conducted activities and accomplishments of the potential of using Red Mud and Paper Mill Fly-Ash as precursors for alkali-activated materials. The experimental work was designed to fully characterize the received Red Mud and Paper Fly-Ash from the precursor point of view. This was followed by evaluating the effect of the proposed precursors on alkali-activated materials properties.

5.1 Introduction

Aluminum and wood pulp industries are considered major Canadian economy tributaries [114,115]. From Canada's national resources statistics "NRCAN" In 2018, Canada ranked the 4th Aluminum producers in the world with total revenue of 7.2 B$. Moreover, the Pulp industry made 8.5 B$ of total revenue in 2017. The massive production of Aluminum and wood pulp products generates a vast amount of waste by-products. In the case of aluminum production, NRCAN mentioned that every 2 tons of Aluminum need 4-5 tons of Bauxite Ore, which generates a large amount of Red Mud as a by-product of Bauxite manufacturing operations. On the other hand, wood pulp production produces several by-products, water effluent, sludge, and pulp mill Fly-Ash [116]. This chapter is assigned to examine different practices to reuse and recycle these by-products in construction applications fulfilling the concepts of green building materials and sustainability.

5.2 Benefits to The Industry Business

Understanding the behavior of the different applications that involve the red mud and PPFA under different realistic environmental and mechanical loading conditions, can be pervasive gains to Canada`s Aluminum and Pulping industries, including:

1) Reusing the Red Mud and PPFA will reduce the amount of wastes sent to the waste disposal facilities, which will result in reducing the pollution and environmental disturbance resulting from the disposal operations.
2) Recycling and reusing of Red Mud PPFA in the construction industry will reduce the costs associated with waste management and alleviate its environmental effect while developing sustainable practices and socially responsible industrial production.
3) Conserving non-renewable natural resources and reducing the energy and environmental disturbance, by replacing the Red Mud and PPFA with these valuable resources.

5.3 Study Program and Methodology

This section describes the research program that will be implemented to achieve the stated objectives. The research is divided into three major phases:

1) Characterize of the Red Mud and Paper PPFA.

2) Examine Red Mud and Paper PPFA potentials as construction materials.

3) Potential applications supported with primary results.

5.3.1 Phase 1: Materials Characterization

Various tests were conducted in order to fully characterize the received red mud and PPFA, including their chemical and physical properties, and their interactions with binding materials. Random samples were collected, divided into small quantities, and used in different characterization tests according to recommendations of different construction materials standards. The following tests were conducted:

1) Visual Inspection

Red mud and Paper Mill Fly-Ash samples will be inspected using either or all of raw human senses such as vision, touch and smell, and/or any non-specialized inspection equipment. This test is to give a general idea about the basic features of the red mud and Paper PPFA. Also, it allows identifying the nature of the waste (i.e., pure or combined by other wastes)

2) Physical properties

The behavior of particulate materials is often dominated by the physical properties of the constituent particles. These can influence a wide range of material properties, including, for an instant, how easily ingredients flow, mix, or compressibility. Some of the most important physical properties that will be measured are:

a) Particle Size Distribution

By far, the most important physical property of particulate samples is particle size. Particle size has a direct influence on material properties such as flowability, viscosity, porosity, and packing density. For fine powder residuals, sieve analysis will be conducted according to ASTM C136 (Test Method for Sieve Analysis of Fine and Coarse Aggregates) (**Fig. 5.1**).

Figure 5-1 Sieve analysis test for red mud and PPFA

b) Specific Gravity

Knowledge of specific gravity is necessary for the proper incorporation of Red Mud and PPFA in construction materials mixtures. It represents the ratio between the mass of the particle material and the volume occupied by the individual particles. This volume includes the pores within the particle but does not include voids between the particles. The test will be conducted using pycnometer method according to ASTM C128 "Standard Test Method for Relative Density (Specific Gravity) and Absorption of Fine Aggregate."

c) Bulk density

Bulk density is defined as the ratio of the mass of a given quantity of material and the total volume occupied by it. This volume includes the voids between, as well as the pores within the particles. Bulk density is a function of particle shape, density, size, grading, and moisture content, as well as the method of packing the material (loose or compacted). Bulk density for red mud will be evaluated in a loose and compact form.

d) Water Content

Evaluate the water content according to ASTM D4959-07 "Standard Test Method for Determination of Water (Moisture) Content of Soil By Direct Heating." Water content is

measured by heating the materials in a furnace at 105 °C until it reaches constant weight. The water content is the weight of dry soil over the weight of water loss.

e) Microstructure Analysis

Scanning Electron Microscope (SEM) was conducted on red mud samples to get information about the red mud surface topography along with localized chemical information using the Energy-dispersive X-ray spectroscopy (EDX). SEM uses a focused beam of electrons to produce the image. The particles interact with the surface giving information about the topography of the surface.

3) Chemical properties

Precursor chemical composition plays the primary role in the hydration process and the formation of the hydration product [117]. The richer calcium and aluminosilicate precursors have a higher tendency to create strong bonds and dancer microstructures [118]. pH value is another important factor, especially in the alkali-activated systems, which helps higher dissolution to form the new bonds [119].

a) X-ray fluorescence (XRF)

Major element oxides and some trace elements concentrations in different agro-wastes were determined using X-ray fluorescence (XRF) spectrometry and quantitative XRD with X-ray line profile analysis.

b) Surface pH

In order to determine the surface pH for Red Mud and Paper PPFA, samples were sent to the chemical labs. The Red Mud and PPFA samples were diluted in deionized water and put over a shaker for 30 min. The pH was measured for the water thereafter.

5.3.2 Phase 2: Examine Red Mud and PPFA Potentials

The success of implementing red mud and PPFA in construction applications will mainly depend on how efficiently the properties of these by-products were utilized to achieve adequate performance. These include fresh and mechanical performances. Hence, in this phase, the behavior of different cementitious mixtures (i.e., cement-based and alkali-activated) incorporating Red Mud and PPFA were investigated.

5.3.2.1 Materials

General use (GU) hydraulic cement, according to the CSA-3001-03, was used as the binding material for reference mixtures. Granulated blast furnace slag (GBFS, hereafter referred to as slag) with specific gravity 2920 kg/m^3, and Blaine fineness 515 m^2/kg and an average particle size value around 14.5 μm was used as the precursor material for all alkali-activated mixtures. The basicity coefficient [Kb = (CaO + MgO)/ (SiO_2+ Al_2O_3)] for the used slag was 1.06. **Table 5.1** shows the chemical composition for the used cement and GBFS. The used fine aggregate was natural riverside sand with a fineness modulus of 2.70, according to ASTM C136 (2014), specific gravity and water absorption of 2.51 and 2.73% determined by ASTM C 128 (2015), respectively. The coarse aggregate was siliceous/calcareous aggregates with a maximum size of 20 mm (3/4 inch), the specific gravity of 2.697 kg/m^{3,} and water absorption of 0.6%. Sieve analyses for both fine and coarse aggregates meet ASTM C33 (2018), as illustrated in **Fig. 5.2**. All mortar mixtures were prepared using a binder to a fine aggregate ratio of 1: 2.75.

Table 5-1 Chemical and physical properties of cement

		OPC	GBFS
SiO_2	(%)	19.80	36.50
Al_2O_3	(%)	4.90	10.20
CaO	(%)	62.30	37.60
Fe_2O_3	(%)	2.30	0.50
SO_3	(%)	3.70	3.10
Na_2O	(%)	0.34	0.30
MgO	(%)	2.80	11.80

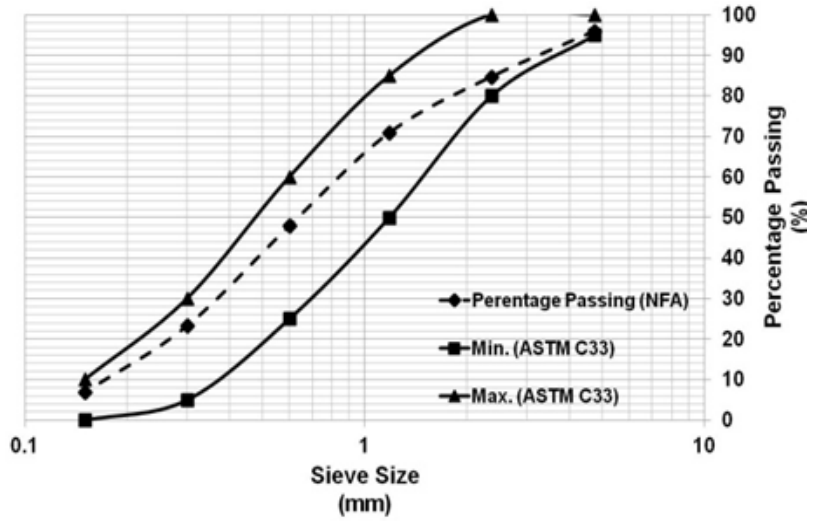

Figure 5-2 Sieve analysis of Fine aggregate.

5.3.2.2 Mixtures Proportions

Mixtures differentiated based on the type of binder and portion of red Mud and PPFA. For Red Mud and OPC mixtures, OPC replaced partially by 0%,10%,20%, and 30% of Red Mad. For Red Mud and GBFS alkali-activated based mixtures, GBFS replaced partially by 0%,25%,50%, of Red Mud. The water/cement ratio of 0.40 was used for all mixtures. Moreover, the alkali-activated based blends had been divided into two subgroups i) activated by meta-silicate, at which red Mud is considered as filler, ii) activated by red Mud only to examine its potential as an activator.

The same procedure was used to evaluate PPFA performance with both systems, For the OPC mixtures, OPC was partially replaced by 0%,10%,20%, and 30% of PPFA, and by 0% and 25% by GBFS in the AAM system.

5.3.2.3 Specimens Preparation

Compressive strength was evaluated on 50 mm cubes at the ages of three and seven days. Immediately after casting, cubes inside molds were stored in double-sealed plastic bags until demolding at 23 ± 1°C. After demolding, specimens were kept in a humid environment (Temperature (T) = 23 ± 1°C and relative humidity (RH) = 85 ± 3%) until the testing age.

5.3.2.4 Testing Procedure

1) Fresh Properties

a) Flowability

Flowability was evaluated for all tested mixtures using the flow table, as shown in **Fig. 5.3**. According to ASTM C230 (Standard Specification for Flow Table for Use in Tests of Hydraulic Cement). The fresh mortar sample was placed in the flow mold on a drop table and stroked for 25 times. Then the diameter of the collapsed mortar was measured at four different locations using the caliper. The flow reading represented the average of the four different readings.

Figure 5-3 Flow table test for flowability evaluation

b) Setting time

Setting time will be measured using the Vicat needle, according to ASTM (C 191-13). In this method, the paste is mixed to normal consistency ten placed in a moist cabinet to set. The penetration test is performed periodically using the 1 mm Vicat needle. The initial setting time is the time between the initial contact between cement and water and the time when the needle penetrates the paste for 25 mm. The final setting time is the time elapsed between the initial contact between the cement and water and the time when the needle does not leave a complete circular impression in the paste surface.

Figure 5-4 Vicat needle apparatus for setting time evaluation

2) Mechanical Properties

a) Strength Activity Index Testing

The strength activity index of red mud will be evaluated following the procedure of ASTM C311, "Standard Test Methods for Sampling and Testing Fly Ash or Natural Pozzolans for Use in Portland-Cement Concrete." In this test, the 7 and 28 days' compressive strengths of mortar cubes with a 20 % mass replacement of cement by red mud and Paper Mill Fly-Ash are compared to those of a control mix without OSTT, at constant flow conditions.

b) Compressive strength

Compressive strength will be determined on 50 mm cube specimens corresponding to ASTM (C109/C109M-13). Three specimens will be used for each mixture at each testing date for each curing condition. The mortar used consists of one-part cement and 2.75 parts of sand proportioned by mass. The mortar mixed at a constant water/cement ratio that obtains a flow

of 110 ± 5 in 25 drops of the flow table. The cubes are cured for one day in the mold then removed from the molds and immersed in lime water until the test.

5.4 Results and Discussion

5.4.1 Phase 1: Materials Characterization

5.4.1.1 Red Mud

1) Visual Inspection

Figure 5.5 shows the Red Mud as received. It had a dark red color with a wet texture and soil odor. After drying the red mud sample was dried inside an oven at temperature 105 C for 24 hrs, the color turned to a lighter red. This indicates that the received sample had relatively high moisture content. Some weight stones were found in the received sample. In addition, wood residuals and organic materials were identified. The received sample had different sizes of particles that were easy to crush them to smaller sizes by hand. The agglomerated particles' sizes ranged from fine powders and up to 11 cm.

Figure 5-5 Different visual aspects for the received Red Mud sample

2) Physical properties

a) Particle Size Distribution

The particle size distribution based on the sieve analysis is shown in **Table 5.2**. It confirms that most around 55% of the received sample had particles less than 4.75 mm, which agrees with size requirements for fine aggregate. In order to overcome agglomeration, a sample was milled with ceramic cylpebs (**Fig. 5.6**). After milling for about 1 hour, more than 92% of the particles had a size of less than 1.00 mm (**Fig. 5.7**).

Table 5-2 Sieve analysis for received Red Mud

Sieve	Weight Retained	Cumulative Weight Retained	Calculation Percent Weight	
			Retained	Passing
¾"	323.0	323.0	11.3	**88.7**
½"	42.2	365.2	12.8	**87.2**
⅜"	175.0	540.2	18.9	**81.1**
#4	703.0	1243.2	43.6	**56.4**
#8	497.0	1740.2	61.0	**39.0**
#16	462.0	2202.2	77.2	**22.8**
#30	0.0	2202.2	77.2	**22.8**
#50	530.0	2732.2	95.8	**4.2**
#100	75.0	2807.2	98.4	**1.6**
Pan	46.0	2853.2	100	**-**

Figure 5-6 Milling the received red mud sample using Rotary Milling Machine

Figure 5-7Red mud sample after milling inside the Rotary Milling Machine.

Specific Gravity

The specific gravity for the milled red mud samples was evaluated on both oven dry and saturated surface dry conditions following the gravimetric procedure. The specific gravity based on oven-dry was 1.78, while based on saturated surface-dry was around 2.20.

b) Bulk density

The bulk density for the milled red mud samples was evaluated for loose and compacted conditions. The bulk density for the loose sample was around 1.1 g/cm3 and 1.24 g/cm3 for the compacted one.

c) Water Content

The moisture content for as received red mud sample was 20.8%.

d) Microstructure Analysis

Figure 5.8 shows the shape of red mud particles at the micro-level. The particles had an irregular shape with a rough surface. The particle seems to be porous and has a high amount of voids. This explains the high absorption rate (i.e., around 23%). Some spots were also examined by EDX, as shown in **Fig. 5.9**. Results indicate that the tested sample is rich in iron, alumina, Titanium, and calcium, as mentioned in several studies about Red Mud chemical and physical properties [120].

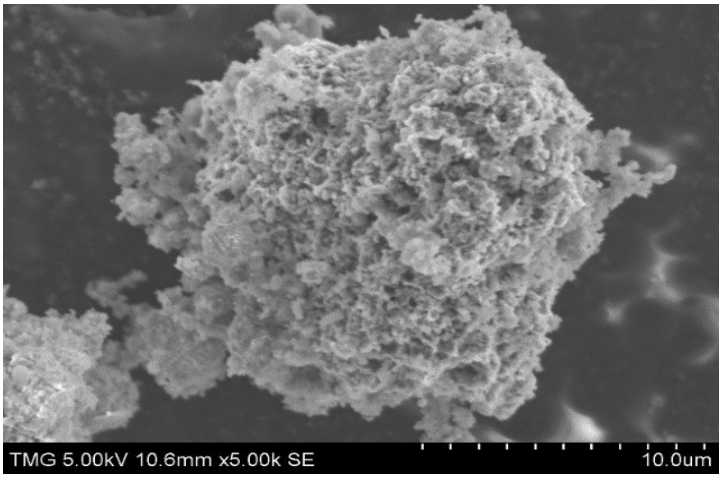

Figure 5-8 SEM for a Red Mud sample.

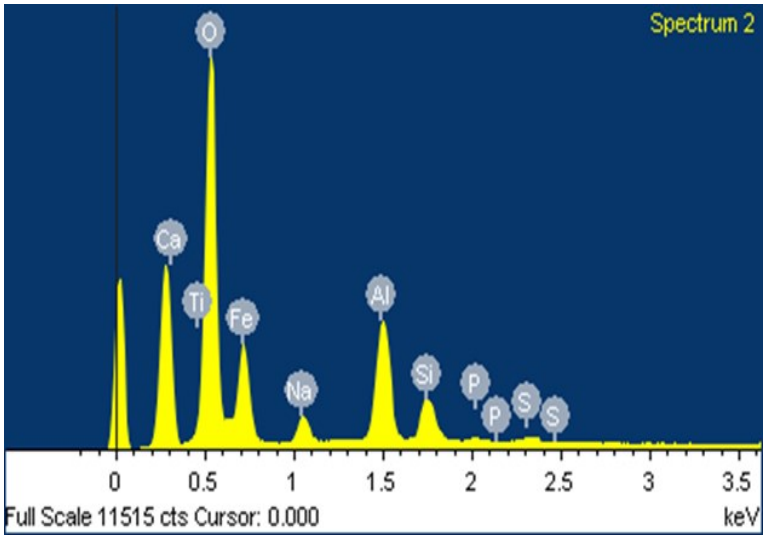

Figure 5-9 EDX for a selected spot in the red mud sample.

3) Chemical properties

a) X-ray fluorescence (XRF)

Fig 5.10 shows the XRD pattern for the red mud sample. The main components are aluminum hydroxide ($Al(OH)_3$), calcium carbonate ($CaCO_3$), and iron oxide (Fe_2O_3), along with some silica (SiO_2). This confirms the EDX results.

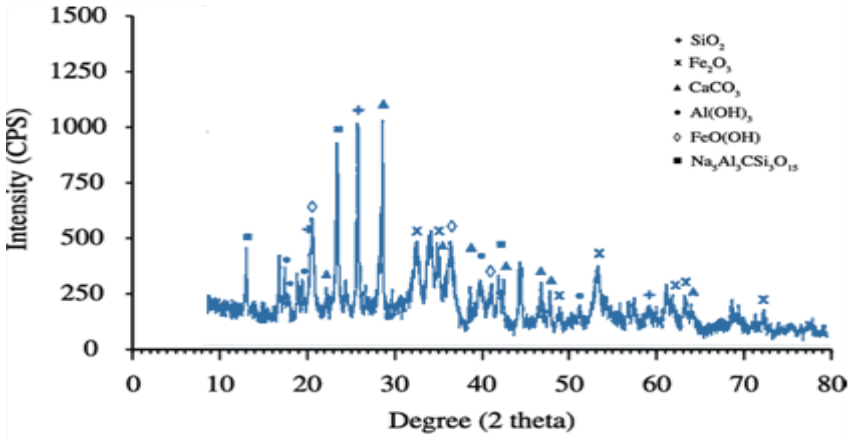

Figure 5-10 XRD pattern for a red mud sample

b) Surface pH

Red Mud is known as high alkaline material with high pH ranges between (10.5–12.5) [121]. Two samples of the red mud, before milling and after milling, were tested to find the surface pH for the solid **Fig. 5.11**. The pH values for samples before and after milling were 9.37 and 9.80, respectively. These values are less than the expected values. Hence, a more advanced test will be conducted in the chemistry department to verify the results.

Figure 5-11 Measuring the surface pH value for solid Red Mud sample

5.4.1.2 PPFA

1) Visual Inspection:

As shown in **Fig. 5.12**, the fly ash was wet-black material with big weak lumps.

Figure 5-12 PPFA Sample

2) Physical Properties:

a) Particle size distribution:

A milling machine was needed to breakdown big lumps into small particles. **Fig. 5.13**. The milling process had been applied for 6 hours to reduce particle size from coarse lumps retained on sieve 4.75 mm to fine materials that pass through sieve #50 (i.e., 0.297 mm). As shown in **Fig. 5.14**, particle sizes average after milling was between (0.15 mm-0.6 mm).

Figure 5-13 PPFA after milling.

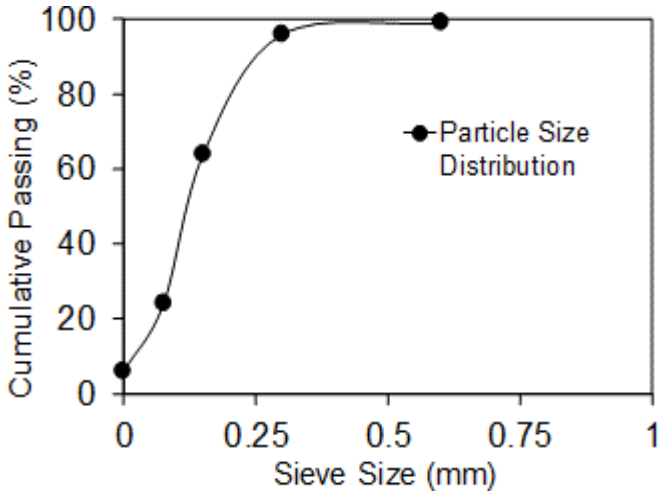

Figure 5-14 PPFA particle size distribution after milling.

b) Water content: 34%

c) Dry bulk density: 1340 kg/m^3

3) Reactivity Index:

PPFA is a high calcium precursor [124]. ASTM C311 "Standard Test Methods for Sampling and Testing Fly Ash or Natural Pozzolans for Use in Portland-Cement Concrete" procedure was followed to check whether this fly ash can be used with other binding systems.

28 days' reactivity index (%) compared to control OPC mixture = 82%.

4) Microstructure Analysis:

Scanning Electron Microscope (SEM) was conducted on fly ash samples to get information about its topography. Pulp and Paper Mill Fly-Ash was not spherical like regular Fly-Ash produced for the Coal industry [123] (**Fig. 5.15**).

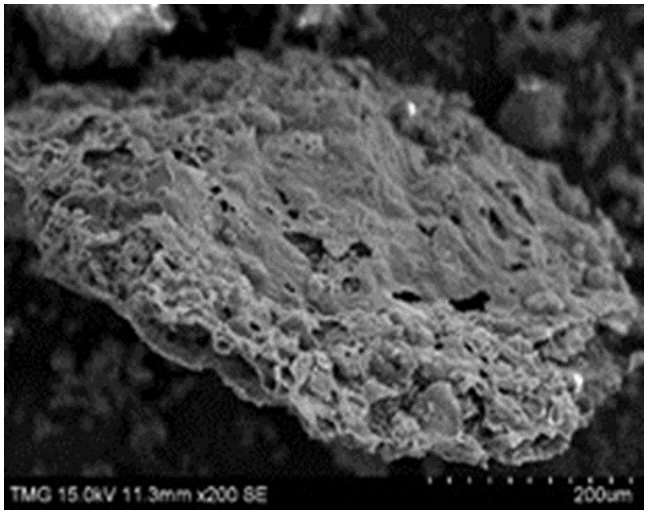

Figure 5-15 SEM for Fly ash sample after milling.

5.4.2 Phase 2: Examine Potential to Implemented in Construction Applications.

5.4.2.1 Red Mud

1) Fresh Properties

a) Flowability

Three mortar mixtures were prepared and tested to evaluate the changes in flowability as the Red Mud content increased. **Figure 5.16** shows the flow results for the three mixtures. The first mixture (i.e., Cement and Red Mud), increasing the Red Mud content resulted in a

reduction in the flowability. For instance, at 30% red mud as a replacement of cement, the flowability value decreased from 150 mm to 116 mm, this can be attributed to the high absorption of the Red Mud [124]. For the second mixture, slag, and Red Mud, there was no significant change in the flowability. It seems that two compensating effects are affecting the flowability. Adding Red Mud as a replacement of slag reduced the surface area of the binder (i.e., Slag is finer than Red Mud), leading to more free water. Simultaneously, Red Med will absorb a higher amount of water, leading to a lower amount of available water. Hence, each factor offset the effect of the other, leading to a slight reduction in the flowability. The mixture of slag, red mud, and metasilicate was examined. The higher the Red Mud, the lower the flowability. This can be attributed to the increase in the alumina content (as explained earlier), which accelerates the formation of gel lead to more viscous mixtures [125].

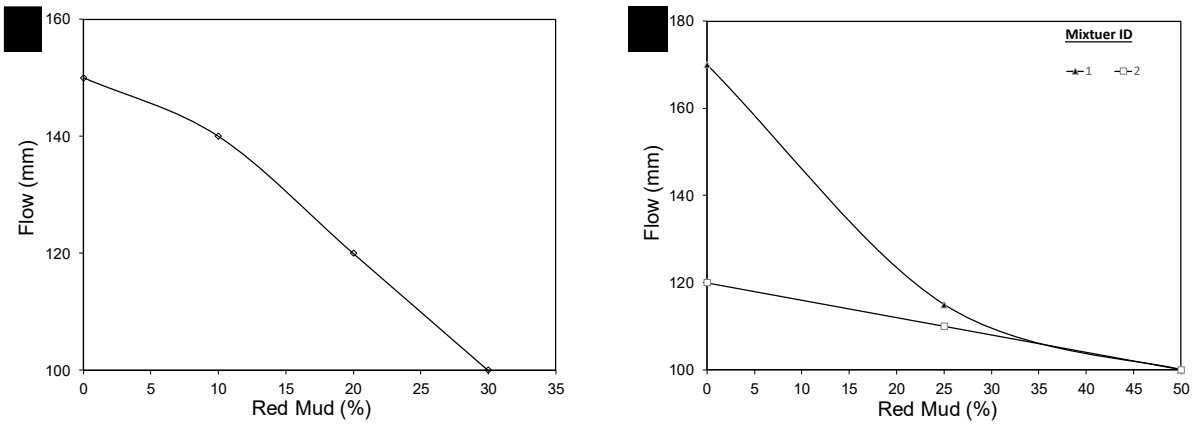

Figure 5-16 Flowability for different mixtures a) cement + Red Mud; b) (1) Slag + Red mud + meta-silicate, (2) Slag + Red Mud

2) Mechanical Properties

a) Strength Activity Index Testing

The reactivity index for milled red mud was 74%. It is anticipated that using finer Red Mud will result in a higher reactivity. Also, at later ages, Red Mud will act as a filler leading to a denser microstructure, which may also contribute to strength.

b) Compressive strength

Figure 5.17 shows the compressive strength development for different mixtures. As expected, adding Red Mud resulted in a reduction in the compressive strength. Three and seven days' strength results show that the higher the red mud content, the lower the achieved strength; this is attributed to the low hydraulic properties of Red Mud [117]. However, all mixtures are exhibiting the same strength indicating that there is another factor offsetting the dilution effect. This factor can be the packing effect induced by such fine Red Mud. Mixtures of slag activated by Red Mud only had exhibited seven days' strength higher than mixtures with Slag alone. Hence, the activation for Slag by the alkali medium developed by Red Mud was more efficient in developing strength than the hydraulic behavior of slag. However, increasing the Red Mud higher than 25% had significantly reduced the achieved strength, this can be attributed to the high absorption of Red Mud; hence, a lower amount of alkali pore solution is available to dissolve the slag [127]. Compressive strength for mixtures of slag and Red Mud and activated by meta-silicate are shown in (**Fig 17c)**. Adding Red Mud did not significantly affect the three days' strength. However, higher reductions were found at a later age (i.e., seven days); this can be attributed to the contribution of alumina to the early strength [120]. At a later age, reduction in silicate (due to replacing slag with Red Mud) seems to dominate the strength development.

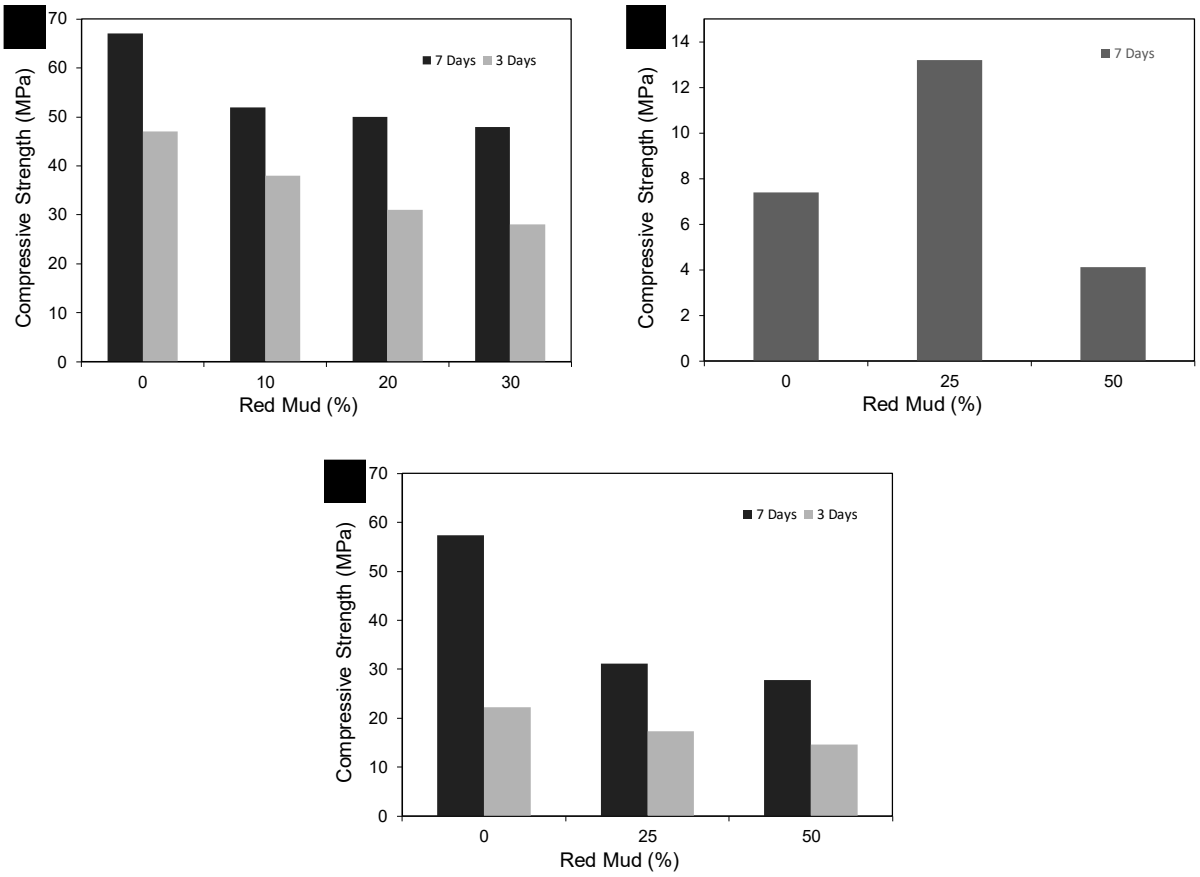

Figure 5-17 Compressive strength for different mixtures a) OPC and Red mud; b) Slag and Red Mud; and c) Slag, Red Mud, and meta-silicate.

5.4.2.2 PPFA

Pulp and Paper Mill Fly-Ash is a high calcium material that can replace cement, or it can be part of Alkali Activated Materials (AAM) binding systems. This replacement will initiate a partnership with cement and concrete manufactures based on the produced quantities of PPFA and its properties. This will convert such kind of waste into a valuable product.

As binding material pressure, PPFA showed high potential as a precursor for AAM systems. As shown in (**Fig. 5.18)**, acceptable strength results were recorded at ages 7 and 28 days. Samples' failure shape indicates shear failure (i.e., the sample is strong).

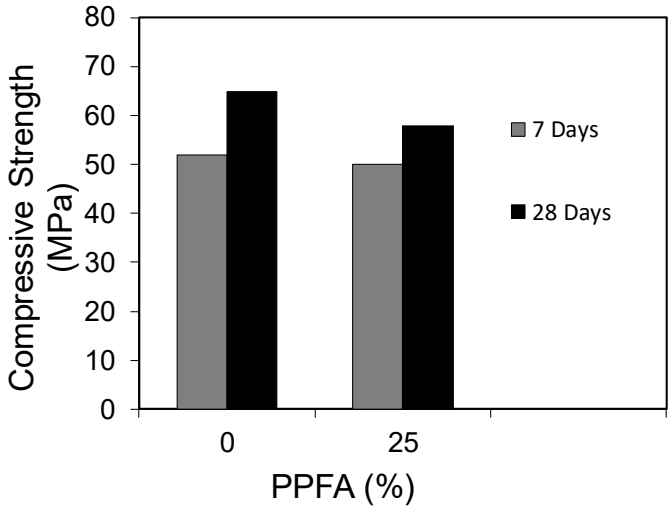

Figure 5-18 Compressive strength for AAM with paper mill fly ash at ages 7 and 28 days

Figure 5-19 Cube failure shape after testing under compression load.

5.4.3 Phase 3: Potential Applications:

5.4.3.1 Using Red Mud as Filling Material in Concrete Low Strength Materials

5.4.3.1.1 CLSM

Based on the primary findings of the previous phases, Red Mud has a high potential to be used in the construction sector. The following section examined the potential of using CLSM. In the literature, many researchers had highlighted the possibility of using red mud as a filling material and for phosphorus and nitrate removal, that are mainly generated from fertilizers, and livestock farming activities [128]. Hence, the potential of using the Red Mud in non-structural filling construction materials was examined. The red mud was used to produce a control low strength filling materials [129]. Results will be compared with data generated from a previous research project conducted using only conventional materials. The concept and primary results are discussed in the following section.

5.4.3.1.2 Concept

The agricultural waste material was used as a replacement for sand, and Red Mud was added as a replacement of cement in order to produce a special type of concrete known as “control low strength materials” [129]. Based on ACI 229R definition, controlled low-strength material (CLSM) is a self-consolidating, cementing material used primarily as backfill as an alternative to compacted fill, according to ACI 229R. CLSM is characterized by its low targeted compressive strength, which is about 8.3 MPa or less. This increases the potential for incorporating a large amount of waste materials in CLSM without concern about reductions in its mechanical performance. In addition, binding materials for CLSM are composed mainly of fly ash with a very low amount of cement. Therefore, this part focused on evaluating the properties of CLSM

incorporating agriculture waste material as a replacement for sand and Red Mud as a replacement of cement along with activating the fly ash.

5.4.3.1.3 Materials and Experimental Work

General used (GU) hydraulic cement according to the CSA-3001-03, and Class F fly ash (FA) according to ASTM C618 was used as binding materials for all tested CLSM mixtures. The chemical composition and the physical properties of the cement and fly ash are shown in **Table 5.3**. Red mud was added as a replacement of cement at rates 50% and 100%. Control mixtures were prepared based on proportion guidelines reported by ACI committee 229. Natural river bed sand with a specific gravity of 2.65 was used as fine aggregate. The same mixture was modified to incorporate agro-waste as a 10% partial replacement of sand by volume. The water was adjusted to achieve the same workability of 150-200 mm, which is the specified range by ACI committee 229. **Table 5.4** shows the composition for all tested mixtures.

Table 5-3 Chemical and physical properties of cement and fly ash.

		GU	FA
SiO_2	(%)	19.80	43.39
Al_2O_3	(%)	4.90	22.08
CaO	(%)	62.30	15.63
Fe_2O_3	(%)	2.30	7.74
SO_3	(%)	3.70	1.72
Na_2O	(%)	0.34	1.01
MgO	(%)	2.80	------
Na_2Oeq	(%)	0.87	------
Loss on ignition	(%)	1.90	0.58
Specific gravity	--	3.15	2.50

Table 5-4 Mixture compositions for CLSM mixtures

	Cement	Fly ash	Sand	Agro-waste (%)	Red mud
G0%RM	90	148	1570	10	0
G50%RM	45	148	1490	10	45
G100%RM	0	148	1325	10	90

5.4.3.1.4 Results and Discussion

1) Fresh Properties

Table 5.5 summarizes the fresh properties for different CLSM mixtures. For CLSM, the water content must be adjusted to achieve am adequate flowability within the range of 150–200 mm. The flow values were in the range from 170 to 200 mm, which falls within the normal flowability category according to the ACI committee 229R report. Hence, all mixtures were still within the acceptable range. Moreover, it is clear that all mixtures were stable and did not exceed the bleeding limit (maximum of 5% for stable CLSM). As expected, increasing the cement content had reduced the bleeding. This is ascribed to the high consumption of water in hydration; hence, less free water is available for bleeding. Replacing cement with red mud had slightly increased the bleeding. This can be attributed to the surface area of the grinded Red Mud sample, which replaced the OPC.

Table 5-5 Results for tested CLSM mixtures

	Flowability (mm)	Bleeding (%)	Compressive strength (MPa)			
			3 Days	7 days	14 Days	28 Days
G0%RM	170	1.5	0.60	0.90	1.50	2.00
G50%RM	200	2.0	0.56	1.12	1.90	2.85
G100%RM	220	2.0	0.00	0.45	0.75	*-----

2) Compressive Strength

Table 5.5 summarizes the compressive strength results for tested CLSM at ages 3,7, 14, and 28 days. Mixtures cement and Red Mud exhibited higher strength compared to mixtures with cement only. This indicated that both cement hydration and activation of the Fly-Ash had contributed to the strength development. The increase in alkalinity of the pore solution was able to partially activated the Fly-Ash leading to a higher strength. This is confirmed by strength results for mixtures incorporating Fly-Ash and Red Mud only. The strength development for Fly-Ash and Red Mud is slower than other mixtures; however, this a good indication and mixtures can be optimized to achieve higher strength. In addition, for some CLSM applications, it may be essential to maintain a low strength to facilitate future excavation. The ACI committee 229 recommends a compressive strength lower than 2.1 (MPa) if future excavation is anticipated. Hence, there is still the potential to add more agricultural waste or increase Red Mud content for G50W10R50 to achieve adequate strength.

5.4.3.2 Using PPFA as Filling Material in Concrete Low Strength Materials CLSM:

Based on ACI (American concrete institute), CLSM is known as self-consolidating backfill Controlled low strength materials (CLSM). It is known as an alternative to compacted fills. This material required low strength (under 8.2 MPa and usually around 2.0 MPa) with excellent flowability that makes it an excellent material for unreachable places, especially around pipes and underground structures. The low strength of these materials makes it easier to be excavated without damaging the instruments.

5.4.3.2.1 Materials and Experimental Work

General used (GU) hydraulic cement according to the CSA-3001-03 with Blaine fineness of 360 m^2/kg and a specific gravity of 3.15, and Class F fly ash (FA) according to ASTM C618 were used as binding materials for all tested CLSM mixtures. **Table 5.6** shows the chemical and physical properties for cement and fly ash. Natural river sand with a specific gravity of 2.65 and particle size distribution complies with that of fine aggregate for concrete according to ASTM C33 was used. Fly Ash samples have been examined as a replacement for sand used in CLSM. In this study, the control mixture composition was selected based on the proportion guidelines reported by ACI committee 229. The control mixture was modified by the incorporation of paper mill fly ash as partial replacement of sand by volume at rates of 0%, 5%, 10%, and 20%. Mixture proportions are shown in **Table 5.7**.

Table 5-6 Chemical and physical properties of cement and fly ash.

		GU	FA
SiO_2	(%)	19.80	43.39
Al_2O_3	(%)	4.90	22.08
CaO	(%)	62.30	15.63
Fe_2O_3	(%)	2.30	7.74
SO_3	(%)	3.70	1.72
K2O		0.83	--
Na_2O	(%)	0.34	1.01
MgO	(%)	2.80	------
P_2O_5	(%)	0.11	------
Na_2Oeq	(%)	0.87	------
Loss on ignition	(%)	1.90	0.58
Specific gravity	--	3.15	2.50
Surface are	(m^2/kg)	360	280

Table 5-7 Mixture compositions for CLSM mixtures with PPFA

	Cement (Kg)	Fly ash (Kg)	PPFA (%)
G0%PPFA	90	148	0
G5%PPFA	90	148	5
G10%PPFA	90	148	10
G20%PPFA	90	148	20

1) Mixing procedure

Initially, dry mixture components (i.e., cement, fly ash, and paper fly ash) were mixed without water addition for 1 min to ensure a homogeneous distribution. Mixing water was then divided into two halves. The first half of the mixing water was added gradually to the mixture while continue mixing for one more minute. The second half was then added and mixed for another 1

minute. The mixture was allowed to rest for 1 min after adding the whole amount of mixing water. Then, the mixture was mixed for an additional 2 min before sampling. For all tested mixtures, the flowability was continuously measured with various mixing water addition targeting the desired normal flowability in the range of 150 mm to 200 mm.

2) Testing procedure

Effects of paper mill fly ash addition on CLSM fresh properties, including bleeding and flowability, were evaluated following ASTM standards D6103-04 (Flow Consistency of Controlled Low Strength Material), ASTM D6023-07 (Density, Yield, Cement Content, and Air Content (Gravimetric) of CLSM) and ASTM test method C232 (Standard Test Method for Bleeding of Concrete), respectively. Cubic specimens 50 ×50 ×50 mm was used to evaluate the compressive strength for CLSM mixtures incorporating different percentages of agro-waste according to the ASTM test method D4832-10 (Standard Test Method for Preparation and Testing of CLSM Test Cylinders). The compressive test was conducted using a strain-controlled unconfined compressive strength machine at age 28 days. Specimens were kept inside the mold uncovered inside a curing room (temperature 22 ± 2°C and relative humidity 95% ± 3%) until the testing age due to the insufficient early-age strength of CLSM mixtures.

5.4.3.2.2 Results and Discussion

1) Bleeding

A maximum of 5% of bleeding is allowed for stable CLSM. **Fig. 5.20** illustrates and compares the bleeding of the CLSM, incorporating Pulp and Paper Mill Fly-Ash with controlled samples. The bleeding amount is in the allowed range.

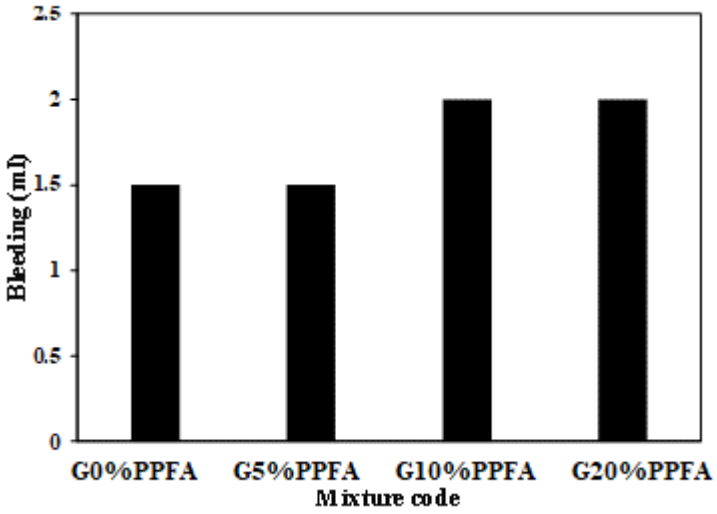

Figure 5-20 Bleeding for CLSM with different percentage of PPFA

2) Flowability

Regarding ACI 299 standard, flowability for all mixtures was within the range of 150-200 mm, which is acceptable for this construction application (**Fig. 5.21**).

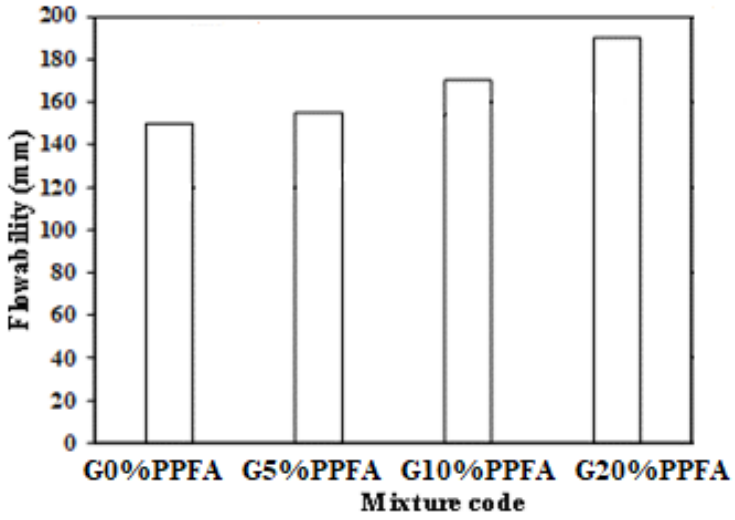

Figure 5-21 Flowability of CLSM with different percentage of PPFA

3) Compressive Strength

For a material to be considered as a CLSM, it must have a compressive strength of less than 8.2 MPa at 28 days. As shown in (**Fig. 5.22)**, all samples exhibited strength below the limit.

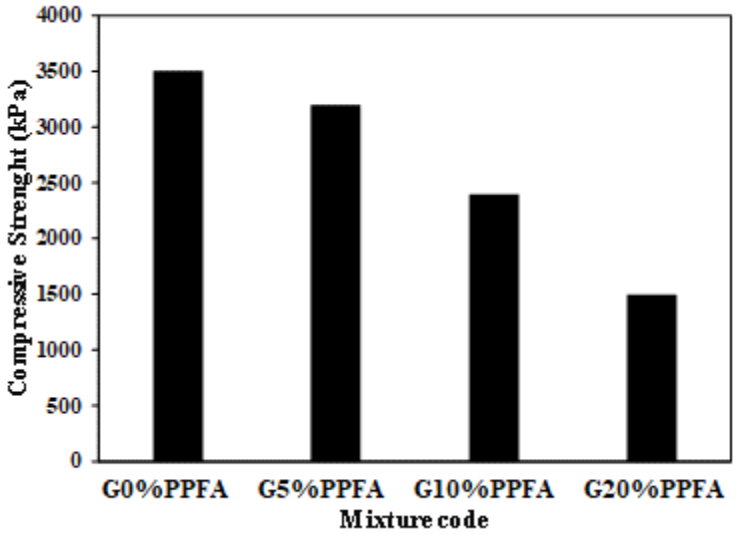

Figure 5-22 Compressive strength for CLSM with different percentage of PPFA

5.5 Conclusion

Red Mud and Pulp and Paper Mill Fly-Ash are the by-products of huge industries in Canada; dealing with a massive amount of these by-products is a challenge facing the sustainability of these businesses. This chapter offers several construction applications that can consume large volumes of these wastes. Both by-products showed reasonable fresh, and mechanical performance makes them fit for many applications such as cement replacement and CLSM.

CHAPTER SIX

EFFECT OF UTILIZING LOCAL PAPER MANUFACTURING INDUSTRY WASTE IN CONSTRUCTION MATERIALS

This chapter focuses on examining the potential of reducing paper industry environmental impacts through new reusing/recycling various wastes in the construction sector. This is anticipated to convert these wastes into valuable products. The chapter started by examining various wastes and identifying their chemical and physical characteristics. Then, multiple mixtures were tailored to incorporate high percentages of these wastes while meeting the performance criteria for selected construction applications.

6.1. Introduction

Pulp and paper manufacturing is an old Canadian industry that started in the 1800s. Three central regions, namely, Quebec, Ontario, and Novascotia, were the first business incubators. Paper manufacturing relies on "pulping"; this terminology is known as converting wood fibers into cellulose components mechanically and chemically [130]. Kraft pulping with sequence processes produce large volumes of wastes that vary in its physical and chemical properties. Globally, the paper industry produces over 403 Mt of paper and over 179 Mt of pulp production in 2013. Massive amounts of wastes are associated with such large production, which needs to be disposed of safely. Paper manufacturing has six main operations, including pulping, washing, evaporation,

combustion, clarification, and causticizing. Sodium hydroxide (NaOH) and (Na2S) Sodium Sulfide are involved in the pulping process. Moreover, high organic substances contribute to the increase of biological oxygen demand levels in water bodies [131,132]. The special precautions needed for disposing of pulp and paper manufacturing wastes had urged legislators to control the industry through lows and regulations such as Pulp and Paper Effluent Regulations (SOR/92-269).

From the waste management point of view, reducing waste volumes is an urgent goal. Reusing and recycling such wastes will reduce the amounts sent to the landfills. However, several factors affect the reusing and recycling of these wastes. For example, recycling sludge has to comply with specific quality criteria like breaking length, elongation, and stiffness to be recycled as new papermaking components [133]. Recently, construction marked became the biggest waste landfill for many types of industrial by-products and wastes. For instance, slag and fly ash were considered hazardous wastes that need special precautions to dispose of safely. Today, these by-products represent essential components in the construction industry to enhance construction materials properties [134]. By using the same concept, pulp and paper production could be tributary with new techniques fulfilling sustainability and environmental concepts while gaining economic benefits.

6.2. Study Methodology

Initially, all received materials were characterized and classified to understand their properties and allocate them for suitable construction applications. The outcome of this stage was used as a benchmark for the next phases. Suitability of each type of waste for proposed applications was examined. Realistic manufacturing procedures for each application were set to simulate the actual future implementation. Validation procedures complying with the international standards and

market needs were applied to each final product to validate its potential to compete with existed products in the market.

6.3. Experimental Program

The experimental program is divided into two phases. Initially, all received materials were characterized and classified to understand their properties and allocate them for suitable construction applications. The outcome of this stage was used to select the right application for each type of waste. Different properties for produced construction materials incorporating wastes were examined.

6.3.1. Materials Characterization

Various tests were conducted to characterize chemical and physical properties for the wastes. Also, the interactions between each waste and binding materials were investigated. Random samples had been collected and divided into small quantities for characterization tests. The following tests were conducted:

1) **Visual Inspection**: Sludge samples had been inspected by raw human senses such as vision, touch and smell, and/or any non-specialized inspection equipment. This test gave a general idea about the basic features of the received samples. Also, it allowed identification for the nature of the wastes (i.e., pure or contaminated by other wastes).

2) **Physical Properties:** The behavior of particulate materials is often dominated by the physical properties of the constituent particles. These can influence a wide range of material behaviors, including, for instance, how easily ingredients can flow, mix, or compress. Some of the most important physical properties that were measured are:

a) Bulk Density: Bulk density is defined as the ratio of the mass of a given quantity of material and the total volume occupied. This volume includes the voids between, as well as the pores within the particles. Bulk density is a function of particle shape, density, size, grading, and moisture content, as well as the method of packing the material.

b) Water Content: The water content was evaluated according to ASTM D4959-07 "Standard Test Method for Determination of Water (Moisture) Content of Soil By Direct Heating." Samples were heated in a furnace at 110 °C until they reached a constant weight. The water content was evaluated as the weight of dry material over the weight of water-loss.

3) **Chemical Properties:** Chemical properties were investigated for water effluent based on the potential application assigned, Chemical composition such as Chloride as Cl-, Sulfate as SO4, and Alkalis as (Na2O + 0.658 K2O) for water effluent samples, those tests had been chosen based on the potential application "concrete mixing water" according to ASTM C 1602.

6.3.2. Selected Applications for Various Wastes

Successful implementation of pulp and paper wastes in building applications will mainly depend on how efficiently the properties of these wastes were utilized to achieve adequate performance. Hence, in this phase, the behavior of different cementitious mixtures incorporating water effluent, sludge, and paper ash was investigated.

1) Wastewater effluent: Activator for alkali-activated materials:

The high alkaline of the water effluent increased its potential as an activator for alkali-activated materials [135]. The use of such non-treated water effluent could reduce the cost of the final product (replacing activator cost) and lead to environmental and economic benefits. (i.e., saving water treatment cost).

2) Pulp and Paper Sludge

Sludge is the solid paper production waste generated at the end of the mechanical treatment process. It is classified as a non-hazardous and fiber-rich by-product. Large quantities of sludge produced in this process ended at landfills. A previous study had suggested reusing up to 12% of sludge in the manufacturing of papers and boards industry [136]. The lightweight and rich fiber content of the pulp and paper sludge make it suitable for sound and heat insulation boards and lightweight masonry units.

One of the main common building materials in the Canadian market is sound and heat insulation boards. Sludge could be a cheap and sustainable solution in the production of partitioning and insulation [137]. The proposed product has zero virgin material. On the other hand, Lightweight masonry units have very low dead loads, easy mobilizing, and higher workmanship productivity [138]. Moreover, lightweight masonry units are considered a heat and sound insulated barrier [139]. Hence, the same concept was applied to use sludge in masonry unit production. This will offer masonry units with similar features with less expensive and environmental impacts.

6.4. Laboratory Testing for Proposed Applications

6.4.1. Materials

General use (GU) hydraulic cement, according to the CSA-3001-03, was used as the binding material for reference mixtures. Granulated blast furnace slag Grade 80 (GBFS, hereafter referred to as slag) with specific gravity 2920 kg/m^3, and Blaine fineness 515 m^2/kg and an average particle size value around 14.5 μm was used as the precursor material for all alkali-activated mixtures. The basicity coefficient [$K_b = (CaO + MgO)/ (SiO_2 + Al_2O_3)$] for the used slag was 1.06. **Table 6.1** shows the chemical composition for the used cement and GBFS. The

used fine aggregate was natural riverside sand with a fineness modulus of 2.70 (according to ASTM C136 (2014)), specific gravity and water absorption of 2.51, and 2.73% determined by ASTM C 128 (2015), respectively. The sand particle distribution is shown in **Fig. 6.1**. Sludge had been added at two percentages 25% and 50% by volume of sand.

Table 6-1 Chemical and physical properties of cement

		OPC	GBFS
SiO_2	(%)	19.80	36.50
Al_2O_3	(%)	4.90	10.20
CaO	(%)	62.30	37.60
Fe_2O_3	(%)	2.30	0.50
SO_3	(%)	3.70	3.10
Na_2O	(%)	0.34	0.30
MgO	(%)	2.80	11.80

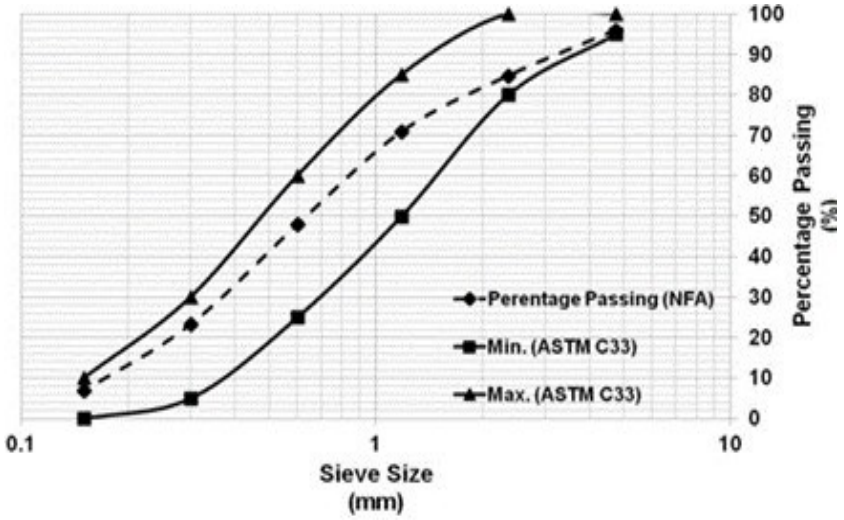

Figure 6-1 Sand particle distribution.

Two binding systems had been used to prepare the OPC system and AAM with activator dosage of 10% Sodium meta-silicate. Fixed water to binder ratio of 0.5 for both systems to achieve semi-dry mixtures. Binder to sand ratio was 1:2.75. **Table 6.2** shows mixtures proportions.

Table 6-2 Mixtures proportions.

Mixture ID	Binding material	Activator (%)	Water to binder ratio	Sludge (% by volume)
A1	OPC	0	0.50	0
A2				25
A3				50
B1	GBFS	10%	0.50	0
B2				25
B3				50

6.4.2. Mixing and Mixtures Preparation

All mixtures were prepared by using an electrically driven mechanical mixer following ASTM C305. Initially, sludge (**Fig. 6.2**) had been mixed for 3 minutes to confirm its dismantling into fibers instead of big lumps. Slag had been added and mixed with the sludge for 1 minute, then sodium meta-silicate and water effluent had been added gradually to the mixture and mixed for an additional 2 minutes. Finally, 3 minutes of continuous mixing had been applied to ensure a homogeneous mixture. For OPC binding system, the same procedure had been repeated to

prepare OPC specimens with the treated water effluent, which is neutralized the alkaline water effluent.

Figure 6-2 Mixture consistency (semi-dry).

6.4.3. Specimens Preparation

Various specimen shapes and sizes had been prepared. For sound insulation tests, cylindrical segments with dimensions (D=100 mm, t= 20 mm) and (D=30 mm, t=20 mm), as shown in Fig. 6, For thermal tests, (300 mm*300*50 mm) sample had been prepared to fit into the thermal conductivity testing machine as follows in **Fig. 6.3**.

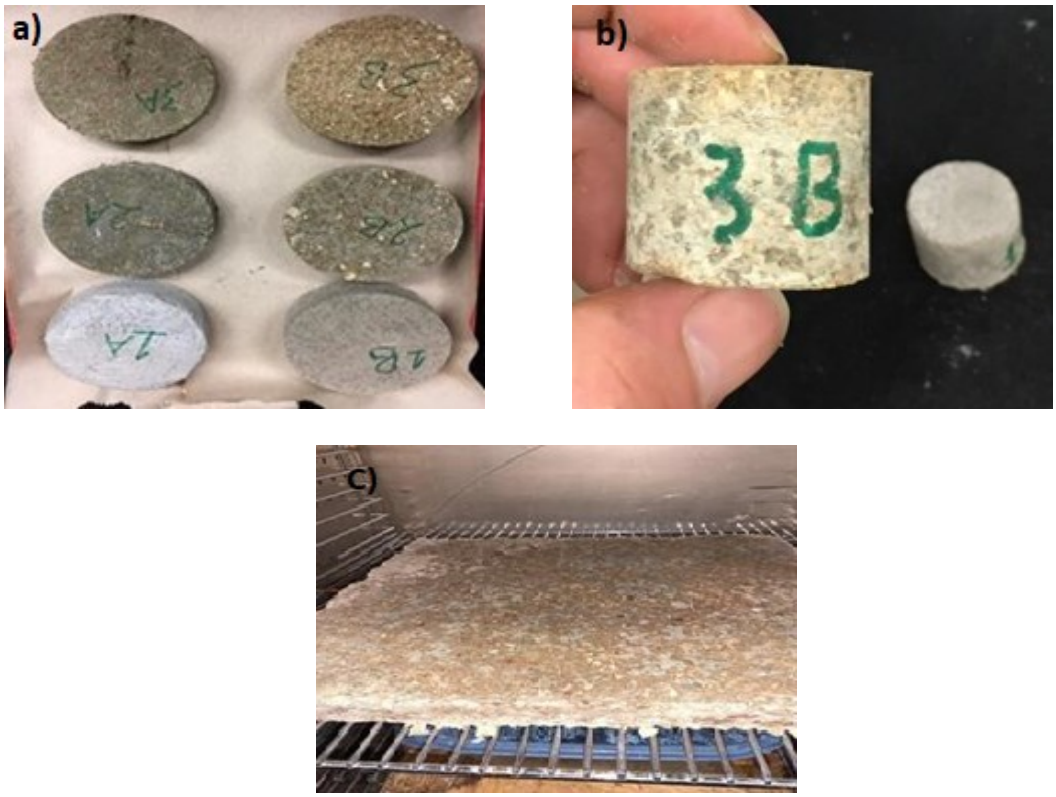

Figure 6-3 a) large Sound insulation samples, b) Small Sound insulation samples, and c) Thermal conductivity test sample.

6.4.4. Samples Curing

All specimens had been covered with plastic to prevent moisture evaporation and cured under 60°C for 24 hours in the curing chamber, simulating precast elements curing regimes (**Fig. 6.4)** [140].

Figure 6-4 Samples curing.

6.5. Testing Procedure

6.5.1. Mechanical Performance

Compressive and tensile strength have been investigated to evaluate mechanical performance. Compressive strength had been tested following ASTM C 109 Standard Test Methods for Compressive Strength of Hydraulic Cement Mortars (Using 2-in. or [50-mm] Cube Specimens), while tensile strength was examined according to AAS HTO T132 Tensile Strength of Hydraulic Cement Mortar.

6.5.2. Sound Insulation Performance

Noise Reduction Coefficient (NRC). Acoustic properties rely on sound frequencies. Human hearing ranges (20 Hz — 20 kHz) [141]. Therefore, specific frequencies present acoustic properties. NRC is a number that indicates sound absorption at a specific frequency range. Samples had been tested following ASTM C423 Standard Test Method for Sound Absorption and Sound Absorption Coefficients by the Reverberation Room Method. The absorption coefficient indicates

the material ability to absorb sound energy. For instance, 0 absorbing coefficient means no sound absorption, while one means all sound energy has been dumped.

6.5.3. Thermal Conductivity

Thermal conductivity was investigated following the ASTM C518 Standard Test Method for Steady-State Thermal Transmission Properties utilizing the Heat Flow Meter Apparatus. Using Nietzsche HFM 436 Lambdas — Heat flow meter, which is considered as a high data reliable heat flow meter **Fig. 6.5**, a sample of B3 mixture, which contains 50% sludge, showed comparable values to that of the market board products.

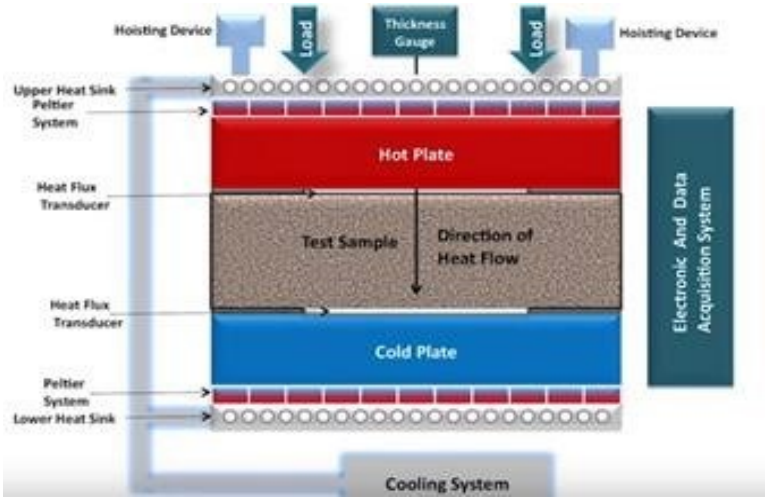

Figure 6-5 Nietzsche HFM 436 Lambdas-Heat flow meter mechanism [142]

6.6. Results and Discussions

6.6.1. Materials Characterization Results

1) Wastewater Effluent

Water samples had a yellowish color **Fig. 6.6**. The water effluent was complied with mixing water limits stated by ASTM C1602 "Standard Specification for Mixing Water Used in the Production of Hydraulic Cement Concrete standards." **Table 6.3** summarizes the results for different acceptance criteria. Using the water effluent resulted in 7 days' compressive strength 93% of that for a mixture made by potable water (i.e., higher than the minimum requirements (90%)). Also, the delay in setting time for cement paste was insignificant compared with the acceptance limit. Using water effluent delay, the setting by only 10 minutes (up to 1.5 hrs. is accepted according to the standard). **Table 6.4** is an optional chemical requirement for specific applications, like reinforcement concrete structures. Samples are under testing, and results will be reported later.

Figure 6-6 Water effluent sample as received.

Table 6-3 Acceptance Criteria and Physical Tests for Mixing Water

	Test Method	Limits	Results
Compressive strength at 7 d, min % of control	ASTM C1602, ASTM C31/39	90 %	93%
Setting time, max. deviation from control, (h:min)	ASTM C1602, ASTM C403	From 1:00 early To 1:30 later	10 min later

Table 6-4 Optional Chemical Limits for Combined Mixing Water.

	Test Method	Limits	Results
Chloride as Cl-, ppm	ASTM C114		
In pre-stressed concrete, bridge decks, or otherwise designated.		500	------*
Other reinforced concrete in moist environments or containing aluminum embedment's or dissimilar metals or with stay-in-place galvanized metal forms.		1000	------*
Sulfate as SO_4, ppm	ASTM C114	3000	-----*
Alkalies as (Na_2O + 0.658 K_2O), ppm	ASTM C114	600	-----*
Total solids by mass, ppm	ASTM C1603	50 000	4480

2) Pulp and Paper Mill Sludge

a) Visual Inspection:

As shown in **(Fig. 6.7)**, the sludge had a greenish color and rich in fibers.

Figure 6-7 Pulp and paper mill sludge.

b) Physical Properties:

Particle sizes/shape: Fibre-like with lengths range between (0.1mm – 7.0 mm).

- Water content: 60%
- Dry bulk density: 160 kg/m^3

c) Chemical Properties:

Alkalinity: Sludge pH was in the normal range of natural materials (6.5 – 8.5).

Microbiological tests: samples from paper mill sludge have been submitted to microbiological laboratories at Concordia universities Layola. (Results will be reported later).

6.6.2. Laboratory Testing Results for Proposed Applications

6.6.2.1. Mechanical Performance

Mechanical properties are essential for any assigned products. Even though the designed products are non-structural elements, a specific load is required for holding its dead load and for mobilization. **Fig. 6.8** demonstrates compressive and tensile strength for all mixtures. Alkali activated materials mixtures showed much higher mechanical performance comparing to that of the OPC mixtures. This performance is due to the high water absorption of sludge. During the compaction, high water content escapes from the mixture. After releasing the piston, sludge retakes the water from the paste. This process consumes the required water for the cement to react and produce hydration products. For AAM, water is just a carrier for the activator [143]. Moreover, the AAM mixture is a sticky paste that has a short initial setting time. Within a few minutes from compaction, initial setting time would take its role and bond all sludge fibers together. The gypsum board's tensile strength ranges between (1-2 MPa) [144]. Therefore, it is potentially high to be a market competitor.

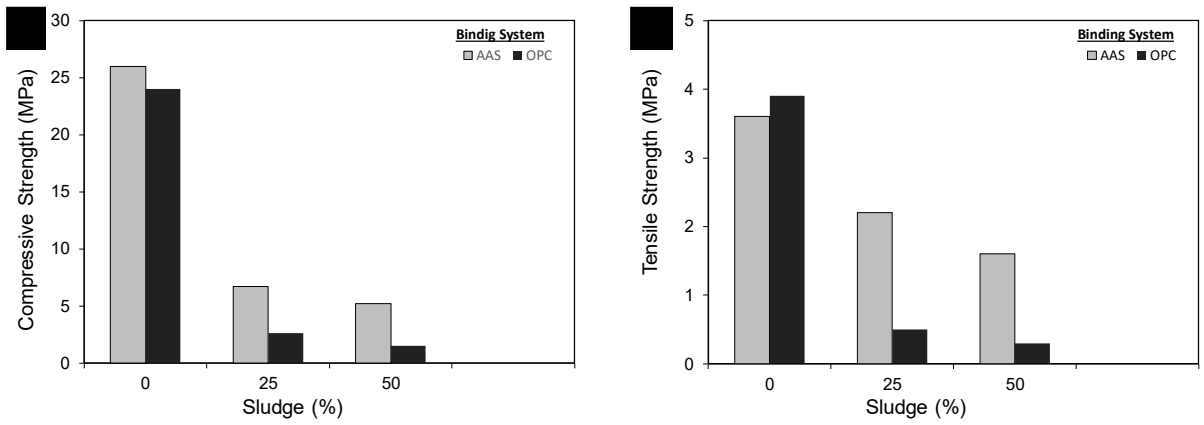

Figure 6-8 a) OPC (A1,A2,A3) and AAM (B1,B2,B3) compressive strength. B) OPC (A1, A2, A3) and AAM (B1, B2, B3) tensile strength.

6.6.2.2. Dry Unit Weight

Lightweight board units can be achieved by adjusting mixtures design. In this research project, 1200 kg/m^3 with reasonable strength results were achieved by the B3 mixture.

6.6.2.3. Sound Insulation Performance

As shown in (**Fig. 6.9)**, all mixtures had been investigated for noise reduction coefficient (NRC) values. Results showed that increasing sludge volume in the mixture provided higher NRC value. OPC mixture with 50% sludge by volume of sand offered the best sound insulation value, but with very low, insufficient mechanical strength compared to market products. Even though AAM samples achieved less noise dumping results compared to the OPC samples. AAM samples achieved noise dumping ranged between (0.3-0.6), which was much higher than the common market gypsum boards (i.e., 0.05 NRC value)

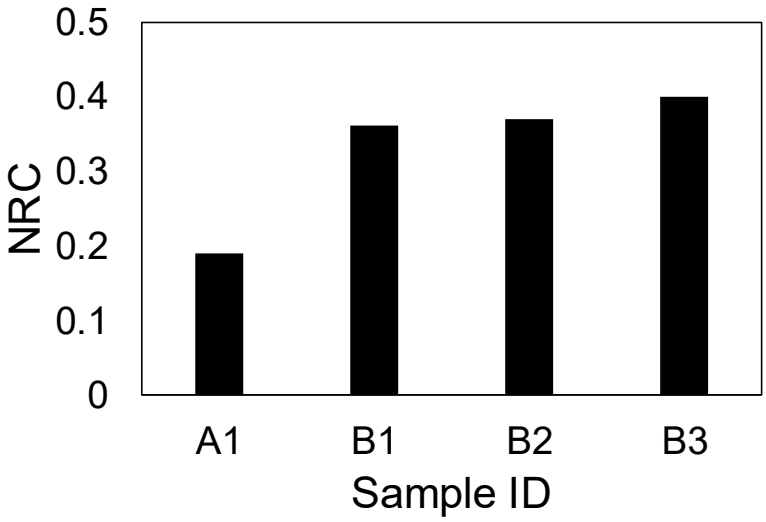

Figure 6-9 Absorption coefficient and frequency relationship for samples OPC (A1) and AAS (B1, B2, B3)

6.6.2.4. Thermal Conductivity Performance

Using Nietzsche HFM 436 Lambdas-Heat flow meter, samples of alkali-activated material with 50% sludge by volume of sand "B3" and construction foam sample have been tested as shown in **Fig. 6.10**. The purpose of testing the foam sample was for comparison purposes.

Figure 6-10 Thermal conductivity test.

From **Table 6.5**, AAM Sludge boards exhibited double thermal resistivity compared to that of the conventional market gypsum boards.

Table 6-5 HFM thermal conductivity results

Material	Thermal Conductivity (W/m·K)
AAS Sludge boards	0.193
Gypsum boards	0.134 - 0.254 [145]
Foam Boards	0.022 - 0.028

6.6.2.5. Extra Features

On top of the above features, AAM sludge boards and masonry units can carry the lateral loads, and it offered good surface bonding for epoxy and plastering applications. **Fig. 6.11**.

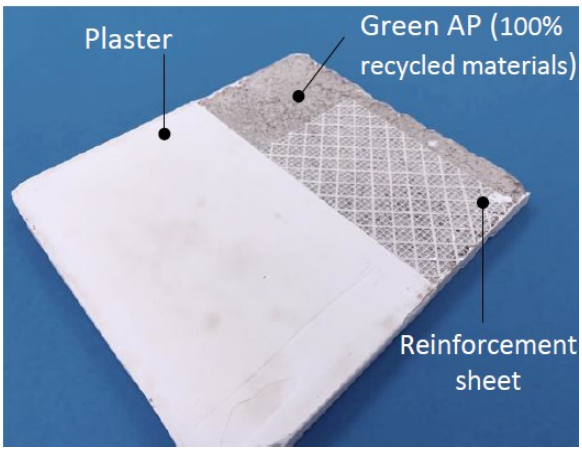

Figure 6-11 Acoustic panels

6.7. Conclusion

Reusing and recycling are the primary tools to reduce the environmental impacts of manufacturing waste, as primary wood pulp and Paper Mill by-products, water effluent, and sludge are manufacturing waste required especial practices to deal with. This chapter applied the concept of reuse these by-products in construction building materials; the treated water effluent shows high potential to be concrete mixing water complying with concrete mixing water standards. Sludge examined to be thermal and acoustic panels using AAM binding system; the final product shows a very high potential of being a real market competitor with almost zero virgin material.

CHAPTER SEVEN

Conclusions and Future Work

7.1 Conclusions

The thesis had two main approaches. The first approach was to explore new green techniques to enhance One-Part Alkali Activated Slag (AAS) properties. The second approach was assigned to engaging local industries wastes in construction building materials. Moreover, both approaches were linked by a sustainable and green building concept, which is the utilization of AAS. Hence, the contribution towards the environment and the economy is tangible.

Away from the conventional methods employed to overcome AAS fresh properties challenges such as the use of chemical admixtures, replace slag with low calcium precursors, or to change activator type and dosage. The new techniques designed to be relying on the physicochemical properties of the ingredient itself without extra additives, which grant this research originality.

The second approach was established based on two sides vision, mitigating the environmental impact of alumina and pulping industries and meeting the construction market needs by innovative green building products. The following is a summary of the work done in the thesis:

- Regardless of mixing water temperature, increasing activator dosage leads to higher slump loss and low setting time.
- Decreasing mixing water temperature extends One-Part AAS workability and setting time for all activator dosages. This is attributed to the lower dissolution rate of the low mixing

water temperature, which is confirmed by heat generation tests. Hence, this would potentially introduce One-Part AAS as a safe material for more construction applications.

- The effect of varying mixing water temperature on the early drying shrinkage was almost negligible.
- Regardless of mixing water temperature, increasing activator dosage increased the early strength while a minimal increase of the ultimate strength.
- Varying mixing water temperatures affect the early, and ultimate strength has been investigated. The findings show that decreasing mixing water temperature increases the early strength, while the impact on the ultimate strength was almost negligible, this is attributed to the dissolution rate, which is controlled by lowering the initial heat generated from the exothermic reaction. These results were confirmed by X-ray and DSC tests.
- The effect of mixing time on One-Part AAS. Generally, increasing mixing time extends both workability and setting time; this is attributed to the continuous braking of the formed networks, this finding would help to implement One-Part AAS in Ready-Mix business.
- It was reported that the continuous mixing for prolonged time increases both early and seven days' strength; this could be attributed to a higher dissolving rate of the anhydrous meta-silicate particles during mixing.
- Red Mud and PPFA were examined as local cement alternatives. Both by-products proved the potential of being sustainable and green building materials for several non-structural applications.
- The findings revealed that increasing the Red Mud portion in OPC mixtures reduced the workability and strength. Even though the achieved strength would be fit for some non-structural applications do not require high strength such as CLSM.

- Replacing slag by 25% of Red Mud offers higher strength; this is attributed to Red Mud high alkalinity. These results could be implemented in Alumina industry waste management procedures for controlling floods in winter.
- PPFA shows very high potential to be OPC alternative where the reactivity index reaches 82% on 28 days; This is attributed to its high calcium content; these results introduce PPFA for a wide range of applications such as CLSM.
- The wood pulping industry has several wastes that vary in their physical and chemical properties. Pulp and paper mill water effluent was examined to be concrete mixing water; the results show that the water effluent is complying with the acceptance criteria of ASTM standers.
- Wood and paper mill sludge was examined as filler material for sound and thermal insulation boards using AAS. The final product was compared to the available market products. The results show that the proposed innovation offers higher insulation performance than what is available in the market. This innovation can be an excellent business opportunity serving both environment and the economy.

7.2 Future Work

It deserves to mention our plan out of this thesis:

1) Combined decreasing water temperature and mixing time techniques and find the right tuning between them to introduce One-Part AAS to Ready-Mix concrete companies.
2) Refine the manufacturing procedures for each application and proposed it to industrial partners.
3) Examine the new products on a larger-scale individually and combined with other

materials.

4) Optimize proposed products based on data collected about each competitor.
5) Enhance proposed product performance and add additional features to distinguish them from other market product.

References

[1] Abdul-Rahman, F., & Wright, S. E. (2014). Reduce, reuse, recycle: alternatives for waste management.

[2] Okoye, F. N. (2017). Geopolymer binder: A veritable alternative to Portland cement. Materials Today: Proceedings, 4(4), 5599-5604.

[3] Sivakrishna, A., Adesina, A., Awoyera, P. O., & Kumar, K. R. (2020). Green concrete: A review of recent developments. Materials Today: Proceedings, 27, 54-58.

[4] Timperley, J. (2018). Q&A: Why cement emissions matter for climate change. Carbon Brief, 13.

[5] Rodgers, L. (2018). Climate change: The massive CO2 emitter you may not know about. BBC News.

[6] Dwivedi, V. N., Das, S. S., Singh, N. B., Rai, S., & Gajbhiye, N. S. (2008). Portland cement hydration in the presence of admixtures: black gram pulse and superplasticizer. Materials Research, 11(4), 427-431.

[7] Mohamed, O. A. (2019). Effect of Mix Constituents and Curing Conditions on Compressive Strength of Sustainable Self-Consolidating Concrete. Sustainability, 11(7), 2094.

[8] Luukkonen, T., Abdollahnejad, Z., Yliniemi, J., Kinnunen, P., & Illikainen, M. (2018). One-part alkali-activated materials: A review. Cement and Concrete Research, 103, 21-34.

[9] Miller, S. A., John, V. M., Pacca, S. A., & Horvath, A. (2018). Carbon dioxide reduction potential in the global cement industry by 2050. Cement and Concrete Research, 114, 115-124.

[10] Montzka, S. A., Dlugokencky, E. J., & Butler, J. H. (2011). Non-CO 2 greenhouse gases and climate change. Nature, 476(7358), 43-50.

[11] Nordbo, A., Järvi, L., Haapanala, S., Wood, C. R., & Vesala, T. (2012). Fraction of natural area as main predictor of net CO2 emissions from cities. Geophysical Research Letters, 39(20).

[12] Bäckstrand, K., & Lövbrand, E. (2019). The road to Paris: Contending climate governance discourses in the post-Copenhagen era. Journal of Environmental Policy & Planning, 21(5), 519-532.

[13] Jackson, R. B., Canadell, J. G., Le Quéré, C., Andrew, R. M., Korsbakken, J. I., Peters, G. P., & Nakicenovic, N. (2016). Reaching peak emissions. Nature Climate Change, 6(1), 7-10.

[14] Lv, W., Sun, Z., & Su, Z. (2020). Study of seawater mixed one-part alkali activated GGBFS-fly ash. Cement and Concrete Composites, 106, 103484..

[15] Proske, T., Hainer, S., Rezvani, M., & Graubner, C. A. (2013). Eco-friendly concretes with reduced water and cement contents—Mix design principles and laboratory tests. Cement and Concrete Research, 51, 38-46.

[16] Hertel, T., & Pontikes, Y. (2020). Geopolymers, inorganic polymers, alkali-activated materials and hybrid binders from bauxite residue (red mud)–Putting things in perspective. Journal of Cleaner Production, 120610.

[17] Gharzouni, A., Ouamara, L., Sobrados, I., & Rossignol, S. (2018). Alkali-activated materials from different aluminosilicate sources: Effect of aluminum and calcium availability. Journal of Non-Crystalline Solids, 484, 14-25.

[18] Nath, P., & Sarker, P. K. (2014). Effect of GGBFS on setting, workability and early strength properties of fly ash geopolymer concrete cured in ambient condition. Construction and Building Materials, 66, 163-171.

[19] Yüksel, İ. (2017). A review of steel slag usage in construction industry for sustainable development. Environment, Development and Sustainability, 19(2), 369-384.

[20] Krivenko, P. (2017). Why alkaline activation–60 years of the theory and practice of alkali-activated materials. Journal of Ceramic Science and Technology, 8(3), 323-333.

[21] De Vries, P. (2018). Geopolymer Concrete Ready Mixed: A Challenge!. In High Tech Concrete: Where Technology and Engineering Meet (pp. 2327-2337). Springer, Cham.

[22] Reddy, M. S., Dinakar, P., & Rao, B. H. (2016). A review of the influence of source material's oxide composition on the compressive strength of geopolymer concrete. Microporous and Mesoporous Materials, 234, 12-23.

[23] Wang, S. D., Scrivener, K. L., & Pratt, P. L. (1994). Factors affecting the strength of alkali-activated slag. Cement and concrete research, 24(6), 1033-1043.

[24] Siddique, R. (2007). Waste materials and by-products in concrete. Springer Science & Business Media.

[25] Xing, J., Zhao, Y., Qiu, J., & Sun, X. (2019). Microstructural and mechanical properties of Alkali activated materials from two types of blast furnace slags. Materials, 12(13), 2089.

[26] Borra, C. R., Pontikes, Y., Binnemans, K., & Van Gerven, T. (2015). Leaching of rare earths from bauxite residue (red mud). Minerals Engineering, 76, 20-27.

[27] Cherian, C., & Siddiqua, S. (2019). Pulp and Paper Mill Fly Ash: A Review. Sustainability, 11(16), 4394.

[28] Naik, T.R.; Kraus, R.N. A new source of pozzolanic material. Concr. Int. **2003**, 25, 55–62.

[29] Chowdhury, S., Mishra, M., & Suganya, O. M. (2015). The incorporation of wood waste ash as a partial cement replacement material for making structural grade concrete: An overview. Ain Shams Engineering Journal, 6(2), 429-437.

[30] Palacios, M., & Puertas, F. (2007). Effect of shrinkage-reducing admixtures on the properties of alkali-activated slag mortars and pastes. Cement and concrete research, 37(5), 691-702.

[31] Gebregziabiher, B. S., Thomas, R., & Peethamparan, S. (2015). Very early-age reaction kinetics and microstructural development in alkali-activated slag. Cement and concrete composites, 55, 91-102.

[32] Puertas, F., González-Fonteboa, B., González-Taboada, I., Alonso, M. M., Torres-Carrasco, M., Rojo, G., & Martínez-Abella, F. (2018). Alkali-activated slag concrete: Fresh and hardened behaviour. Cement and Concrete Composites, 85, 22-31.

[33] Tennakoon, C., San Nicolas, R., Sanjayan, J. G., & Shayan, A. (2016). Thermal effects of activators on the setting time and rate of workability loss of geopolymers. Ceramics International, 42(16), 19257-19268.

[34] Tänzer, R., Jin, Y., & Stephan, D. (2017). Alkali activated slag binder: effect of cations from silicate activators. Materials and Structures, 50(1), 91.

[35] Zuo, Y., Nedeljković, M., & Ye, G. (2019). Pore solution composition of alkali-activated slag/fly ash pastes. Cement and Concrete Research, 115, 230-250.

[36] Xin, L., Jin-yu, X., Weimin, L., & Erlei, B. (2014). Effect of alkali-activator types on the dynamic compressive deformation behavior of geopolymer concrete. Materials Letters, 124, 310-312.

[37] Fang, G., Ho, W. K., Tu, W., & Zhang, M. (2018). Workability and mechanical properties of alkali-activated fly ash-slag concrete cured at ambient temperature. Construction and Building Materials, 172, 476-487.

[38] Provis, J. L. (2018). Alkali-activated materials. Cement and Concrete Research, 114, 40-48.

[39] Li, Y., & Sun, Y. (2000). Preliminary study on combined-alkali–slag paste materials. Cement and concrete research, 30(6), 963-966.

[40] Oderji, S. Y., Chen, B., Shakya, C., Ahmad, M. R., & Shah, S. F. A. (2019). Influence of superplasticizers and retarders on the workability and strength of one-part alkali-activated fly ash/slag binders cured at room temperature. Construction and Building Materials, 229, 116891.

[41] Gebregziabiher, B. S., Thomas, R. J., & Peethamparan, S. (2016). Temperature and activator effect on early-age reaction kinetics of alkali-activated slag binders. Construction and Building Materials, 113, 783-793.

[42] Babu, D. V. (2018). Assessing the performance of molarity and alkaline activator ratio on engineering properties of self-compacting alkaline activated concrete at ambient temperature. Journal of Building Engineering, 20, 137-155.

[43] Mohamed, R., Abd Razak, R., Abdullah, M. M. A. B., Shuib, R. K., Mortar, N. A. M., & Zailani, W. W. A. (2019, August). Investigation of Heat Released during Geopolymerization with Fly Ash based Geopolymer. In IOP Conference Series: Materials Science and Engineering (Vol. 551, No. 1, p. 012093). IOP Publishing.

[44] Khale, D., & Chaudhary, R. (2007). Mechanism of geopolymerization and factors influencing its development: a review. Journal of materials science, 42(3), 729-746.

[45] Winnefeld, F., Leemann, A., Lucuk, M., Svoboda, P., & Neuroth, M. (2010). Assessment of phase formation in alkali activated low and high calcium fly ashes in building materials. Construction and building materials, 24(6), 1086-1093.

[46] Dransfield, J. (2003). Admixtures for Concrete. Mortar and Grout, Advanced Concrete Technologies, 3.

[47] Bilim, C., Karahan, O., Atiş, C. D., & Ilkentapar, S. (2013). Influence of admixtures on the properties of alkali-activated slag mortars subjected to different curing conditions. Materials & Design, 44, 540-547.

[48] Bakharev, T., Sanjayan, J. G., & Cheng, Y. B. (2000). Effect of admixtures on properties of alkali-activated slag concrete. Cement and Concrete Research, 30(9), 1367-1374.

[49] Yao, X., Zhang, Z., Zhu, H., & Chen, Y. (2009). Geopolymerization process of Alkali–metakaolinite characterized by isothermal calorimetry. Thermochimica Acta, 493(1-2), 49-54.

[50] Gu, Y. M., Fang, Y. H., You, D., Gong, Y. F., & Zhu, C. H. (2015). Properties and microstructure of alkali-activated slag cement cured at below-and about-normal temperature. Construction and Building Materials, 79, 1-8.

[51] Chindaprasirt, P., Phoo-ngernkham, T., Hanjitsuwan, S., Horpibulsuk, S., Poowancum, A., & Injorhor, B. (2018). Effect of calcium-rich compounds on setting time and strength development of alkali-activated fly ash cured at ambient temperature. Case Studies in Construction Materials, 9, e00198.

[52] Juilland, P., Kumar, A., Gallucci, E., Flatt, R. J., & Scrivener, K. L. (2012). Effect of mixing on the early hydration of alite and OPC systems. Cement and Concrete Research, 42(9), 1175-1188.

[53] Baskoca, A., Ozkul, M. H., & Artirma, S. (1998). Effect of chemical admixtures on workability and strength properties of prolonged agitated concrete. Cement and concrete research, 28(5), 737-747.

[54] Erdoğdu, Ş., Arslantürk, C., & Kurbetci, Ş. (2011). Influence of fly ash and silica fume on the consistency retention and compressive strength of concrete subjected to prolonged agitating. Construction and Building Materials, 25(3), 1277-1281.

[55] Palacios, M., & Puertas, F. (2011). Effectiveness of Mixing Time on Hardened Properties of Waterglass-Activated Slag Pastes and Mortars. ACI Materials Journal, 108(1).

[56] Palacios, M., Banfill, P. F., & Puertas, F. (2008). Rheology and setting of alkali-activated slag pastes and mortars: effect of organic admixture. ACI Materials Journal, 105(2), 140.

[57] Habert, G. (2014). Assessing the environmental impact of conventional and 'green'cement production. In Eco-efficient Construction and Building Materials (pp. 199-238). Woodhead Publishing.

[58] Ye, H., & Radlińska, A. (2016). Shrinkage mechanisms of alkali-activated slag. Cement and Concrete Research, 88, 126-135.

[59] Singh, B., Ishwarya, G., Gupta, M., & Bhattacharyya, S. K. (2015). Geopolymer concrete: A review of some recent developments. Construction and building materials, 85, 78-90.

[60] Puertas, F., Fernández-Jiménez, A., & Blanco-Varela, M. T. (2004). Pore solution in alkali-activated slag cement pastes. Relation to the composition and structure of calcium silicate hydrate. Cement and Concrete Research, 34(1), 139-148.

[61] Ozturk, M., Bankir, M. B., Bolukbasi, O. S., & Sevim, U. K. (2019). Alkali activation of electric arc furnace slag: Mechanical properties and micro analyzes. Journal of Building Engineering, 21, 97-105.

[62] Criado, M., Fernández-Jiménez, A., & Palomo, A. (2010). Alkali activation of fly ash. Part III: Effect of curing conditions on reaction and its graphical description. Fuel, 89(11), 3185-3192.

[63] Granizo, M. L., Alonso, S., Blanco-Varela, M. T., & Palomo, A. (2002). Alkaline activation of metakaolin: effect of calcium hydroxide in the products of reaction. Journal of the American Ceramic Society, 85(1), 225-231.

[64] Puertas, F., Varga, C., & Alonso, M. M. (2014). Rheology of alkali-activated slag pastes. Effect of the nature and concentration of the activating solution. Cement and Concrete Composites, 53, 279-288.

[65] Atiş, C. D., Bilim, C., Çelik, Ö., & Karahan, O. (2009). Influence of activator on the strength and drying shrinkage of alkali-activated slag mortar. Construction and building materials, 23(1), 548-555.

[66] Thomas, R. J., Ariyachandra, E., Lezama, D., & Peethamparan, S. (2018). Comparison of chloride permeability methods for Alkali-Activated concrete. Construction and Building Materials, 165, 104-111.

[67] Shojaei, M., Behfarnia, K., & Mohebi, R. (2015). Application of alkali-activated slag concrete in railway sleepers. Materials & Design, 69, 89-95.

[68] Elinwa, A. U., Ejeh, S. P., & Mamuda, A. M. (2008). Assessing of the fresh concrete properties of self-compacting concrete containing sawdust ash. Construction and building materials, 22(6), 1178-1182.

[69] Kay, E. A. (2003). Hot and cold weather concreting. Advanced Concrete Technology, Concrete Properties Edited by J. Newman, BS Choo, Elsevier.

[70] ACI Committee 306 (2016) "Guide to Cold Weather Concreting" , American Concrete Institute 14p.

[71] Assal, M. A. (2018). The effect of mixing water temperature on concrete properties in hot weather conditions.

[72] Myers, R. J., Bernal, S. A., & Provis, J. L. (2017). Phase diagrams for alkali-activated slag binders. Cement and Concrete Research, 95, 30-38.

[73] Wardhono, A., Gunasekara, C., Law, D. W., & Setunge, S. (2017). Comparison of long term performance between alkali activated slag and fly ash geopolymer concretes. Construction and Building materials, 143, 272-279.

[74] Coppola, L., Coffetti, D., Crotti, E., Candamano, S., Crea, F., Gazzaniga, G., & Pastore, T. (2020). The combined use of admixtures for shrinkage reduction in one-part alkali activated slag-based mortars and pastes. Construction and Building Materials, 248, 118682.

[75] Gao, X., Yu, Q. L., & Brouwers, H. J. H. (2015). Properties of alkali activated slag–fly ash blends with limestone addition. Cement and Concrete Composites, 59, 119-128.

[76] Bakharev, T., Sanjayan, J. G., & Cheng, Y. B. (2000). Effect of admixtures on properties of alkali-activated slag concrete. Cement and Concrete Research, 30(9), 1367-1374.

[77] Yao, X., Zhang, Z., Zhu, H., & Chen, Y. (2009). Geopolymerization process of alkali–metakaolinite characterized by isothermal calorimetry. Thermochimica Acta, 493(1-2), 49-54.

[78] Chen, W., & Brouwers, H. J. H. (2007). The hydration of slag, part 1: reaction models for alkali-activated slag. Journal of materials science, 42(2), 428-443.

[79] Provis, J. L., & Bernal, S. A. (2014). Geopolymers and related alkali-activated materials. Annual Review of Materials Research, 44, 299-327.

[80] Garcia-Lodeiro, I., Palomo, A., & Fernández-Jiménez, A. (2015). Crucial insights on the mix design of alkali-activated cement-based binders. In Handbook of alkali-activated cements, mortars and concretes (pp. 49-73). Woodhead Publishing.

[81] Luukkonen, T., Abdollahnejad, Z., Yliniemi, J., Kinnunen, P., & Illikainen, M. (2018). One-part alkali-activated materials: A review. Cement and Concrete Research, 103, 21-34.

[82] Alrefaei, Y., Wang, Y. S., & Dai, J. G. (2019). The effectiveness of different superplasticizers in ambient cured one-part alkali activated pastes. Cement and Concrete Composites, 97, 166-174.

[83] Oderji, S. Y., Chen, B., Shakya, C., Ahmad, M. R., & Shah, S. F. A. (2019). Influence of superplasticizers and retarders on the workability and strength of one-part alkali-activated fly ash/slag binders cured at room temperature. Construction and Building Materials, 229, 116891.

[84] Sodium meta-Silicate Nonahydrate (Crystalline/Certified), Fisher Chemical. https://www.fishersci.ca/shop/products/sodium-meta-silicate-nonahydrate-crystalline-certified-fisher-chemical-2/p-34259

[85] Hasanain, G. S., Khallaf, T. A., Mahmood, K. (1989) "Water evaporation from freshly placed concrete surfaces in hot weather," Cement and Concrete Research, Volume 19, Issue 3, pp. 465-475

[86] Kashani, A., Provis, J.L., Qiao, G.G., Deventer, J.S.J (2014) "The interrelationship between surface chemistry and rheology in alkali activated slag paste,' Construction and Building Materials, Vol. 65, pp. 583-591

[87] Yuan, B., Yu, Q.L. and Brouwers, H.J.H. (2017) "Time-dependent characterization of Na_2CO_3 activated slag," Cement and Concrete CompositesVolume 84, pp. 188-197

[88] H.H.C. Wong, A.K.H. KwanRheology of cement paste: role of excess water to solid surface area ratio J Mater Civ Eng, 20 (2008), p. 189

[89] Živica, V. (2007). Effects of type and dosage of alkaline activator and temperature on the properties of alkali-activated slag mixtures. Construction and Building Materials, 21(7), 1463-1469.

[90] Johnson SB, Franks GV, Scales PJ, Boger DV, Healy TW. Surface chemistry–rheology relationships in concentrated mineral suspensions. Int J Miner Process 2000;58:267–304.

[91] Chithiraputhiran, S., & Neithalath, N. (2013). Isothermal reaction kinetics and temperature dependence of alkali activation of slag, fly ash and their blends. Construction and Building Materials, 45, 233-242.

[92] Luukkonen, T., Abdollahnejad, Z., Yliniemi, J., Kinnunen, P., & Illikainen, M. (2018). One-part alkali-activated materials: A review. Cement and Concrete Research, 103, 21-34.

[93] Pardal, X., Pochard, I., & Nonat, A. (2009). Experimental study of Si–Al substitution in calcium-silicate-hydrate (CSH) prepared under equilibrium conditions. Cement and Concrete Research, 39(8), 637-643.

[94] Shi, C., & Day, R. L. (1995). A calorimetric study of early hydration of alkali-slag cements. Cement and concrete Research, 25(6), 1333-1346.

[95] General Chemistry: Principles and Modern Applications, 11th edition, Ralph H. Petrucci, Ralph H. Petrucci, F Geoffrey Herring, Jeffry D. Madura, Carey Bissonnette, Published by Pearson (February 23rd 2016) - Copyright © 2016 11th edition

[96] Hazardous Substances Data Bank, 2003. Sodium Metasilicate; Hazardous Substances Data Bank Number 753. U.S. National Library of Medicine, Toxicology. Data Network. USA.

[97] Vestfálová, M., & Šafařík, P. (2016). Dependence of the isobaric specific heat capacity of water vapor on the pressure and temperature. In EPJ Web of Conferences (Vol. 114, p. 02133). EDP Sciences.

[98] Gebregziabiher, B. S., Thomas, R., & Peethamparan, S. (2015). Very early-age reaction kinetics and microstructural development in alkali-activated slag. Cement and concrete composites, 55, 91-102.

[99] Gruskovnjak, B. Lothenbach, L. Holzer, R. Figi and F. Winnefeld*(2006) “Hydration of alkali-activated slag: comparison with ordinary Portland cement” Advances in Cement Research, 2006,18, No. 3, pp. 119–128

[100] Deng, Z., Zhou,W., Yue, H., and Guo, X. (2019) “Study on the hydration mechanism of a hardened slag-based plugging agent activated by alkalis,” Construction and Building MaterialsVolume 203pp. 343-355

[101] Fernández-Jiménez A, Puertas F. Alkali-activated slag cements: kinetic studies. Cem Concr Res 1997;27:359–68.

[102] Criado, M., Walkley, B., Ke, X., Provis, J. L., & Bernal, S. A. (2018). Slag and activator chemistry control the reaction kinetics of sodium metasilicate-activated slag cements. Sustainability, 10(12), 4709.

[103] Yuan, R., Gao, Q. and Ouyang, S. (1987) "Study on the structure and latenet hydraulic activity of slag and its activation mechanism," Journal of Wuhan university of technolohgy, No.3, pp.297-303.

[104] Burciaga-Díaz, O., & Betancourt-Castillo, I. (2018). Characterization of novel blast-furnace slag cement pastes and mortars activated with a reactive mixture of MgO-NaOH. Cement and Concrete Research, 105, 54-63.

[105] Bernal, S. A., Provis, J. L., Walkley, B., San Nicolas, R., Gehman, J. D., Brice, D. G., ... & van Deventer, J. S. (2013). Gel nanostructure in alkali-activated binders based on slag and fly ash, and effects of accelerated carbonation. Cement and Concrete Research, 53, 127-144.

[106] Burciaga-Díaz, O., & Betancourt-Castillo, I. (2018). Characterization of novel blast-furnace slag cement pastes and mortars activated with a reactive mixture of MgO-NaOH. Cement and Concrete Research, 105, 54-63.

[107] Li, P., Tang, J., Chen, X., Bai, Y., & Li, Q. (2019). Effect of temperature and pH on early hydration rate and apparent activation energy of alkali-activated slag. Advances in Materials Science and Engineering, 2019.

[108] Alonso, S., & Palomo, A. (2001). Alkaline activation of metakaolin and calcium hydroxide mixtures: influence of temperature, activator concentration and solids ratio. Materials Letters, 47(1-2), 55-62.

[109] Ye, H., Cartwright, C., Rajabipour, F., & Radlińska, A. (2014). Effect of drying rate on shrinkage of alkali-activated slag cements.

[110] Jiao, Z., Wang, Y., Zheng, W., & Huang, W. (2018). Effect of Dosage of Alkaline Activator on the Properties of Alkali-Activated Slag Pastes. Advances in Materials Science and Engineering, 2018.

[111] Ishwarya, G., Singh, B., Deshwal, S., & Bhattacharyya, S. K. (2019). Effect of sodium carbonate/sodium silicate activator on the rheology, geopolymerization and strength of fly ash/slag geopolymer pastes. Cement and Concrete Composites, 97, 226-238.

[112] Criado, M., Walkley, B., Ke, X., Provis, J. L., & Bernal, S. A. (2018). Slag and activator chemistry control the reaction kinetics of sodium metasilicate-activated slag cements. Sustainability, 10(12), 4709.

[113] Juilland, P., Kumar, A., Gallucci, E., Flatt, R. J., & Scrivener, K. L. (2012). Effect of mixing on the early hydration of alite and OPC systems. Cement and Concrete Research, 42(9), 1175-1188.

[114] Chevalier, P.,, & Baker, N., Aluminum in Canada (2020). In The Canadian Encyclopedia. Retrieved from https://www.thecanadianencyclopedia.ca/en/article/aluminum

[115] Kuhlberg, M., Pulp and Paper Industry (2015). In The Canadian Encyclopedia. Retrieved from https://www.thecanadianencyclopedia.ca/en/article/pulp-and-paper-industry

[116] Simão, L., Hotza, D., Raupp-Pereira, F., Labrincha, J. A., & Montedo, O. R. K. (2018). Wastes from pulp and paper mills-a review of generation and recycling alternatives. Cerâmica, 64(371), 443-453.

[117] Ribeiro, D. V., Labrincha, J. A., & Morelli, M. R. (2011). Potential use of natural red mud as pozzolan for Portland cement. Materials research, 14(1), 60-66.

[118] Vafaei, M., & Allahverdi, A. (2017). High strength geopolymer binder based on waste-glass powder. Advanced Powder Technology, 28(1), 215-222.

[119] Provis, J. L., Palomo, A., & Shi, C. (2015). Advances in understanding alkali-activated materials. Cement and Concrete Research, 78, 110-125.

[120] Wang, P., & Liu, D. Y. (2012). Physical and chemical properties of sintering red mud and bayer red mud and the implications for beneficial utilization. Materials, 5(10), 1800-1810.

[121] Rai, S., Lataye, D. H., Chaddha, M. J., Mishra, R. S., Mahendiran, P., Mukhopadhyay, J., ... & Wasewar, K. L. (2013). An alternative to clay in building materials: red mud sintering using fly ash via taguchi's methodology. Advances in Materials Science and Engineering, 2013.

[122] Cherian, C., & Siddiqua, S. (2019). Pulp and Paper Mill Fly Ash: A Review. Sustainability, 11(16), 4394.

[123] Saha, A. K. (2018). Effect of class F fly ash on the durability properties of concrete. Sustainable environment research, 28(1), 25-31.

[124] Dodoo-Arhin, D., Nuamah, R. A., Agyei-Tuffour, B., Obada, D. O., & Yaya, A. (2017). Awaso bauxite red mud-cement based composites: Characterisation for pavement applications. Case studies in construction materials, 7, 45-55.

[125] Bayat, A., Hassani, A., & Yousefi, A. A. (2018). Effects of red mud on the properties of fresh and hardened alkali-activated slag paste and mortar. Construction and Building Materials, 167, 775-790.

[126] Hatami, F., & Kermani, M. Effect of Mechanical Behaviour of Steel Making Slags on the Blended Cements by Experimental Study.

[127] Škvára, F. (2007). Alkali activated materials or geopolymers. Ceramics-Silikáty, 51(3), 173-177.

[128] Lopez, E., Soto, B., Arias, M., Nunez, A., Rubinos, D., & Barral, M. T. (1998). Adsorbent properties of red mud and its use for wastewater treatment. Water research, 32(4), 1314-1322.

[129] Do, T. M., & Kim, Y. S. (2016). Engineering properties of controlled low strength material (CLSM) incorporating red mud. International Journal of Geo-Engineering, 7(1), 7.

[130] Kuhlberg, M., Pulp and Paper Industry (2015). In The Canadian Encyclopedia. Retrieved from https://www.thecanadianencyclopedia.ca/en/article/pulp-and-paper-industry.

[131] Hubbe, M. A., Metts, J. R., Hermosilla, D., Blanco, M. A., Yerushalmi, L., Haghighat, F., ... & Elliott, A. (2016). Wastewater treatment and reclamation: A review of pulp and paper industry practices and opportunities. BioResources, 11(3), 7953-8091.

[132] Cabrera, M. N. (2017). Pulp mill wastewater: Characteristics and treatment. Biological Wastewater Treatment and Resource Recovery, 119-139.

[133] de Alda, J. A. O. (2008). Feasibility of recycling pulp and paper mill sludge in the paper and board industries. Resources, Conservation and Recycling, 52(7), 965-972.

[134] Tavakoli, D., Hashempour, M., & Heidari, A. (2018). Use of waste materials in concrete: a review. Pertanika Journal of Science & Technology, 26(2), 499-522.

[135] Jiayu, K. A. N. G., Mengxiao, W. A. N. G., & Zhongjun, X. I. A. O. (2009). Modeling and control of pH in pulp and paper wastewater treatment process. Journal of Water Resource and Protection, 2009.

[136] Balador, Z., Gjerde, M., Isaacs, N., & Imani, M. (2018). Thermal and Acoustic Building Insulations from Agricultural Wastes.

[137] Mazur, W., Drobiec, L., & Jasinski, R. (2016). Research of light concrete precast lintels. Procedia engineering, 161, 611-617.

[138] Li, F., Chen, G., Zhang, Y., Hao, Y., & Si, Z. (2020). Fundamental Properties and

Thermal Transferability of Masonry Built by Autoclaved Aerated Concrete Self-Insulation Blocks. Materials, 13(7), 1680.

[139] Finance, M. B. A., & Marketing, M. B. A. Noise Absorbing Composite Materials Using Agro Waste Products.

[140] Hwang, S. D., Khatib, R., Lee, H. K., Lee, S. H., & Khayat, K. H. (2012). Optimization of steam-curing regime for high-strength, self-consolidating concrete for precast, prestressed concrete applications. PCI journal, 57(3), 48.

[141] Wereski, M. (2015). The Threshold of Hearing. The STEAM Journal, 2(1), 20.

[142]https://www.netzsch-thermal-analysis.com/en/products-solutions/thermal-diffusivity-conductivity/hfm-446-lambda-series/

[143] Škvára, F. (2007). Alkali activated materials or geopolymers. Ceramics-Silikáty, 51(3), 173-177.

[144] Cramer, S. M., Friday, O. M., White, R. H., & Sriprutkiat, G. (2003). Mechanical properties of gypsum board at elevated temperatures. In Fire and materials 2003: 8th International Conference, January 2003, San Francisco, CA, USA. London: Interscience Communications Limited, c2003: pages 33-42.

[145] Manzello, S. L., Park, S. H., Mizukami, T. E. N. S. E. I., & Bentz, D. P. (2008, May). Measurement of thermal properties of gypsum board at elevated temperatures. In Proceedings of the 5th International Conference on Structures in Fire. Nanyang Technological University, Singapore (pp. 28-30).